3-Days Training for Practical Application of ACS SASSI NQA V4 to Seismic SSI Analysis of Nuclear Facility Structures

Ghiocel Predictive Technologies Inc.

Dr. Dan M. Ghiocel

Member of ASCE 4 & 43 Standards

Email: dan.ghiocel@ghiocel-tech.com

Ghiocel Predictive Technologies Inc.

http://www.ghiocel-tech.com

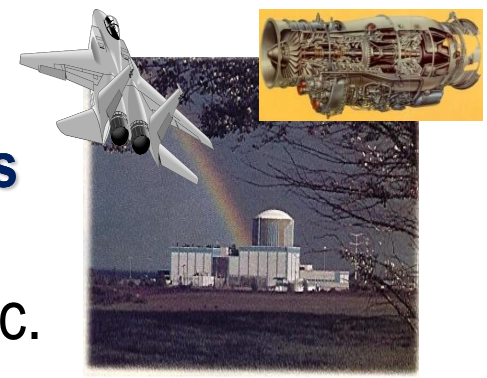

Part 1: ACS SASSI Modeling, Theory and Implementation

USNRC Office, Rockville, MD

June 25-27, 2019

Presentation Content

1. SASSI Flexible Volume Substructuring Methodology. Theoretical and Implementation Aspects.

2. Excavated Soil Modeling for Deeply Embedded Structures

3. ACS SASSI Motion Incoherency Modeling

4. Limitations of RVT SASSI Approach

1. SASSI Flexible Volume Substructuring Methodology.

Theoretical and Implementation Aspects

SSI Analysis Methods and Models

Real

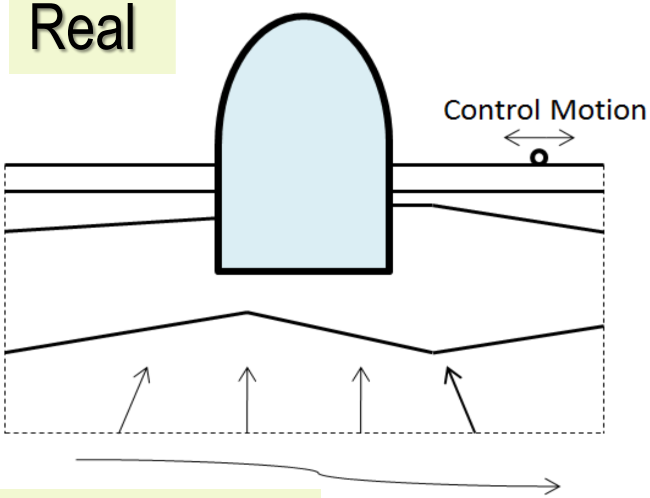

Idealized

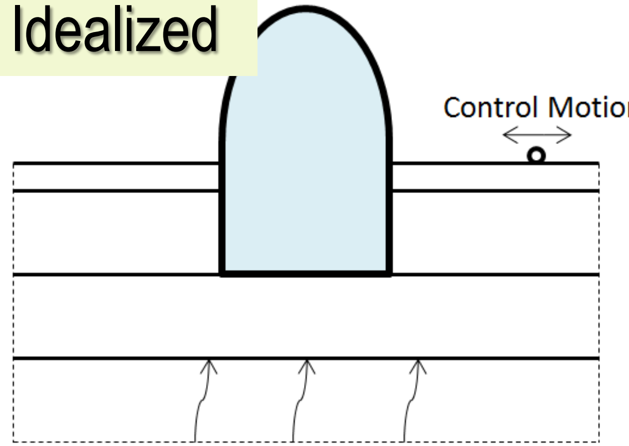

Vertical wave propagation is used to replace actual complex ground motion pattern, but still produce specified motion at control point.

Direct Approach
(Single Step Analysis)
(Single FE Model)

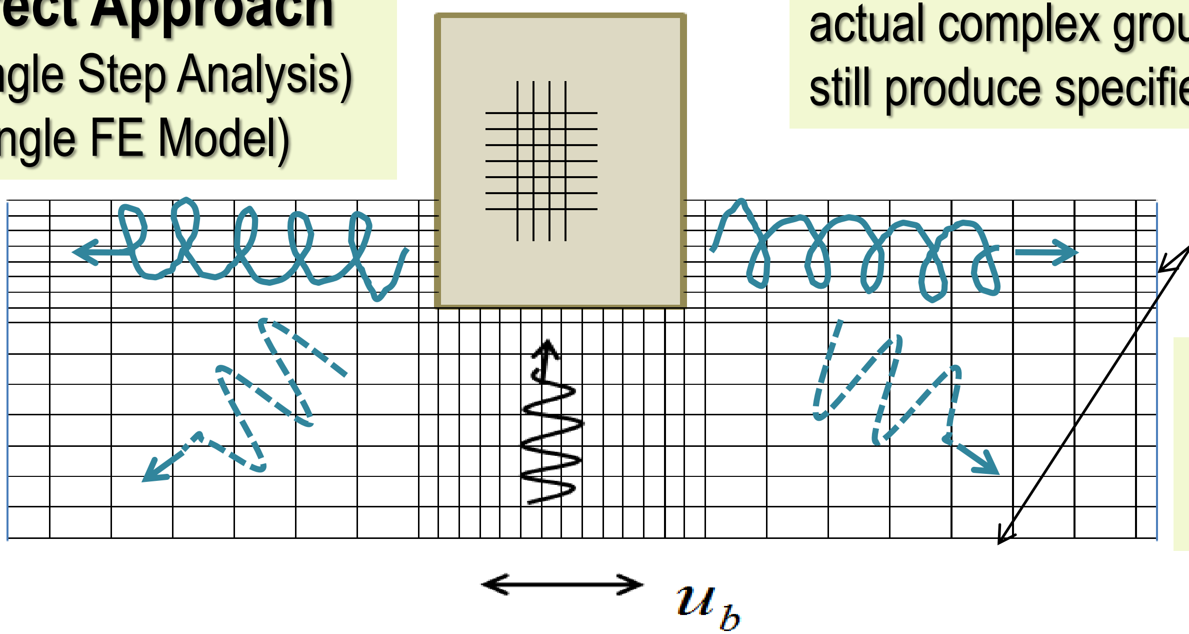

Conventional BCs
(stiffness, damping, soil motion)

Enormous amount of solid elements; 99% of FE elements are in soil media

Linearized SSI Analysis Superposition Theorem

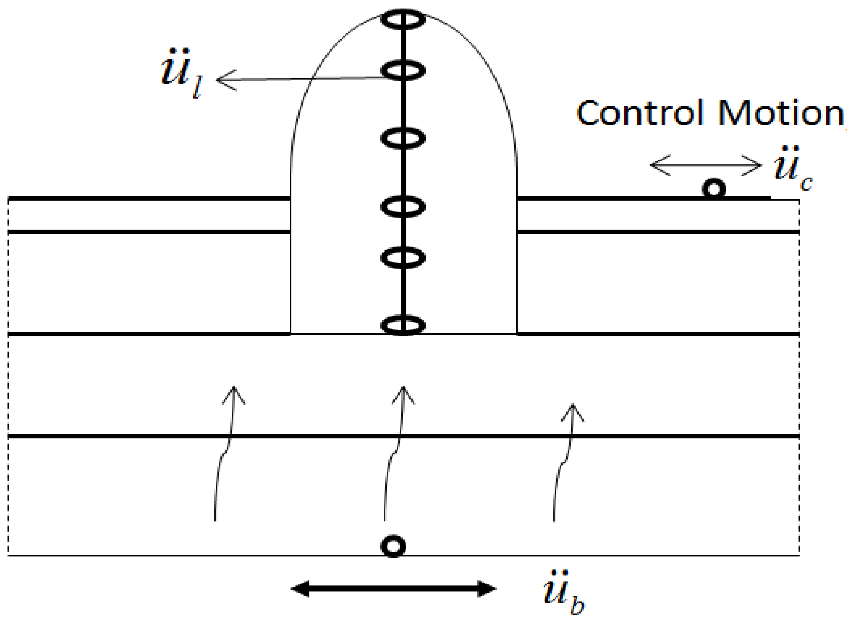

(a) Kinematic Interaction Analysis

Structure has stiffness but no mass.

Analysis leads to determination of motions at different points in structure relative to base control point.

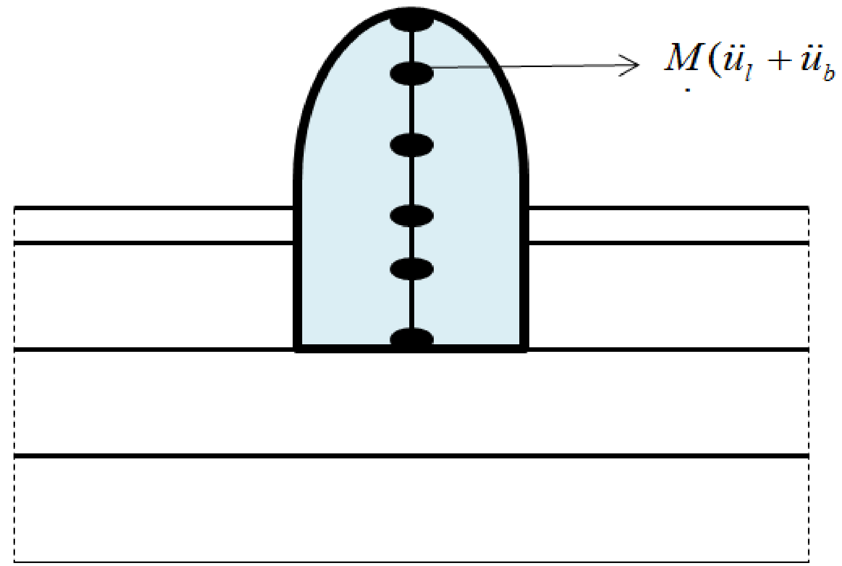

(b) Inertial Interaction Analysis

Motions computed in (a) are applied to masses in structure as shown above.

Analysis leads to computation of new motions at different points in structure.

SSI Substructuring Using Three Step Approach

Rigid Boundary SSI Substructuring (Kausel,1974)

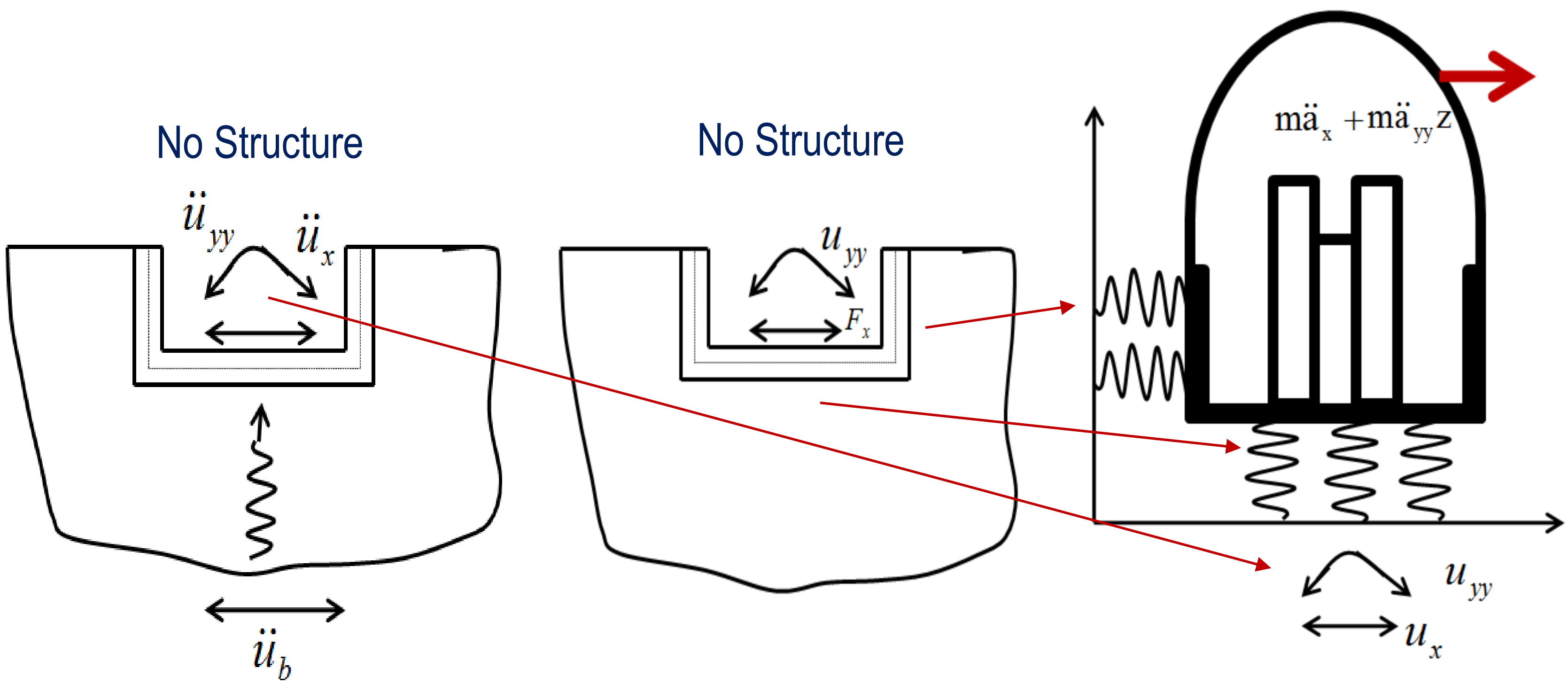

a) Kinematic SSI Analysis (Wave Scattering Problem Pb)

b) Impedance Computation (External Force Pb)

c) Inertial SSI Analysis (Structural Dynamics Pb)

Direct SSI Approach vs. SASSI Approach

Direct Approach (Time-Domain)

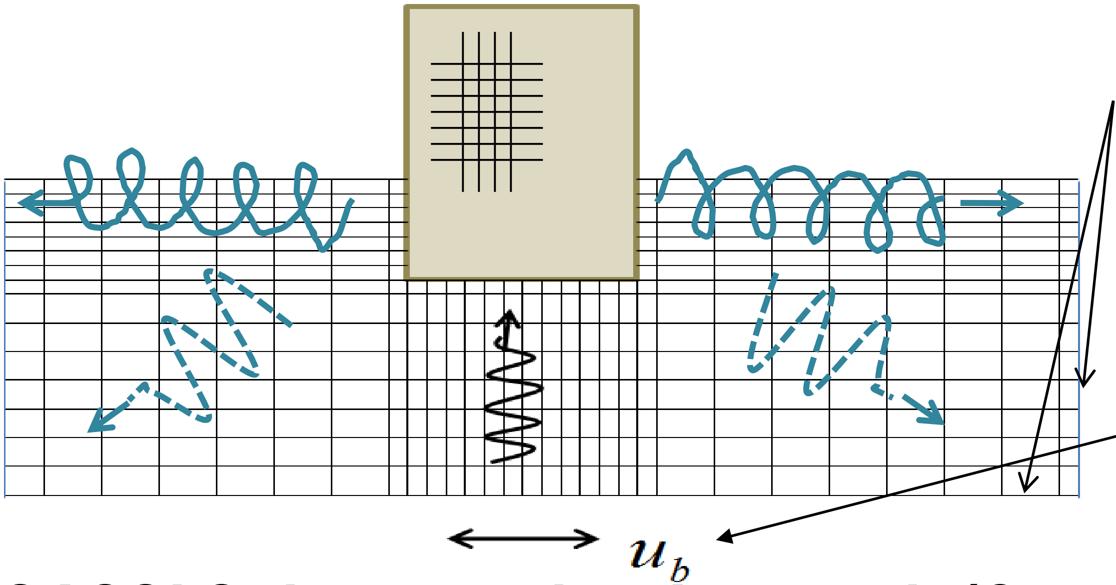

FE Model Boundaries
(stiffness, damping, soil motion)

99% of FE elements are in soil

Input motion

SASSI Substructuring Approach (Complex Frequency)

Structural dynamic analysis step includes *3D Structure FEM* and *Excavated Soil FEM*

Only *1D soil layering variation model* is used to compute the input motions and the soil impedance for SSI analysis via axisymmetric soil deposit modeling

1D Soil Layering FE Model
w/o Excavated Soil
(Free Field Analysis)

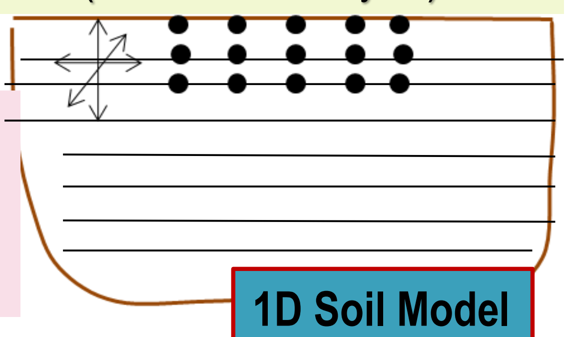

3D Structure w/ Excavated Soil
FE Model (SSI Analysis)

Input motion

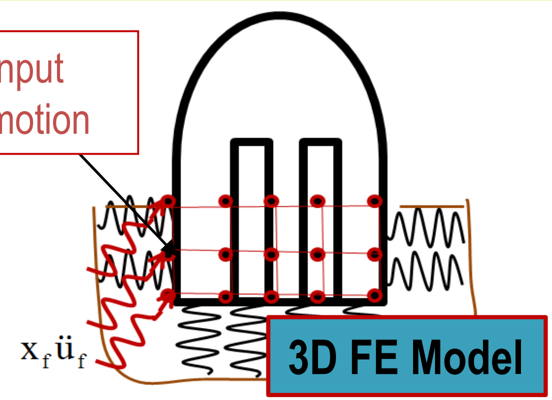

Direct SSI Approach and SASSI Approach Models

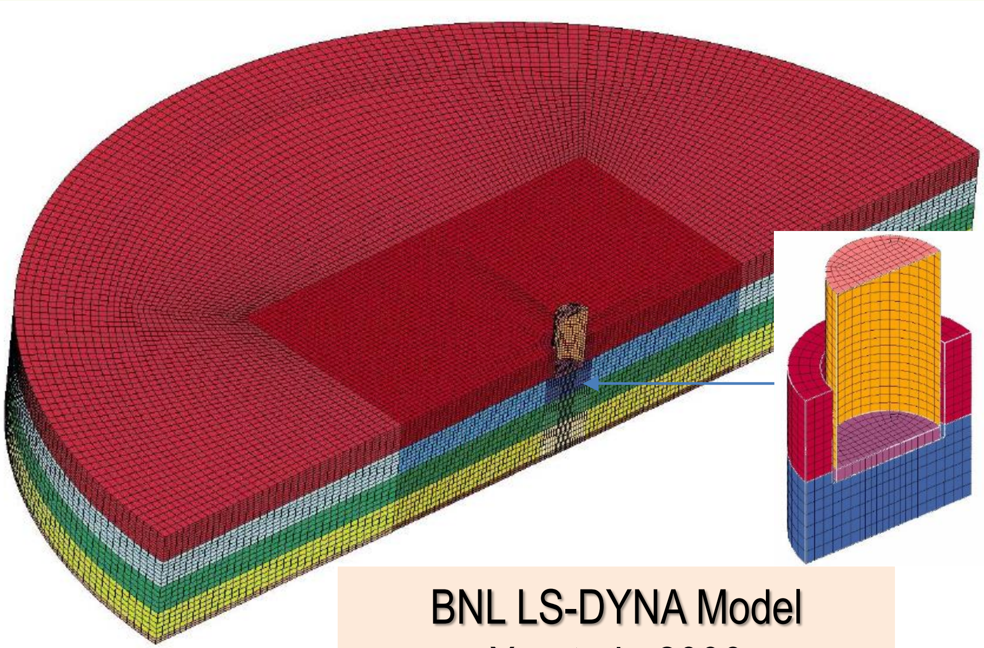

BNL LS-DYNA Model
Xu et al., 2006

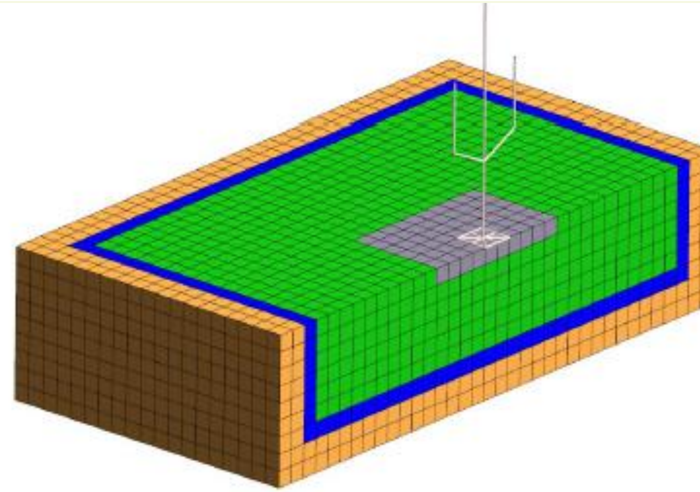

E-SSI Model (Low Frequency)
Neboja et al., 2015

Direct SSI Approach Model

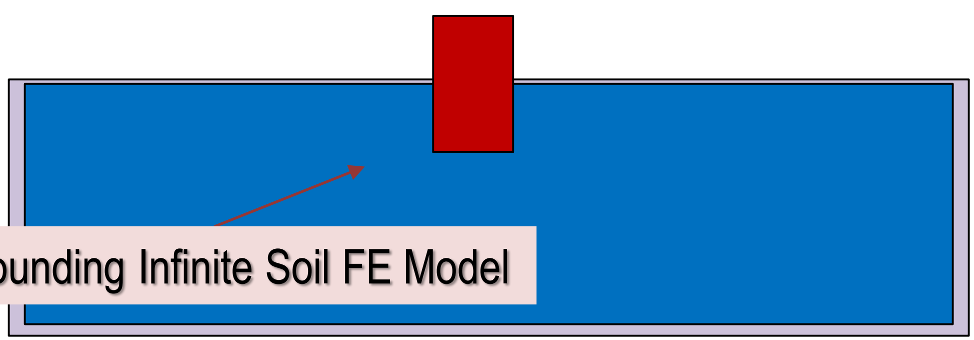

Surrounding Infinite Soil FE Model

SASSI Approach Model

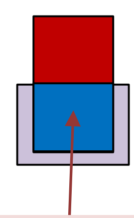

Excavated Soil FE Model

SASSI Flexible Volume (FV) Substructuring Method

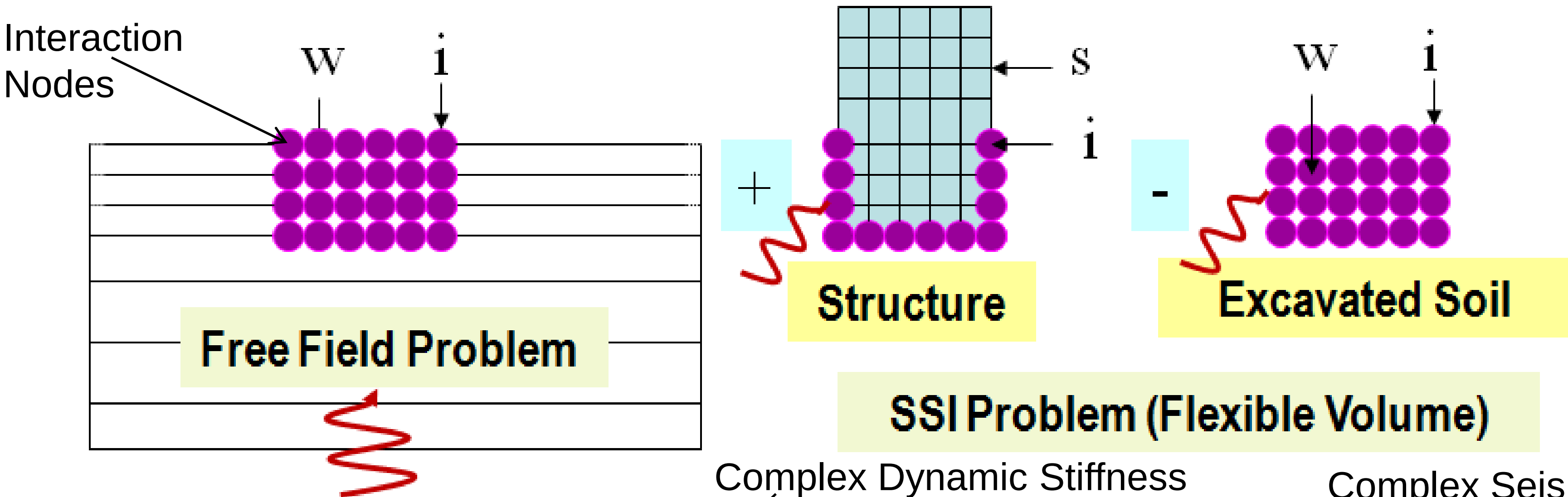

Complex Frequency Domain Formulation:

Complex Dynamic Stiffness

Complex Seismic Load Vector

$$\boxed{C(\omega)\,U(\omega) = Q(\omega)}$$

Complex Absolute Displacements

Complex Soil Impedance Terms

$$\begin{bmatrix} \mathbf{C}^{s}_{ii} - \mathbf{C}^{e}_{ii} + \mathbf{X}_{ii} & -\mathbf{C}^{e}_{iw} + \mathbf{X}_{iw} & \mathbf{C}^{s}_{is} \\ -\mathbf{C}^{e}_{wi} + \mathbf{X}_{wi} & -\mathbf{C}^{e}_{ww} + \mathbf{X}_{ww} & \mathbf{0} \\ \mathbf{C}^{s}_{si} & \mathbf{0} & \mathbf{C}^{s}_{ss} \end{bmatrix} \begin{Bmatrix} \mathbf{U}_{i} \\ \mathbf{U}_{w} \\ \mathbf{U}_{s} \end{Bmatrix} = \begin{Bmatrix} \mathbf{X}_{ii}\mathbf{U}'_{i} + \mathbf{X}_{iw}\mathbf{U}'_{w} \\ \mathbf{X}_{wi}\mathbf{U}'_{i} + \mathbf{X}_{ww}\mathbf{U}'_{w} \\ \mathbf{0} \end{Bmatrix}$$

REMARK: All Excavated Soil nodes are interaction nodes (include exact equations of motion)

SASSI Substructuring Uses 3D1D SSI Models

System Components Aspects:

1) Free-filed Soil Layer Variation (1D)
2) Assembly SSI System and Solve (3D)

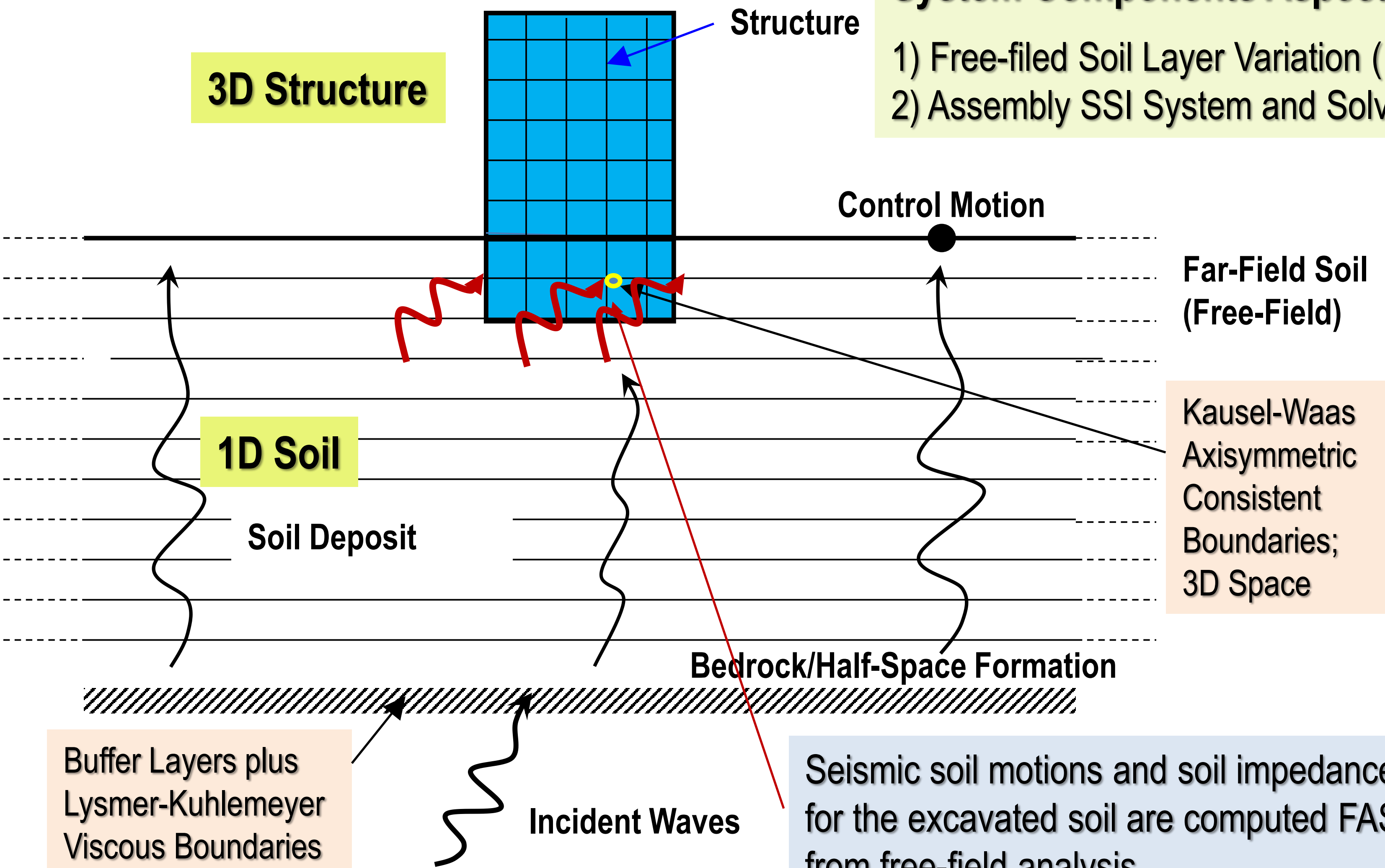

Seismic soil motions and soil impedances for the excavated soil are computed FAST from free-field analysis

Typical Nuclear Island SASSI Modeling (Using 3D FE Models)

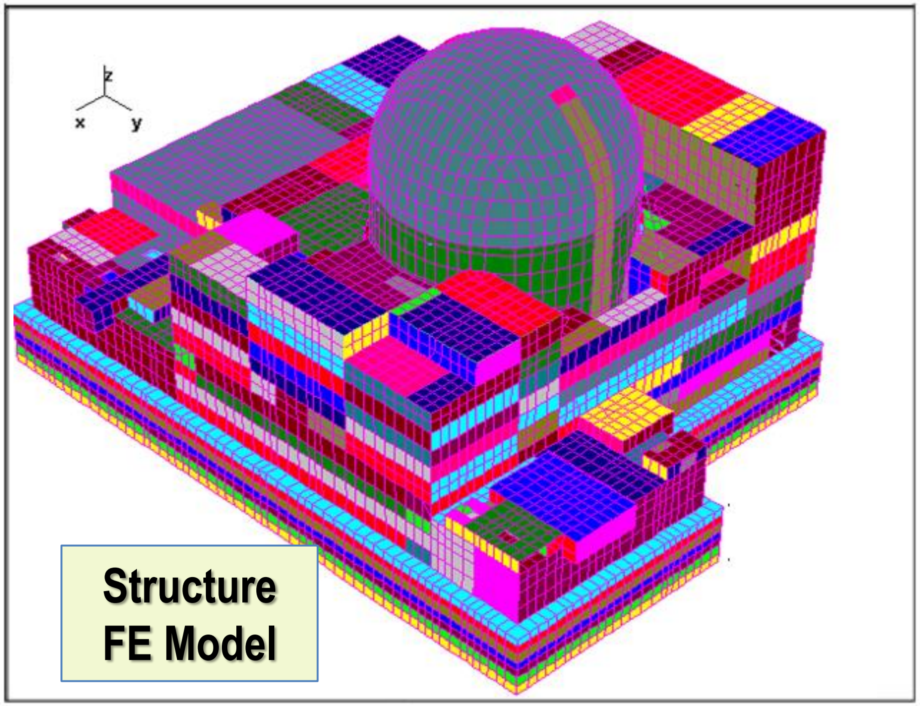

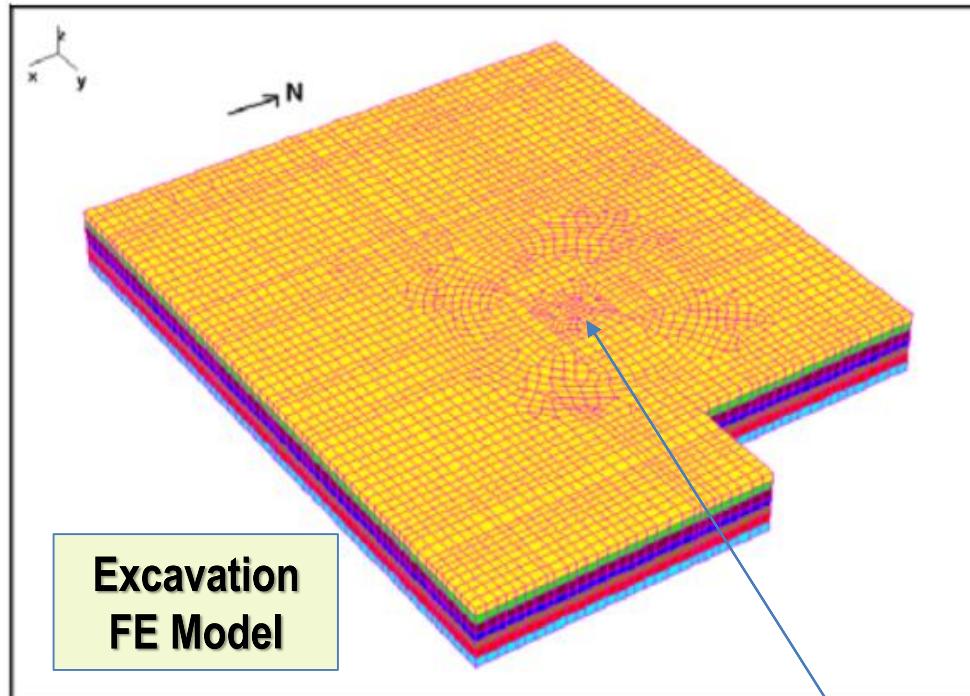

US-APWR RB SSI Model

Ghiocel et. al., 2013, SMIRT22

Adjacent Soil Nonlinear Behavior Via Equivalent-Linear Iterative SASSI Analysis (w/ Octahedral Soil Strains)

US-APWR
ACS SASSI MODEL

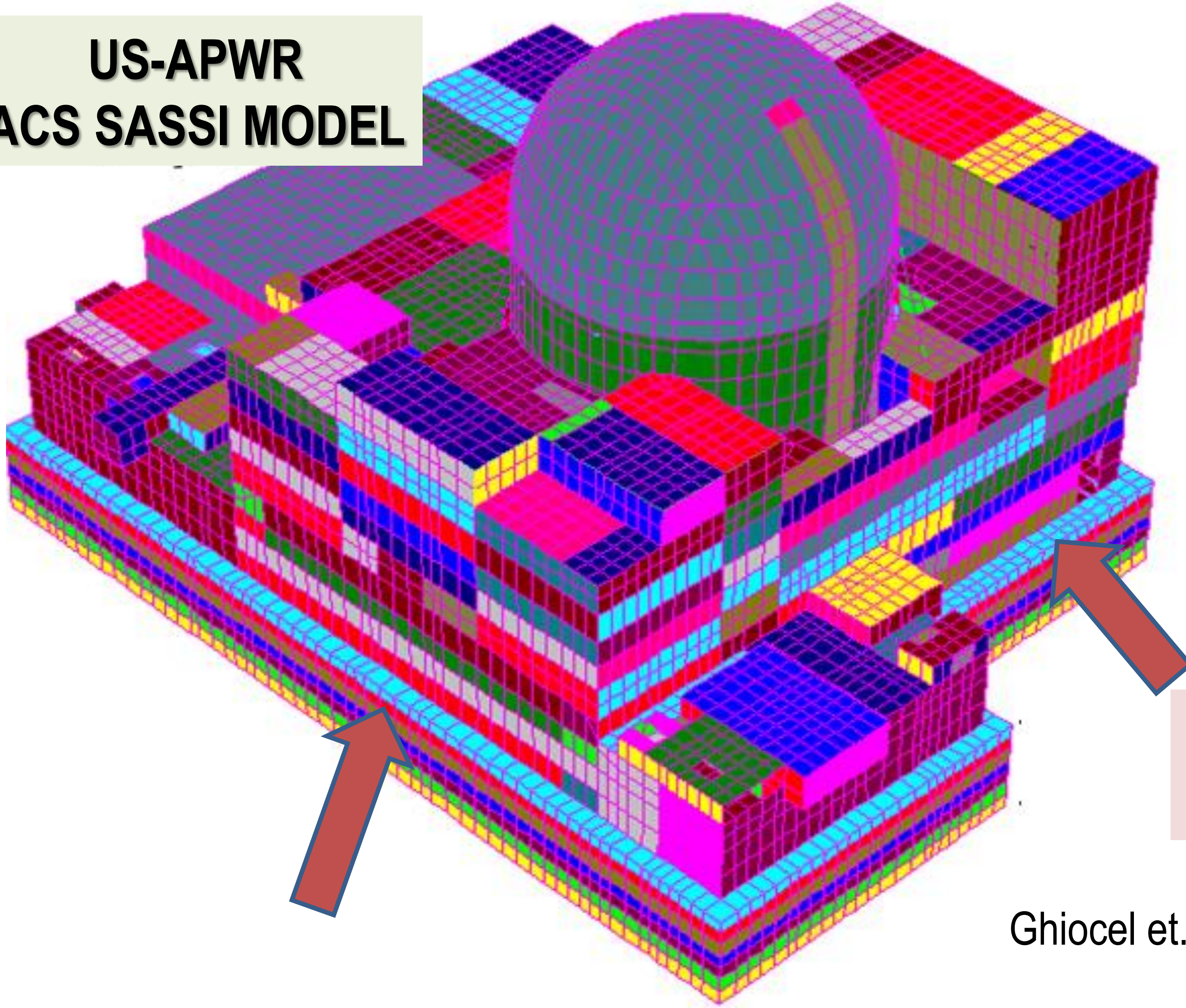

Iterative EQL

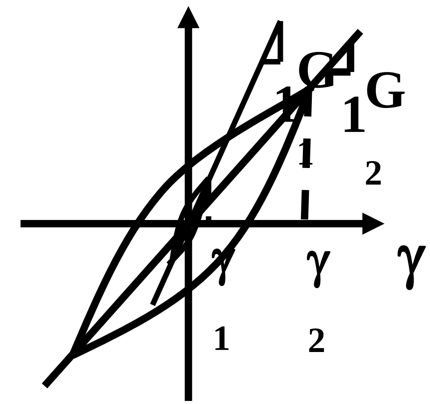

Nonlinear soil solid elements

Ghiocel et. al., 2013, SMIRT22)

27 slides skipped for public version

Layered Soil Impedance Matrix Computation

In this method, the flexibility matrix need be computed for all the interacting nodes using the methods described above.

The impedance matrix is obtained by inverting the flexibility matrix, i.e.,

$$\mathbf{X}_{\mathrm{ff}} = \mathbf{F}_{\mathrm{ff}}^{-1}$$

- The inversion of the matrix is computationally intensive and needs to be performed for every frequency of analysis.
- An efficient in-place inversion routine is used to invert the flexibility matrix which is a full matrix in the direct method of analysis.
- For total number of i interacting nodes, the resultant impedance matrix of the order of 3i x 3i for three-dimensional problems.

Layered Soil Impedance Matrix Computation

Computational Steps:

1. Compute Flexibility Matrix (complex soil displacement amplitudes under unit amplitude harmonic forces at each frequency)

2. Compute Impedance Matrix (complex soil stiffness amplitudes)
   - Flexible Volume Method (FV, uses all excavation interaction nodes)
   - Flexible Interface Method (FV-EVBN or MSM, ESM, SM, FFV, uses only excavation interface nodes)

3. Equivalent Global Impedances (Optional, Old option).
   NOT RECOMMENDED. These are not foundation impedances!

SASSI Flexible Volume Methods for Embedded Structures

Flexible Volume Substructuring Approaches

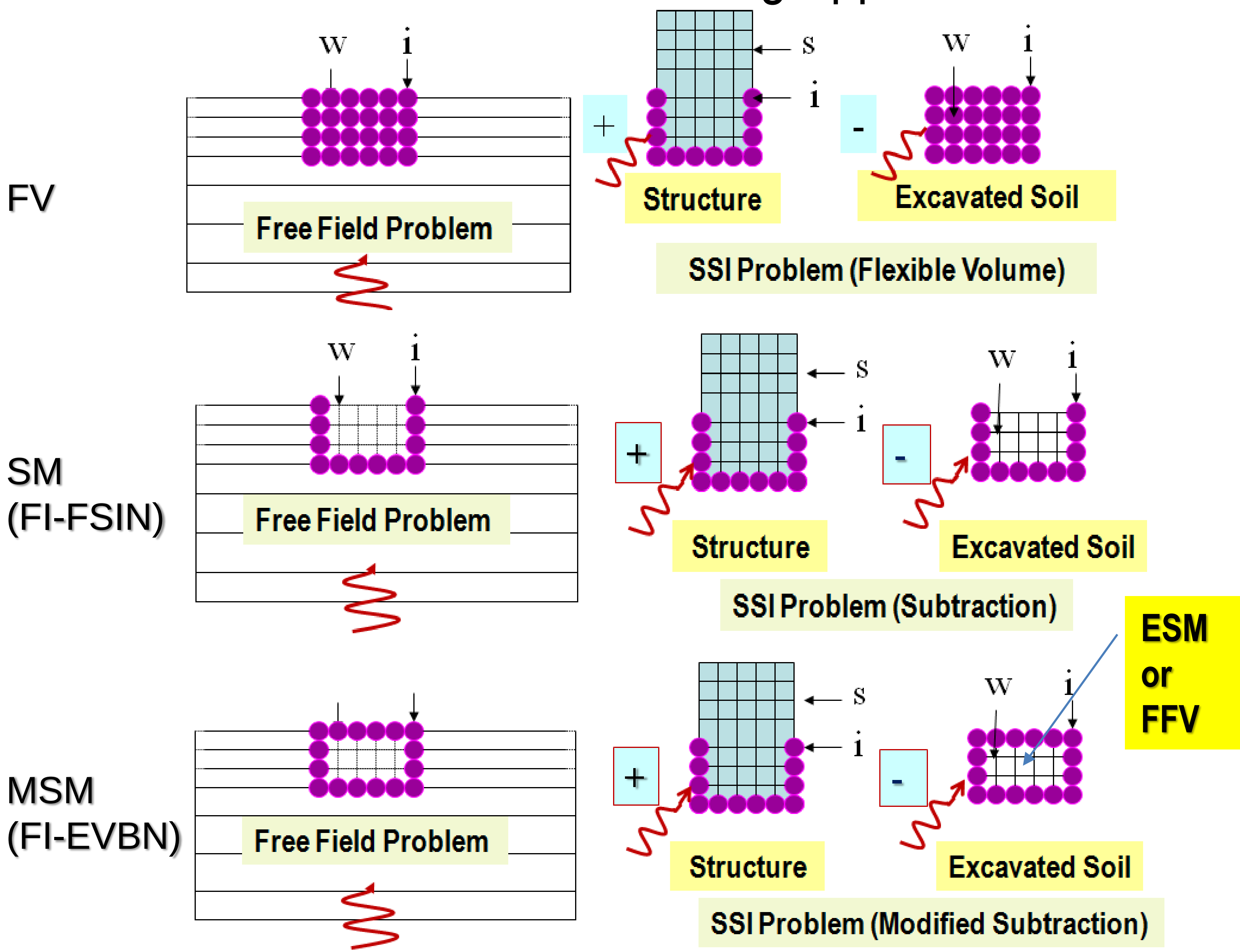

2. Excavated Soil Modeling for Deeply Embedded Structures

Complete SSI Analysis Using RB Complex SSI Model

RB Complex SSI Model

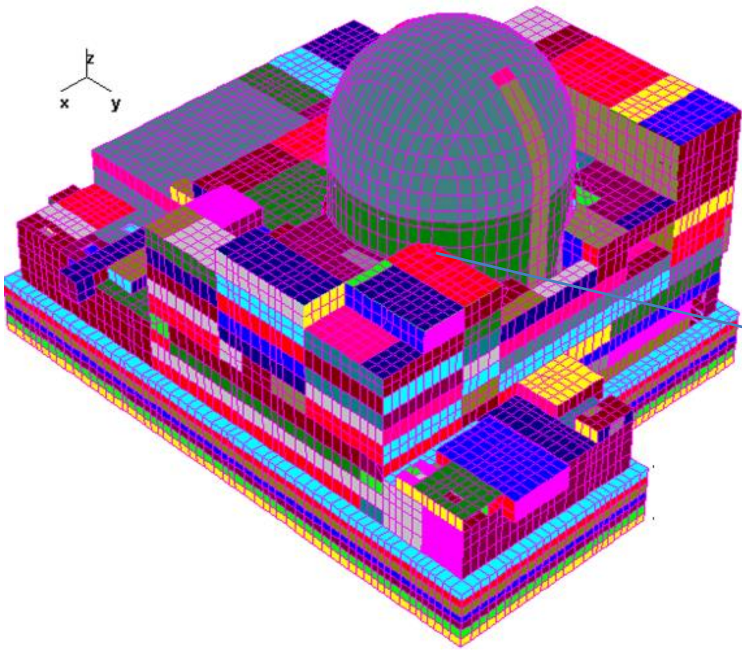

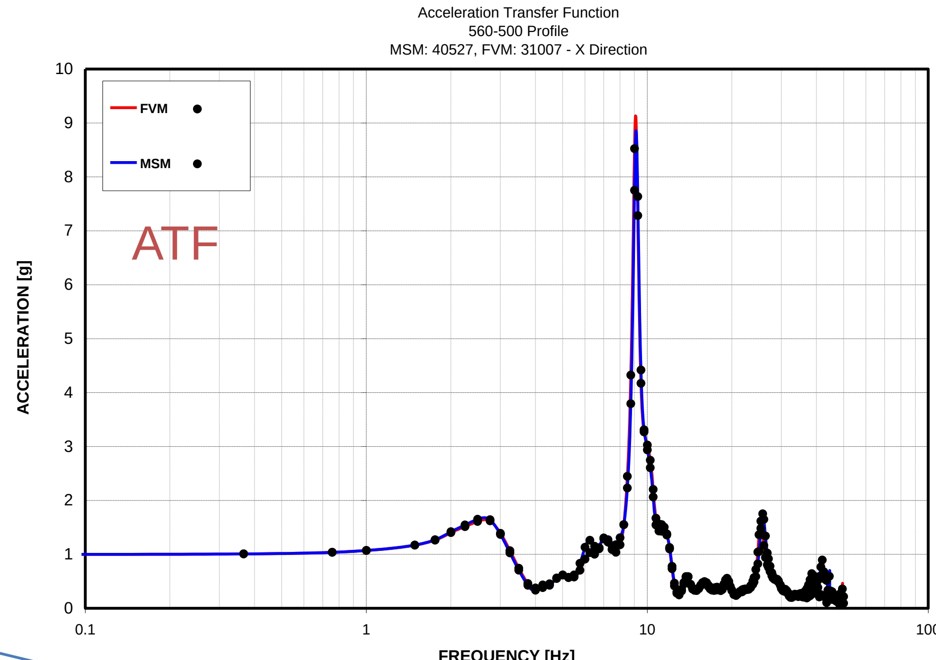

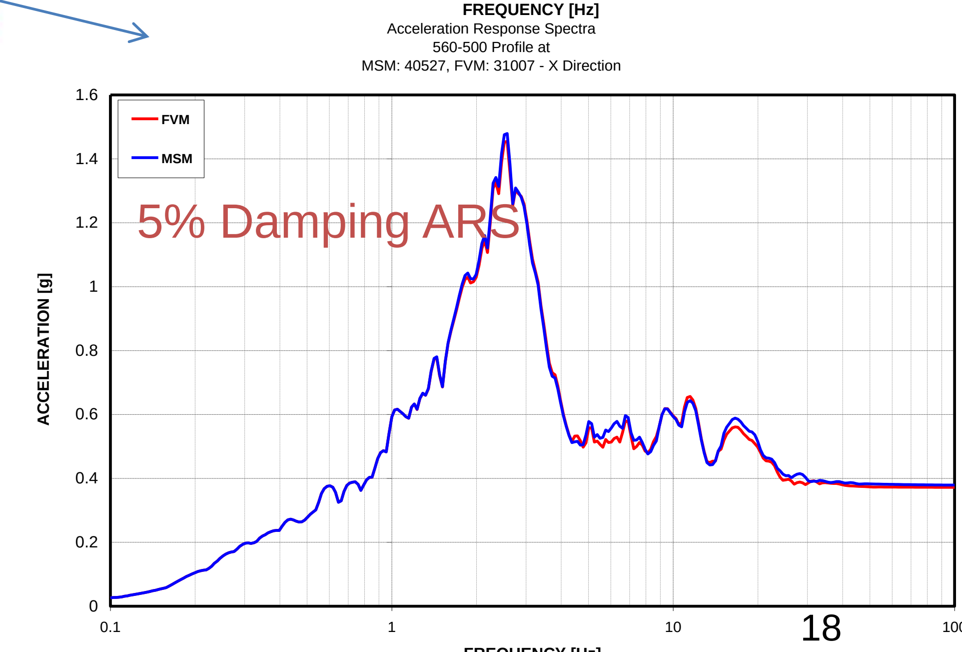

NI RB Complete SSI Model Case Studies

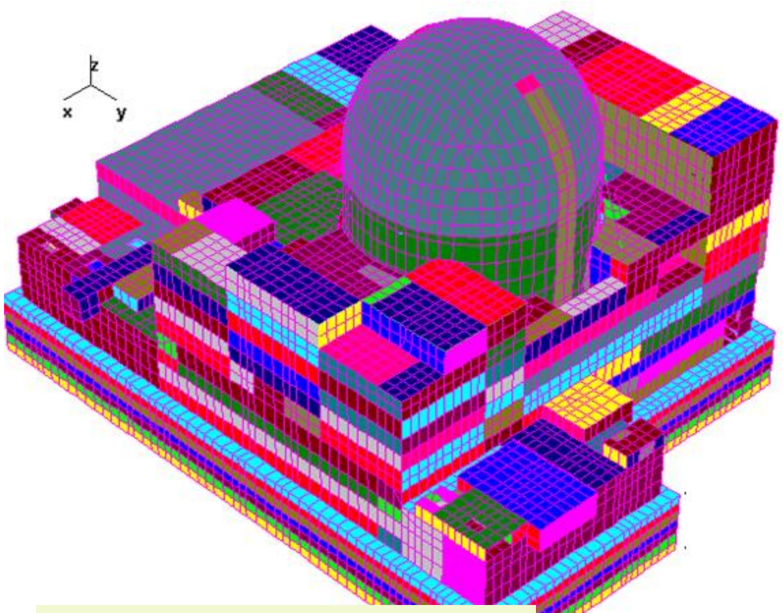

RB Complete SSI Model

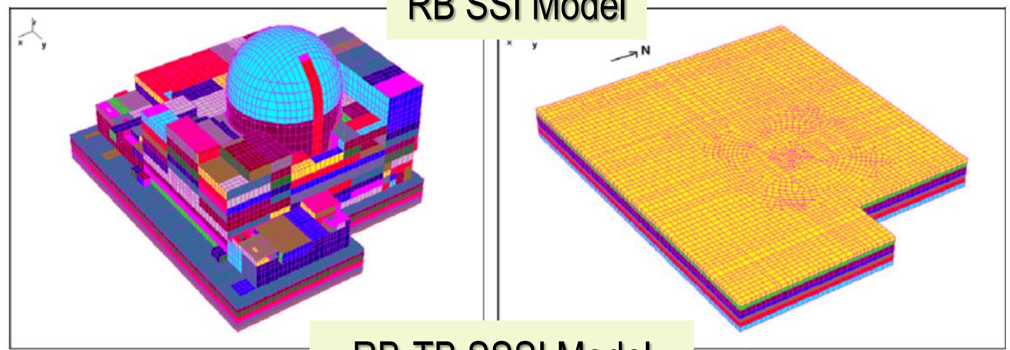

RB SSI Model

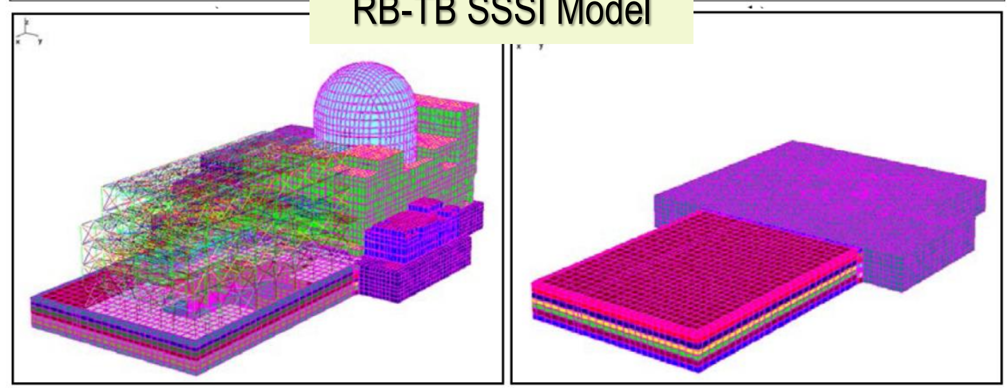

RB-TB SSSI Model

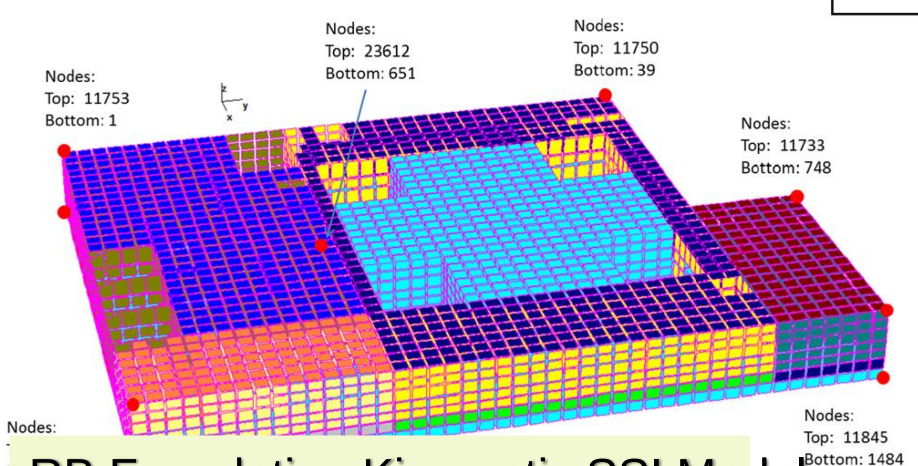

RB Foundation Kinematic SSI Model

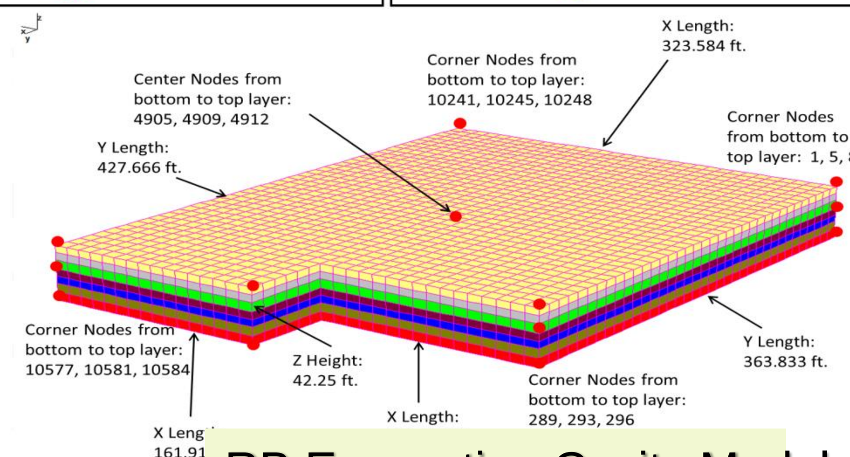

RB Excavation Cavity Model

Excavated Soil Vibration Using FVM, SM and MSM

Effects of Ground Surface Constraints on Scattered Surface Wave Solution

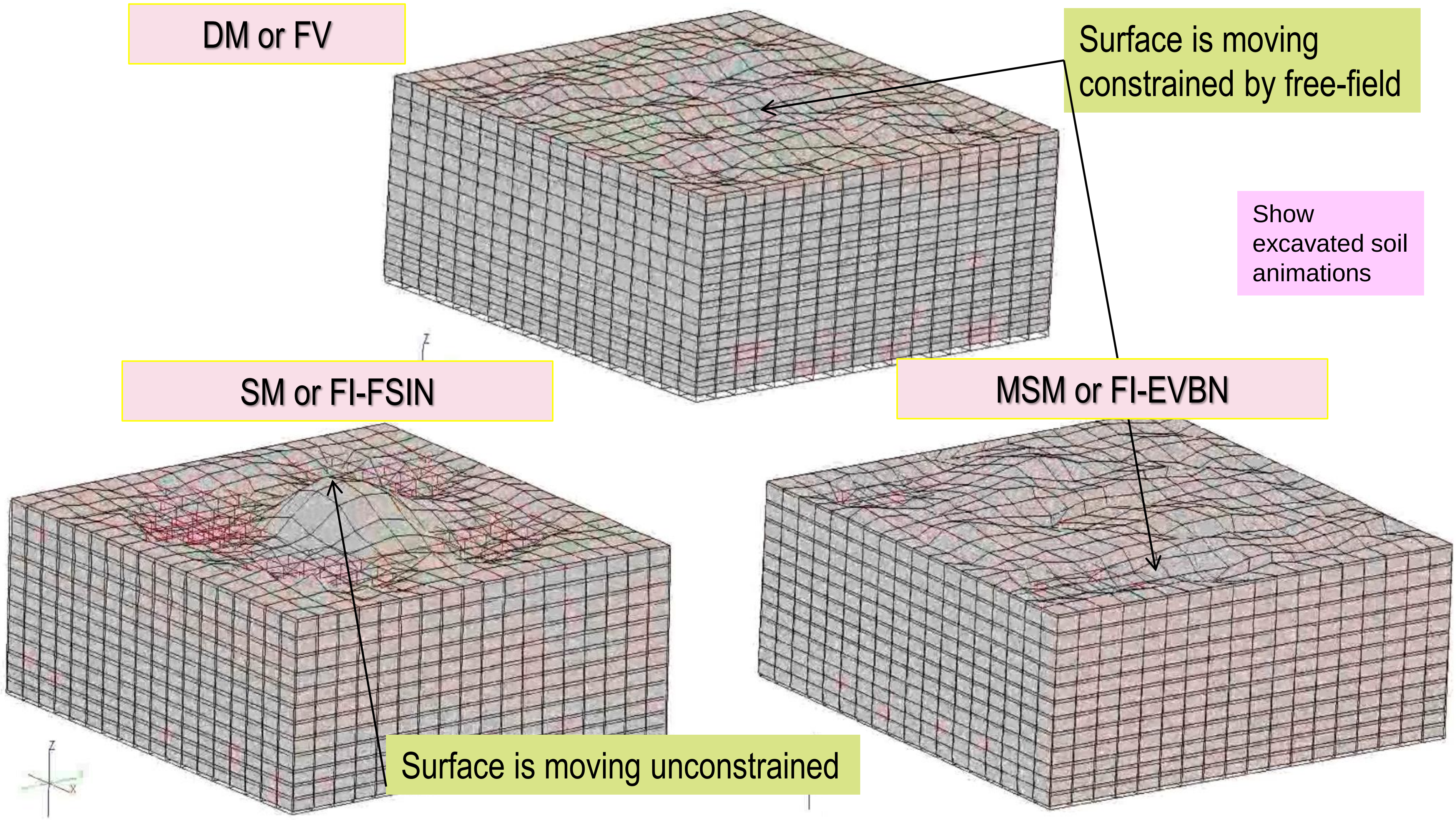

Show excavated soil animations

MSM Approach Failure for Deeply Embedded NI

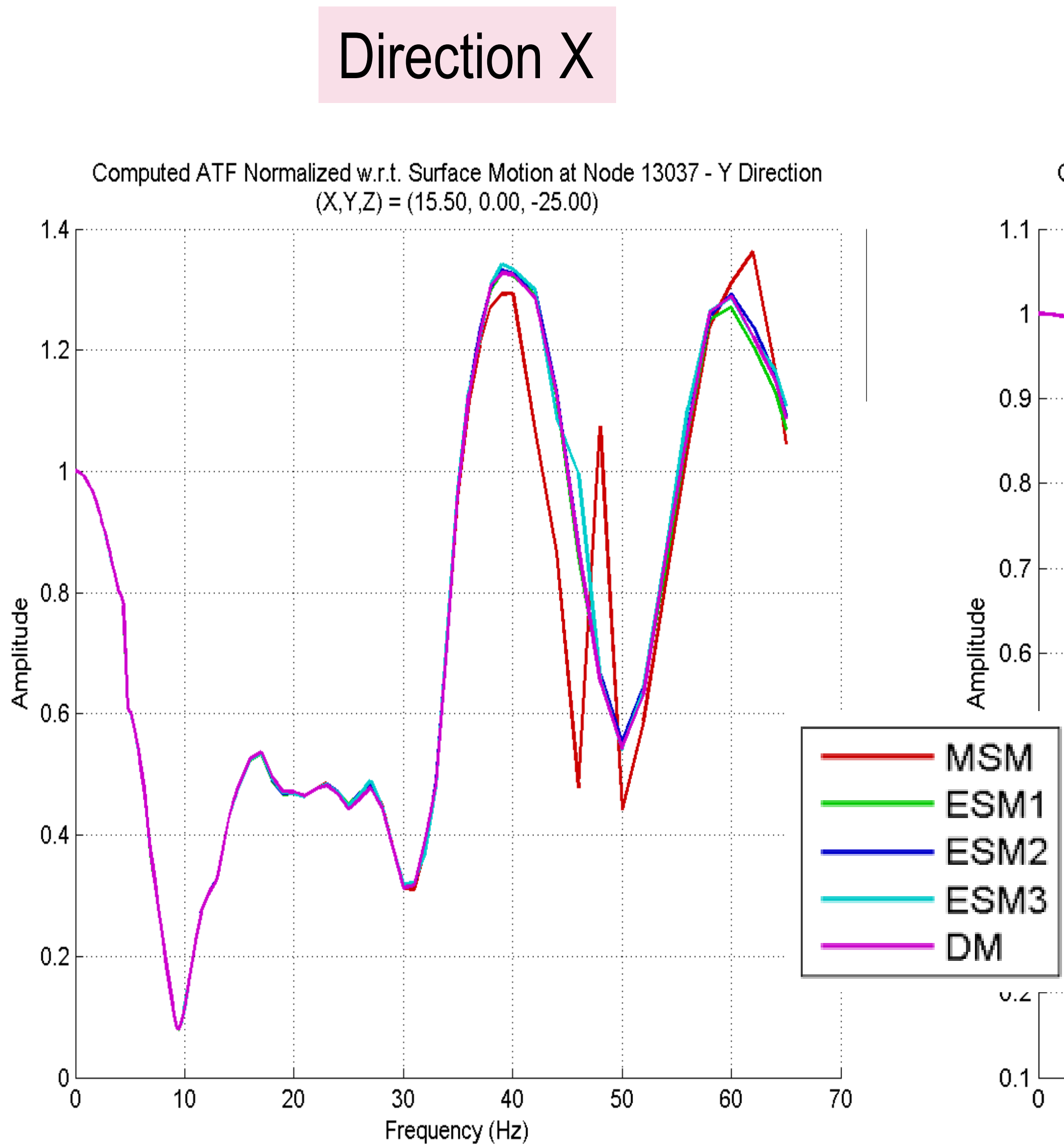

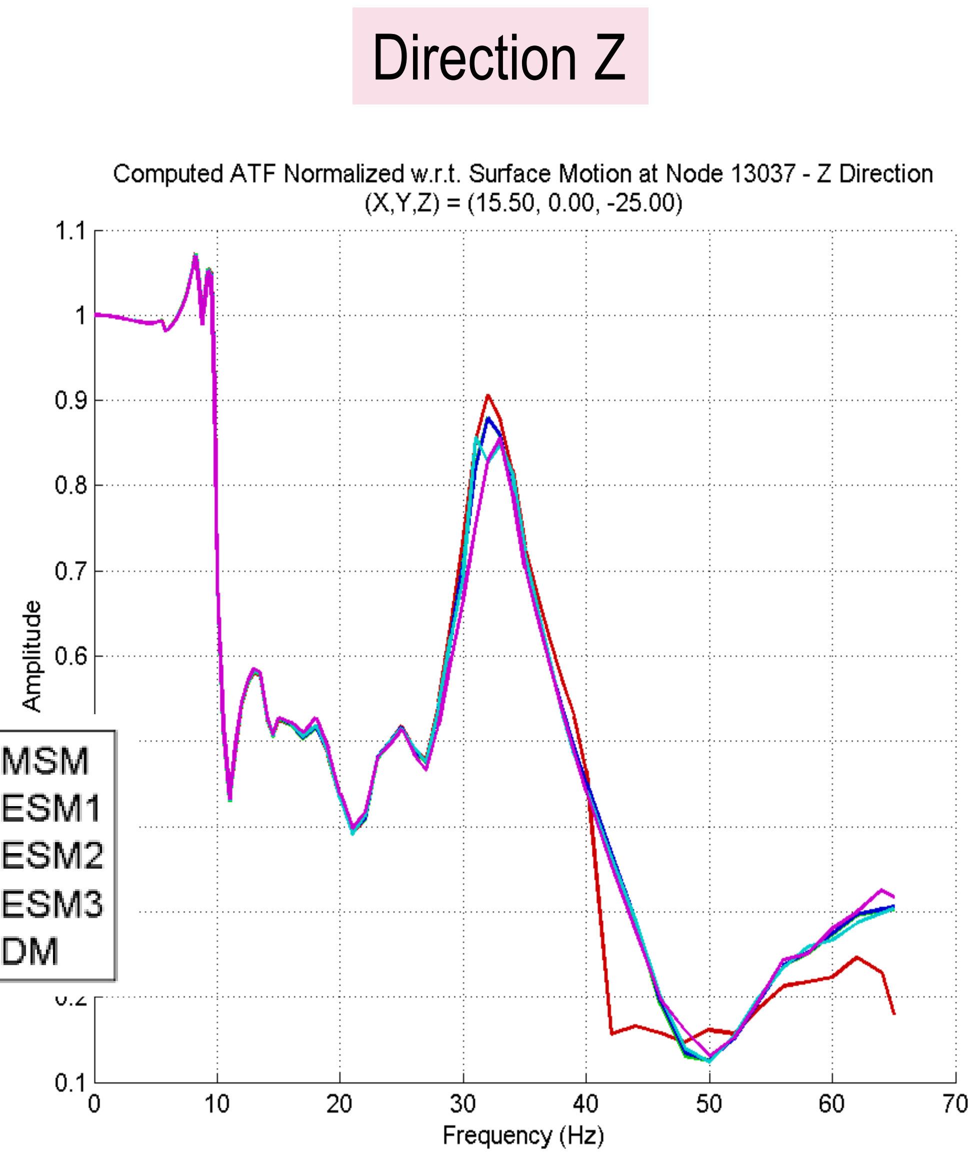

SMR Massless Foundation (Fully Embedded) Model

Volume Size: 120 ft x 80 ft x 80 ft

Model View

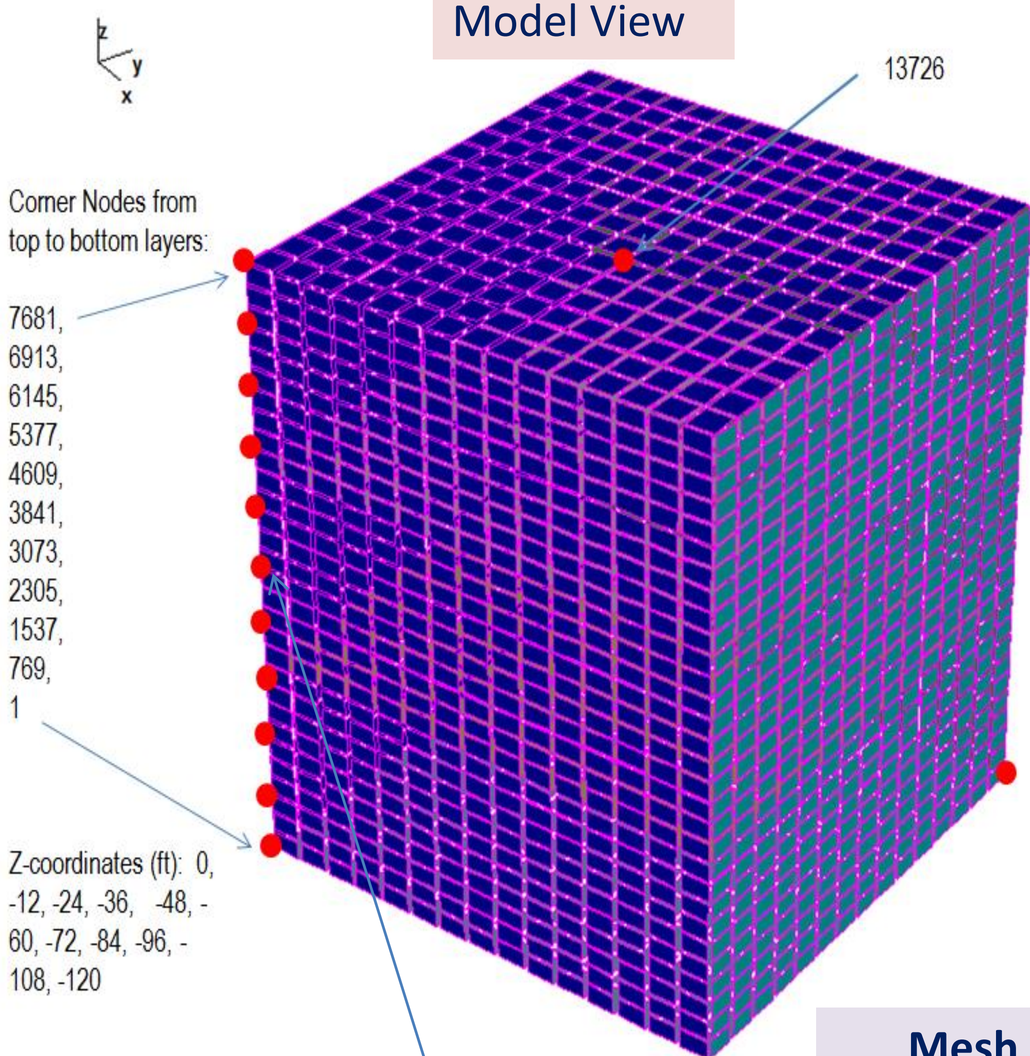

FFV-Skip 2 Levels

Vertical Section

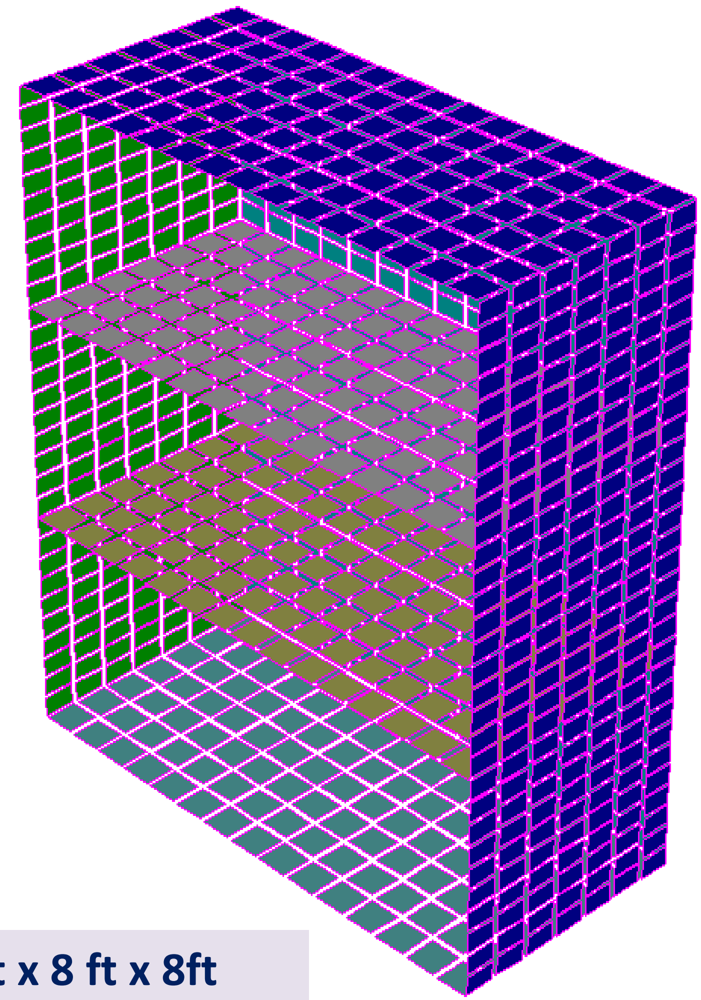

Mesh 4 ft x 8 ft x 8ft
7,938 Interaction Nodes

SMR Case Studies on FV Substructuring Methods

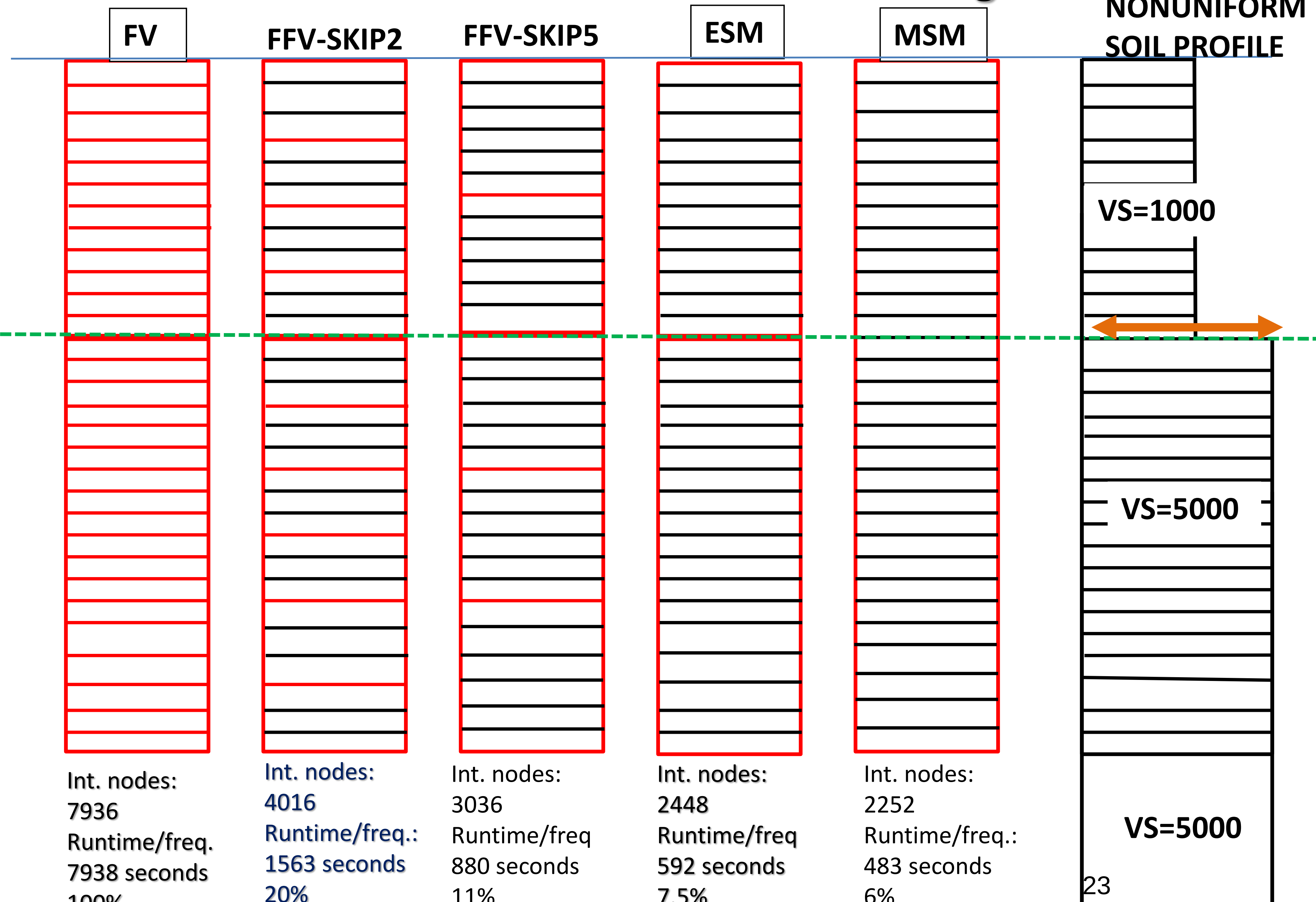

FV	FFV-SKIP2	FFV-SKIP5	ESM	MSM
Int. nodes: 7936	Int. nodes: 4016	Int. nodes: 3036	Int. nodes: 2448	Int. nodes: 2252
Runtime/freq. 7938 seconds	Runtime/freq.: 1563 seconds	Runtime/freq 880 seconds	Runtime/freq 592 seconds	Runtime/freq.: 483 seconds
100%	20%	11%	7.5%	6%

Comparative ATF at -32 ft Depth (1/4 of Embedment)

Direction X

Direction Z

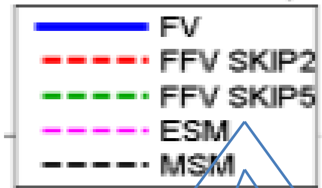

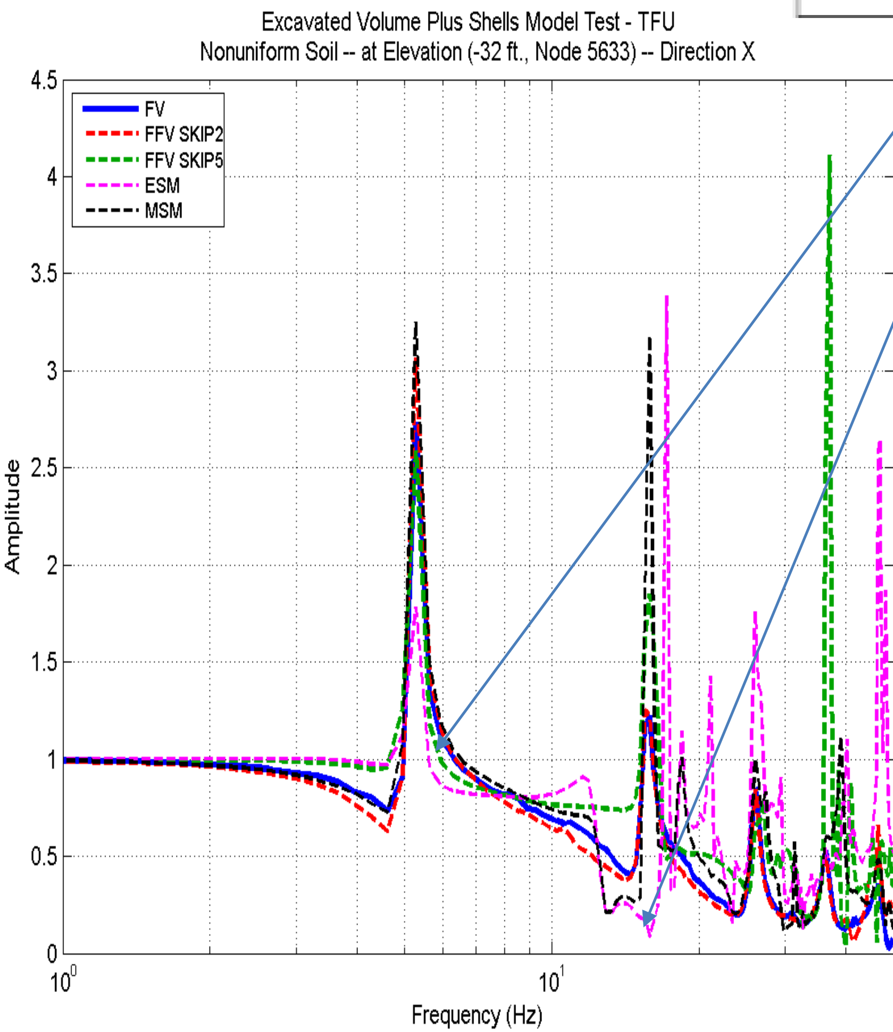

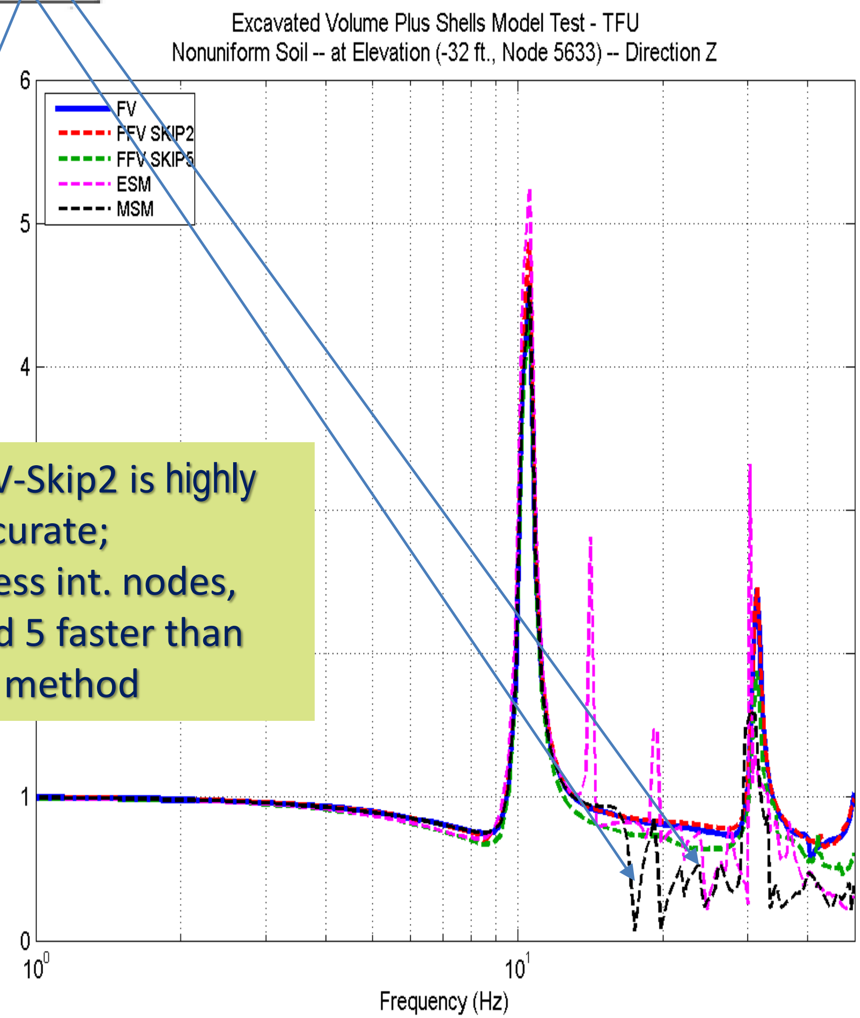

FFV-Skip2 is highly accurate;
5 less int. nodes, and 5 faster than FV method

SASSI Substructuring for Nuclear Islands

- MSM is a highly accurate and robust SSI approach for large-size embedded foundations, as nuclear island (NI) complex foundations. MSM is much more robust than SM.

- MSM could break down for deeply embedded foundations on a case-by-case basis.

Transition Mesh Zones Are Necessary for DES to Get A Regular Mesh Excavated Soil FE Model

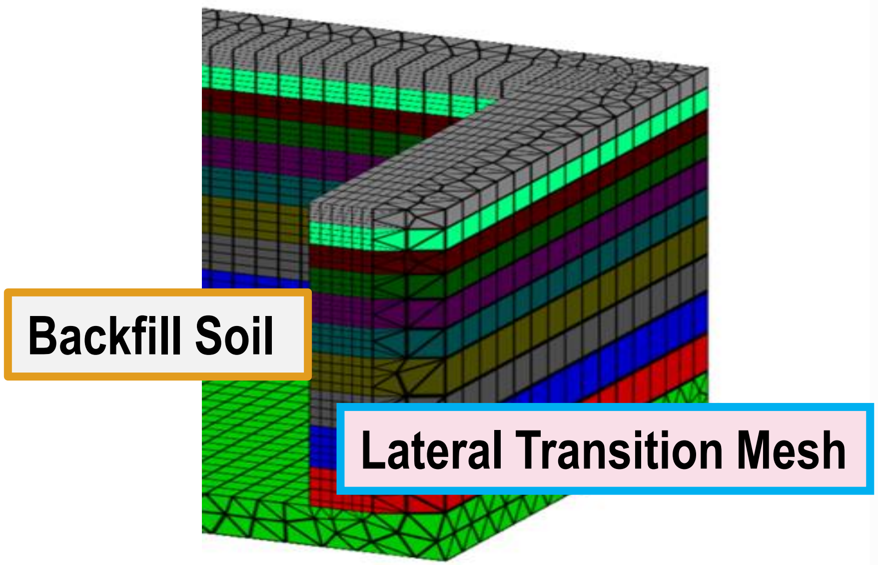

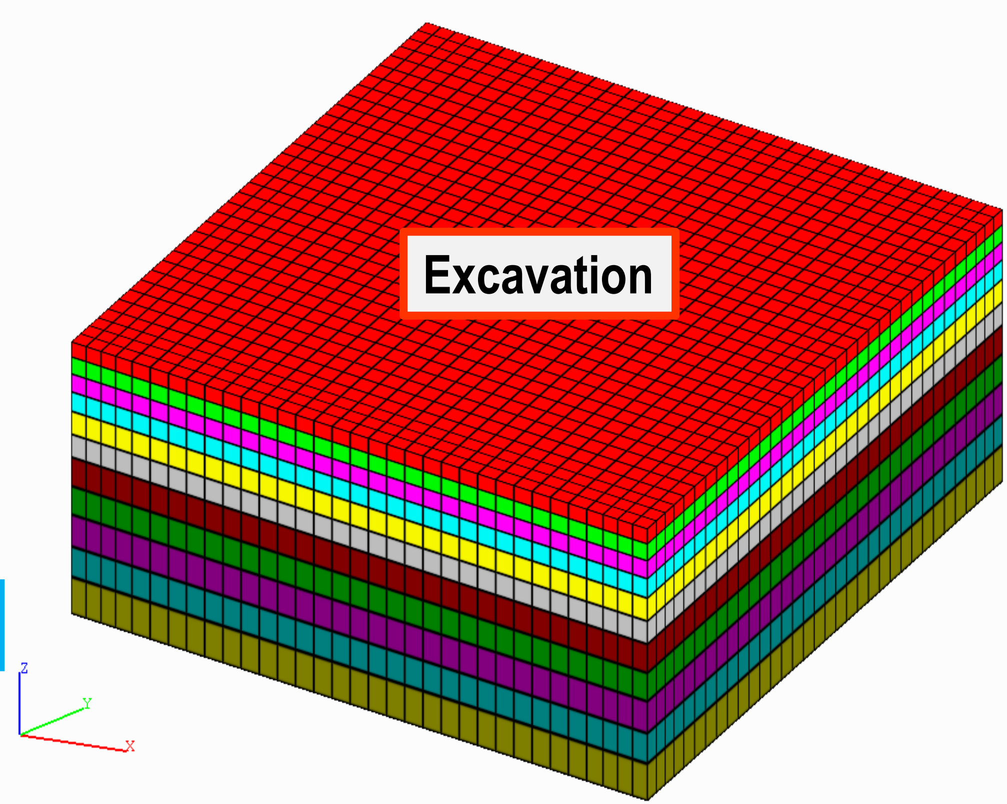

Regular uniform mesh excavation FE models capture accurately the high-frequency wave scattering effects. Also ensures much more efficient SSI runs (less int. nodes). *(Brookhaven National Lab Report BNL-102434 by USNRC BNL Consultants, by Nie et al., 2013)*

RB Complex Pile Foundation Example Includes More Then 200,000 FE Mesh Nodes (10,000/level)

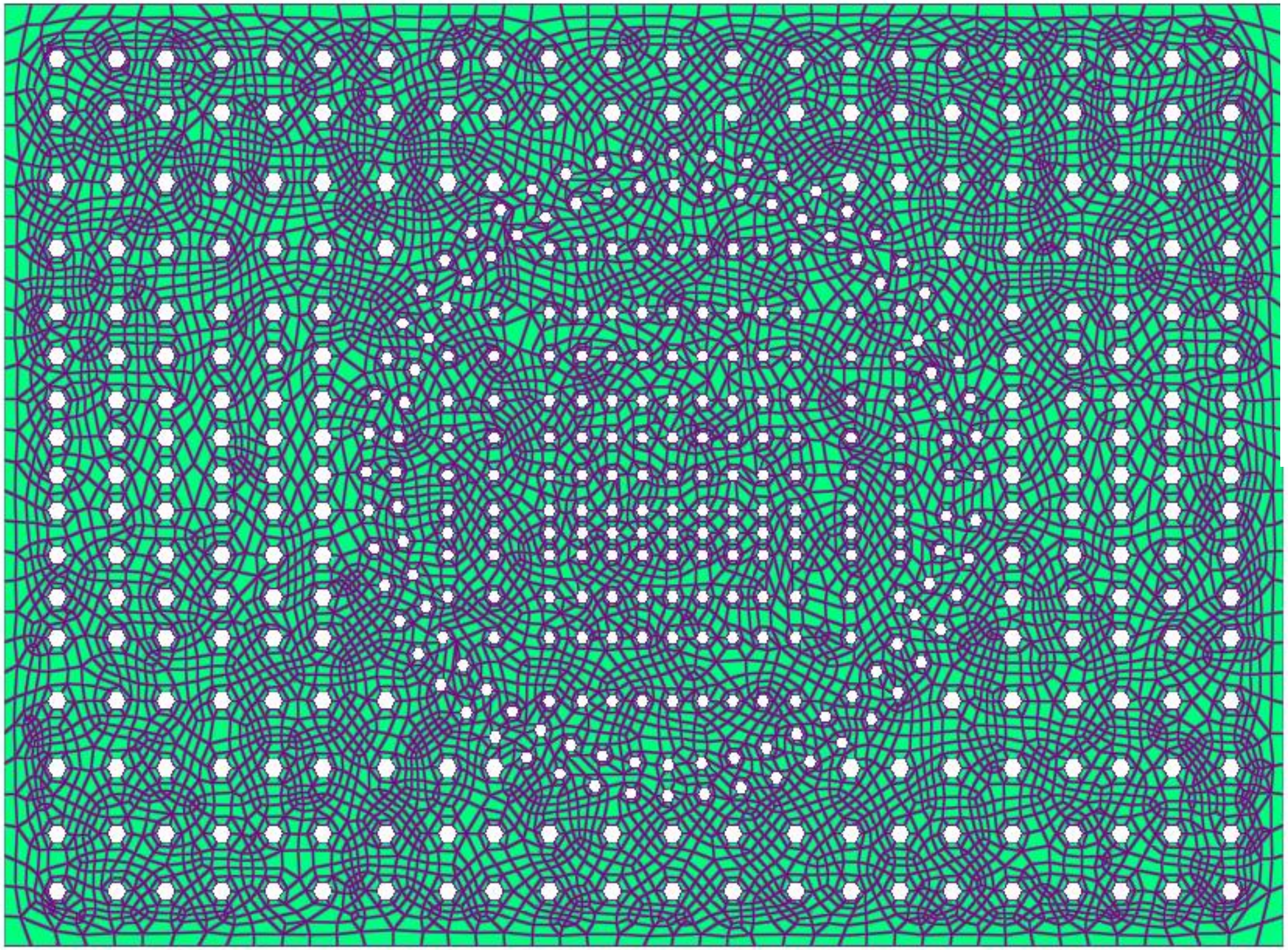

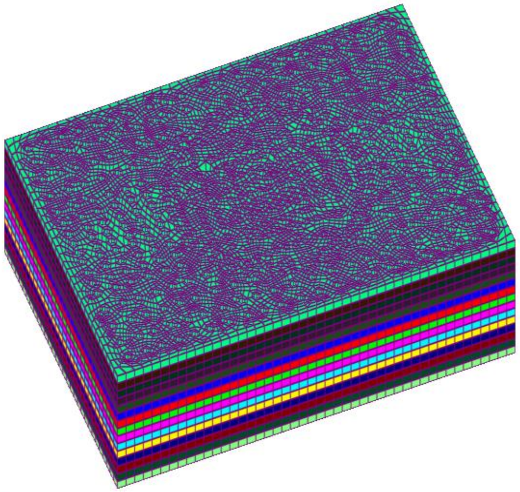

SSI runtime was about 2,600 sec. per frequency on a 128 GB RAM MS Windows PC

BROOKHAVEN NATIONAL LABORATORY

BNL-102434-2013

Seismic Soil-Structure Interaction Analyses of a Deeply Embedded Model Reactor – SASSI Analyses

J. Nie, J. Braverman, M. Costantino

October 2013

Therefore, it is recommended to pursue further improvements in the frequency domain codes in parallel to the ongoing research to develop and benchmark the time domain codes. Some of the key improvements are listed below:

(1) Re-establish/develop a modern, modularized (pluggable for incorporating future capabilities), and parallel code base for SASSI;
(2) "Profile" the code (i.e., analyze the efficiency of various parts of the code) and optimize the code to expedite the execution speed;
(3) Implement/automate certain capabilities based on industry guidelines for using SASSI (e.g., addressing the need for regular excavated soil mesh for any reasonable finite element structural model, approximating local soil nonlinearity, automating the treatment of soil layering, implementing advanced data management, etc.);
(4) Investigate the number-theoretic (e.g., GLP) enhanced subtraction method (ESM, which was proposed and briefly tested in this study); and
(5) Incorporate methods to consider uncertainties in soil properties.

SMR Excavation Mesh Nonuniformity Study

Volume Size: 200 ft x 100 ft x 100 ft

140 ft Embedded SMR Model

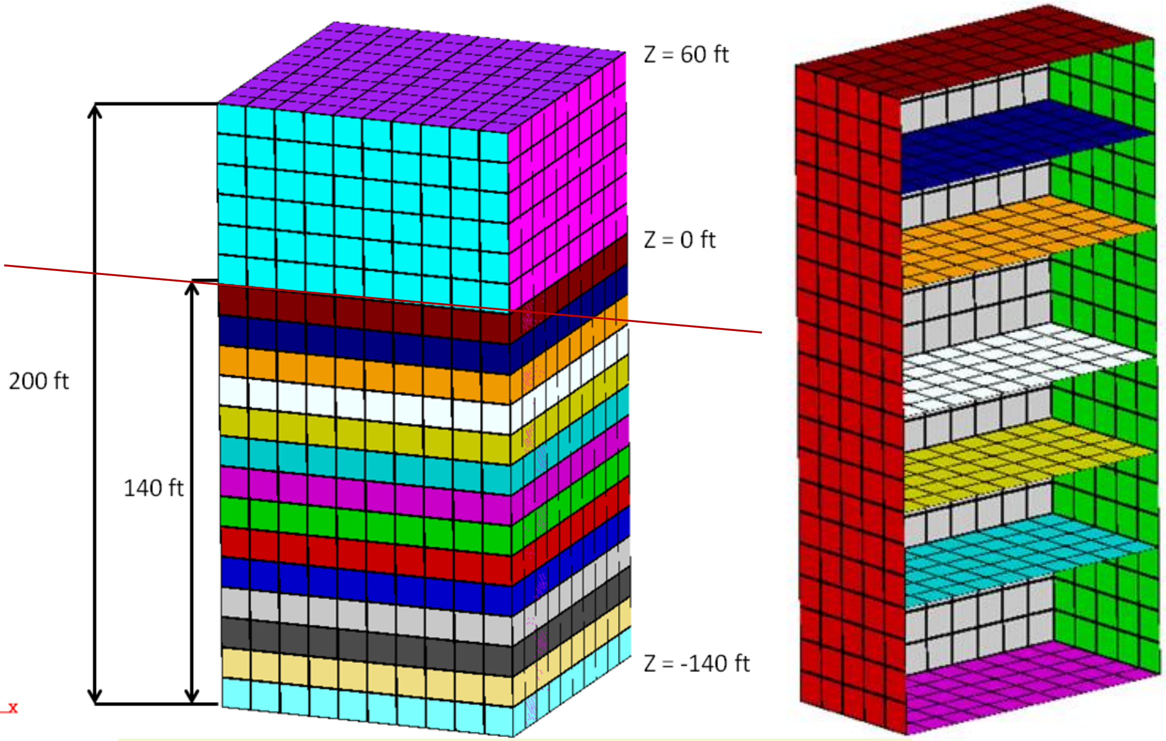

SMR size: 100 ft x 100 ft X 200 ft
Embedment: 140 ft
Mesh size: 10 ft X 10 ft X 10 ft
Number of Nodes: 2,580
Interaction Nodes: 1,815

Vs Soil Profile (fps)

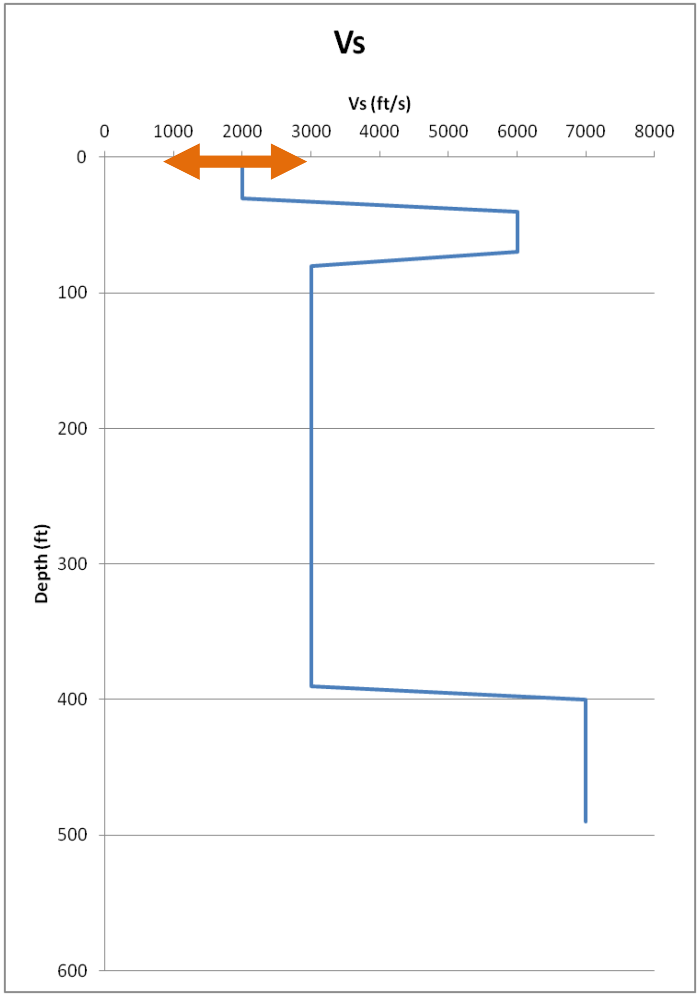

140 ft Embedment SMR Excavation Meshes

Uniform Model

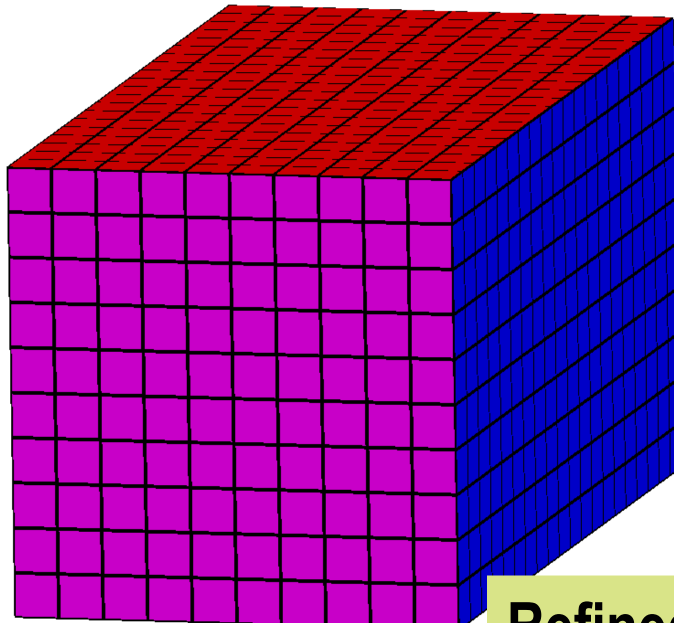

For nonuniform meshes the average radius values are used.

Non-uniform Model

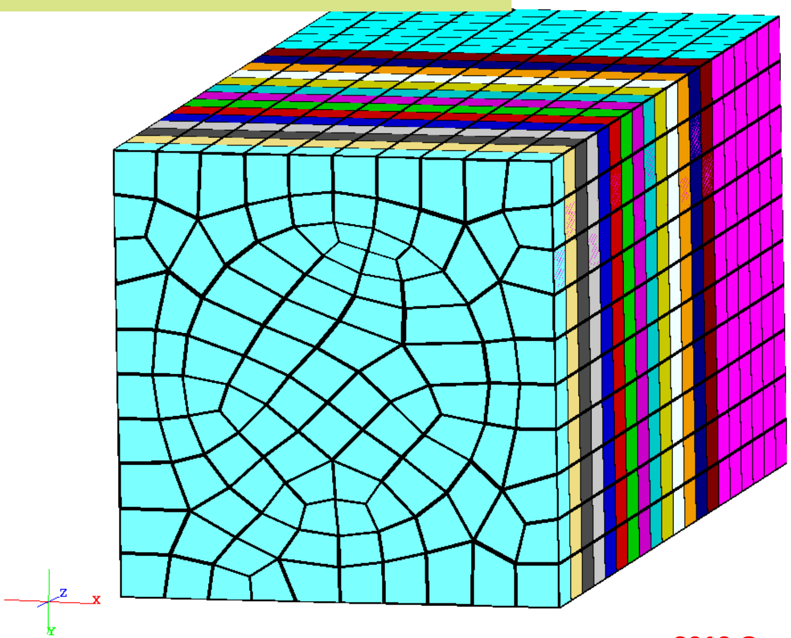

Refined Non-uniform Model

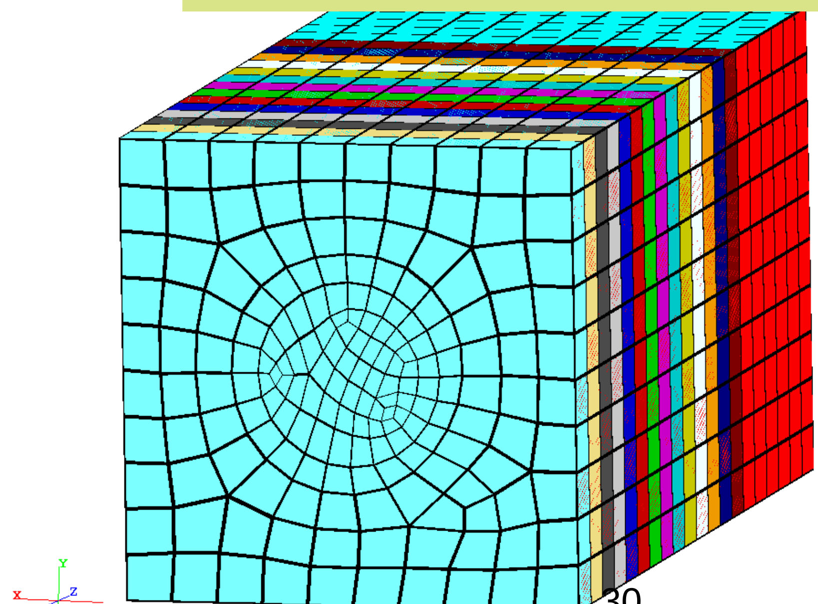

1

Effects of Excavation Volume Meshing. Uniform Mesh vs. Nonuniform Mesh

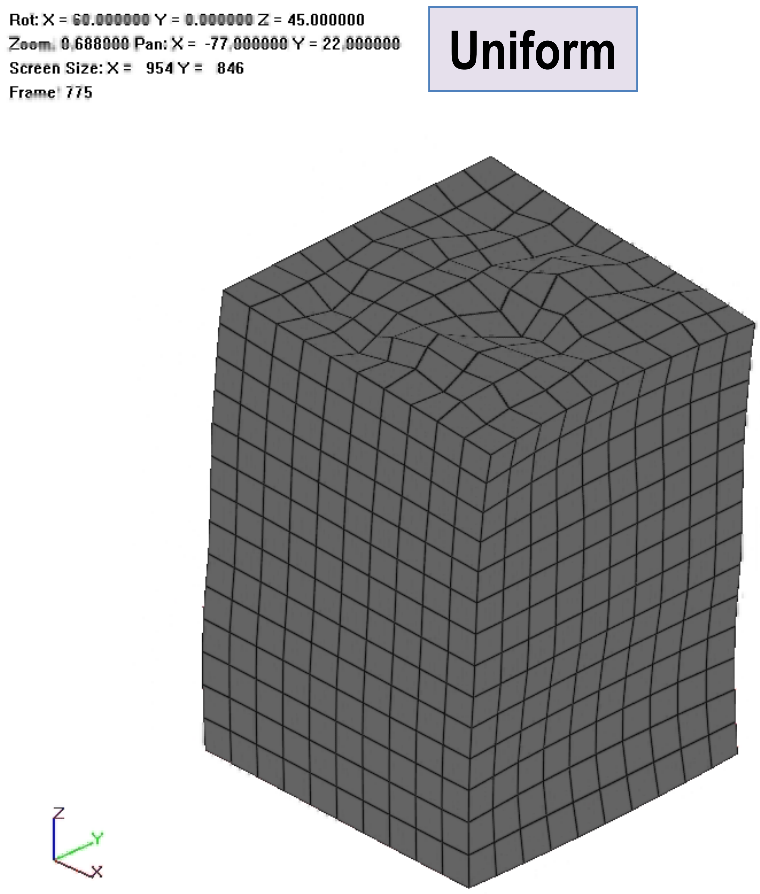

HORIZONTAL

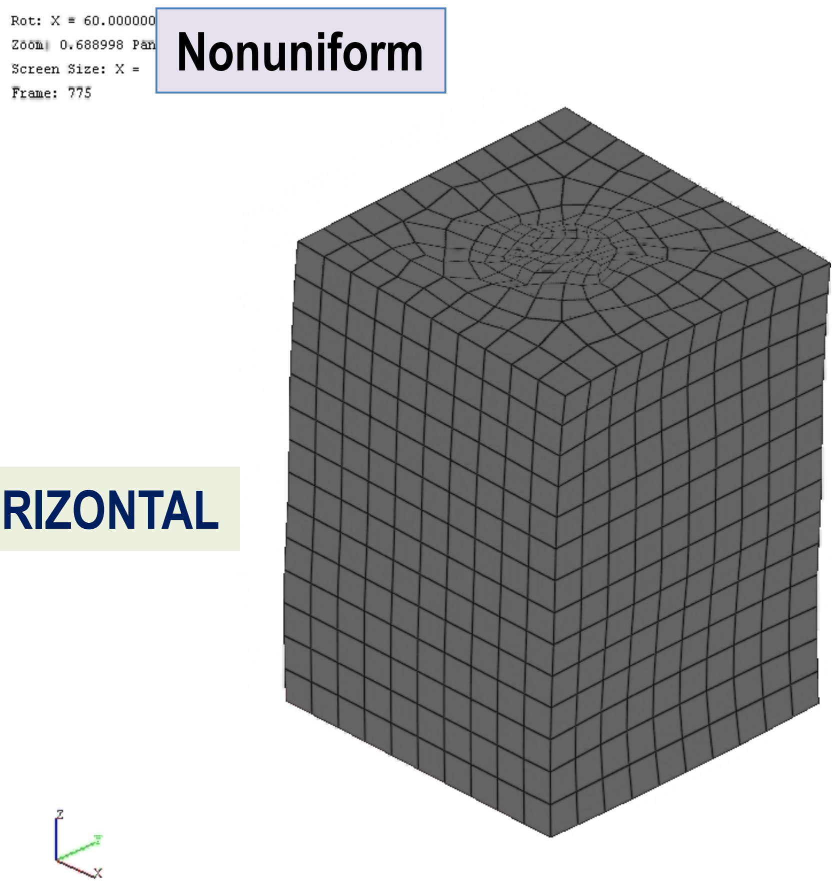

Regular uniform mesh captures correctly the high-frequency wave scattering effects.

Effects of Excavation Volume Meshing. Uniform Mesh vs. Nonuniform Mesh

Uniform

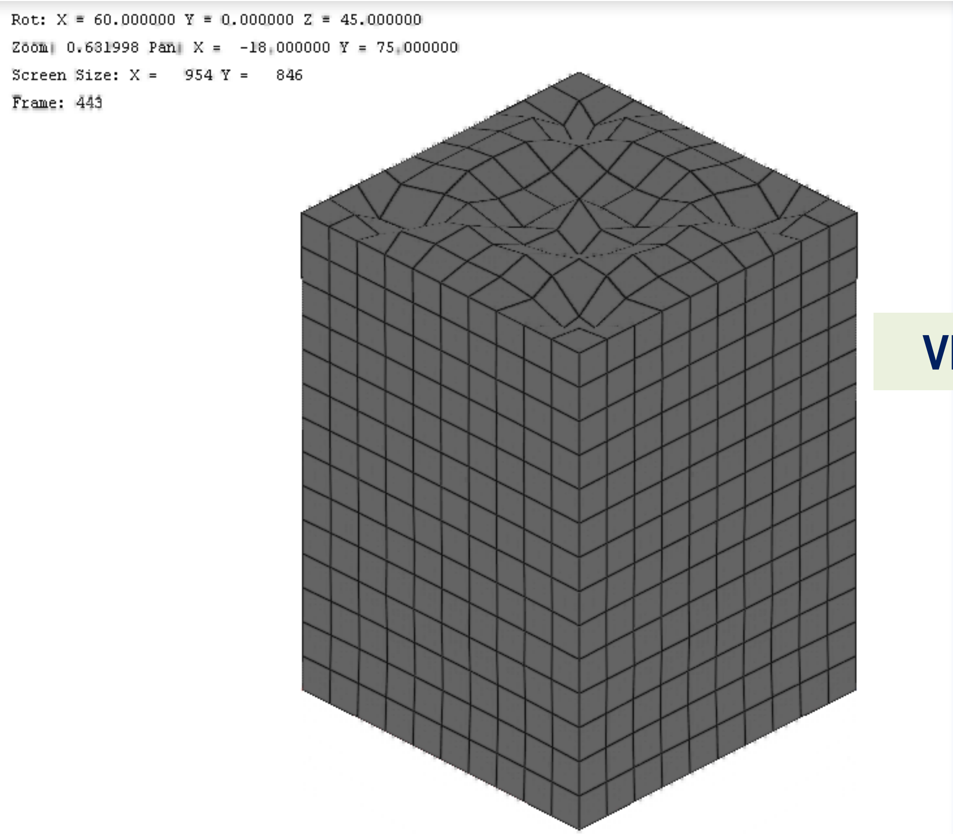

VERTICAL

Nonuniform

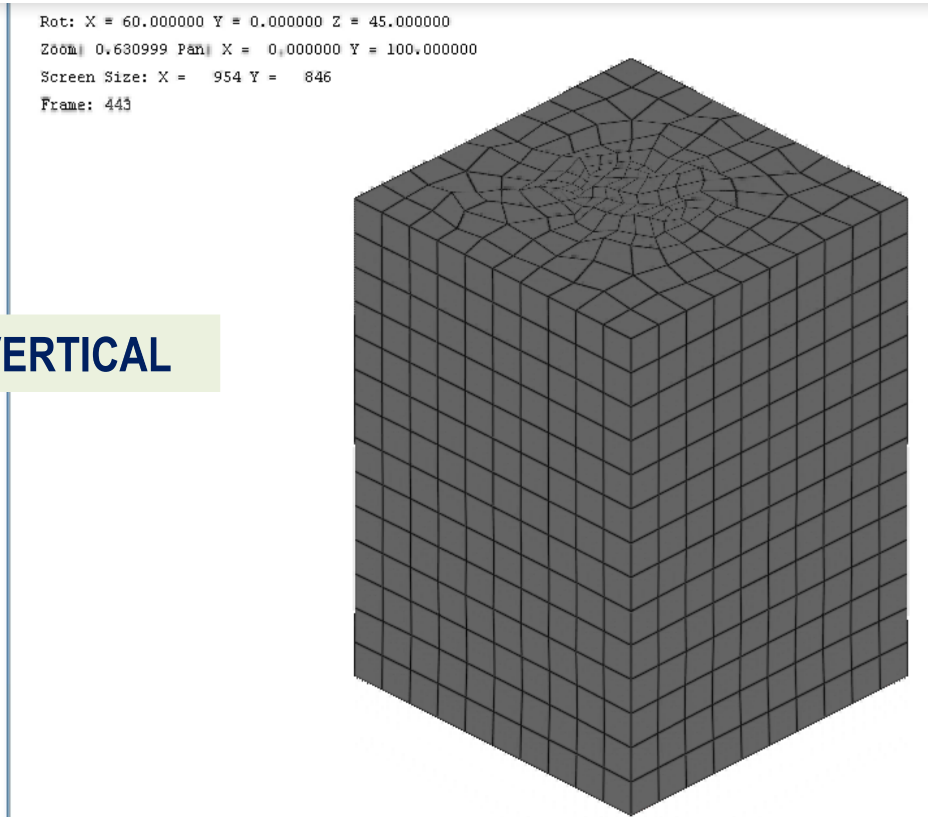

Regular uniform mesh captures correctly the high-frequency wave scattering effects.

SMR Massless Foundation Excavation Mesh Size Study

Volume Size: 120 ft x 80 ft x 80 ft

Original

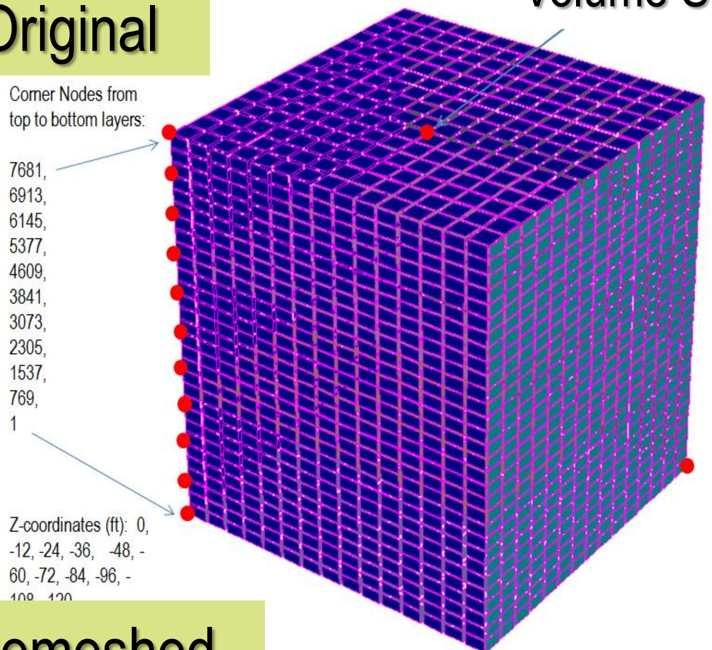

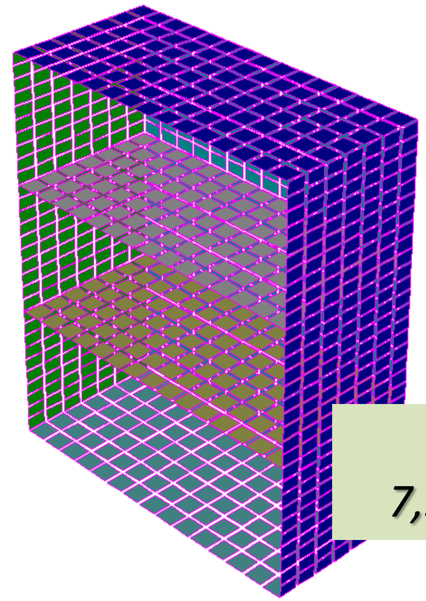

Uniform soil
Vs=1000 fps;

Input at Surface

Mesh 4 ft x 8ft x 8ft
7,938 Interaction Nodes

Remeshed

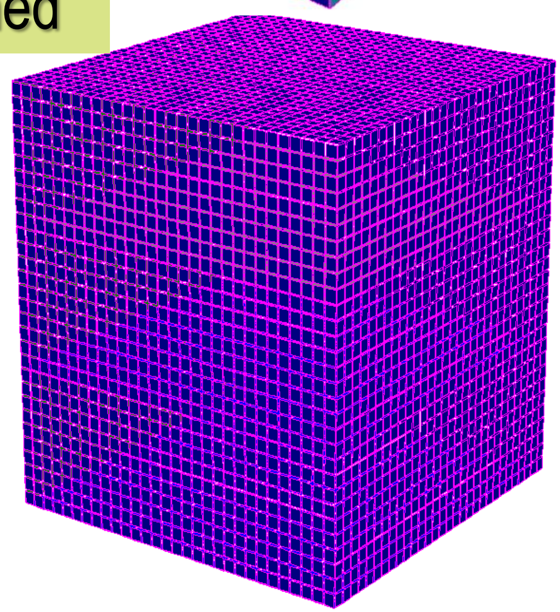

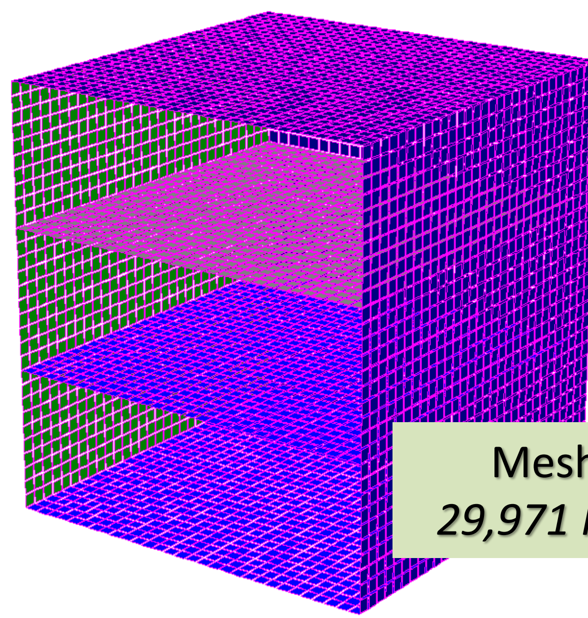

Mesh 4 ft x 4ft x 4ft
29,971 Interaction Nodes

Comparative ATF at Foundation and Surface Levels

120 ft Depth

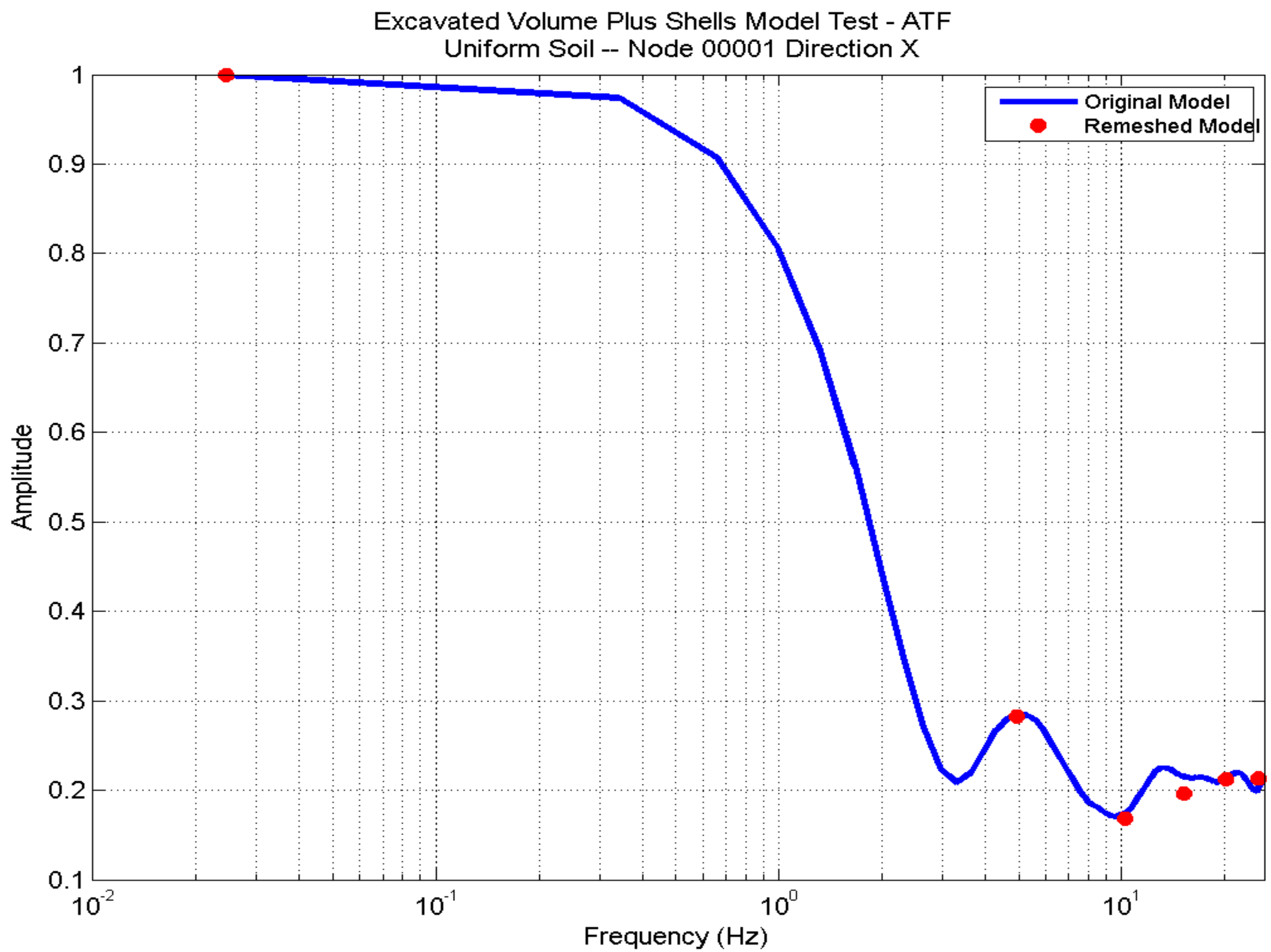

Non-Uniform Soil Insertion Embedment Problem

Large Size Excavation (480ftx360ftx160ft)

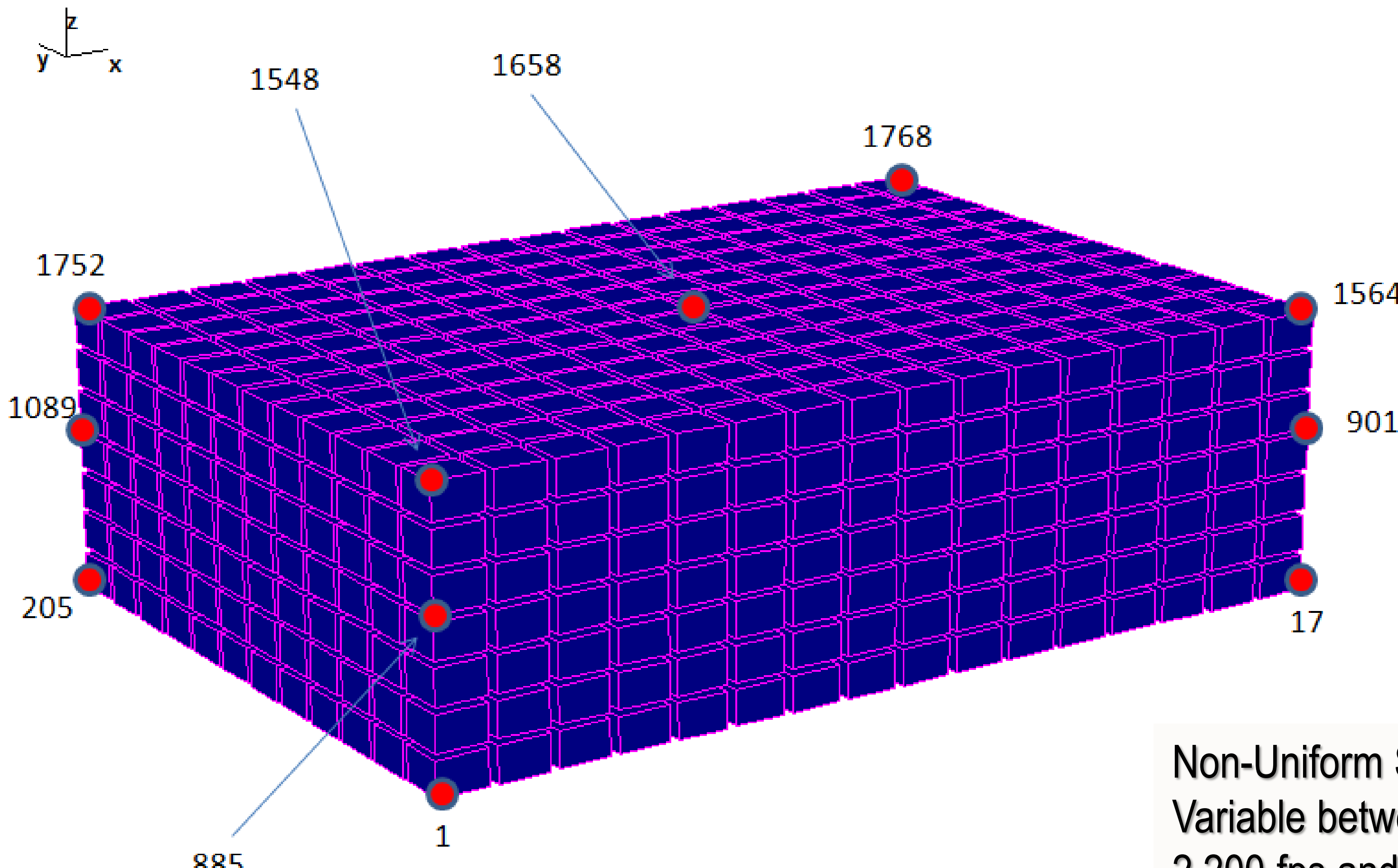

Non-Uniform Soil,
Variable between
2,200 fps and 6,000fps,
EPRI HF Seismic Input

Excavated Soil Mesh Size = 30ft x 30ft x 20ft
Max. Trans. Frequencies = 15 Hz, 15 Hz and 22.5Hz
Cut-off Frequency = 25 Hz

Highly Non-Uniform (Soil Insertion) Embedment Problem Vs Soil Profiles for the 480ft x 320ft Horizontal Area

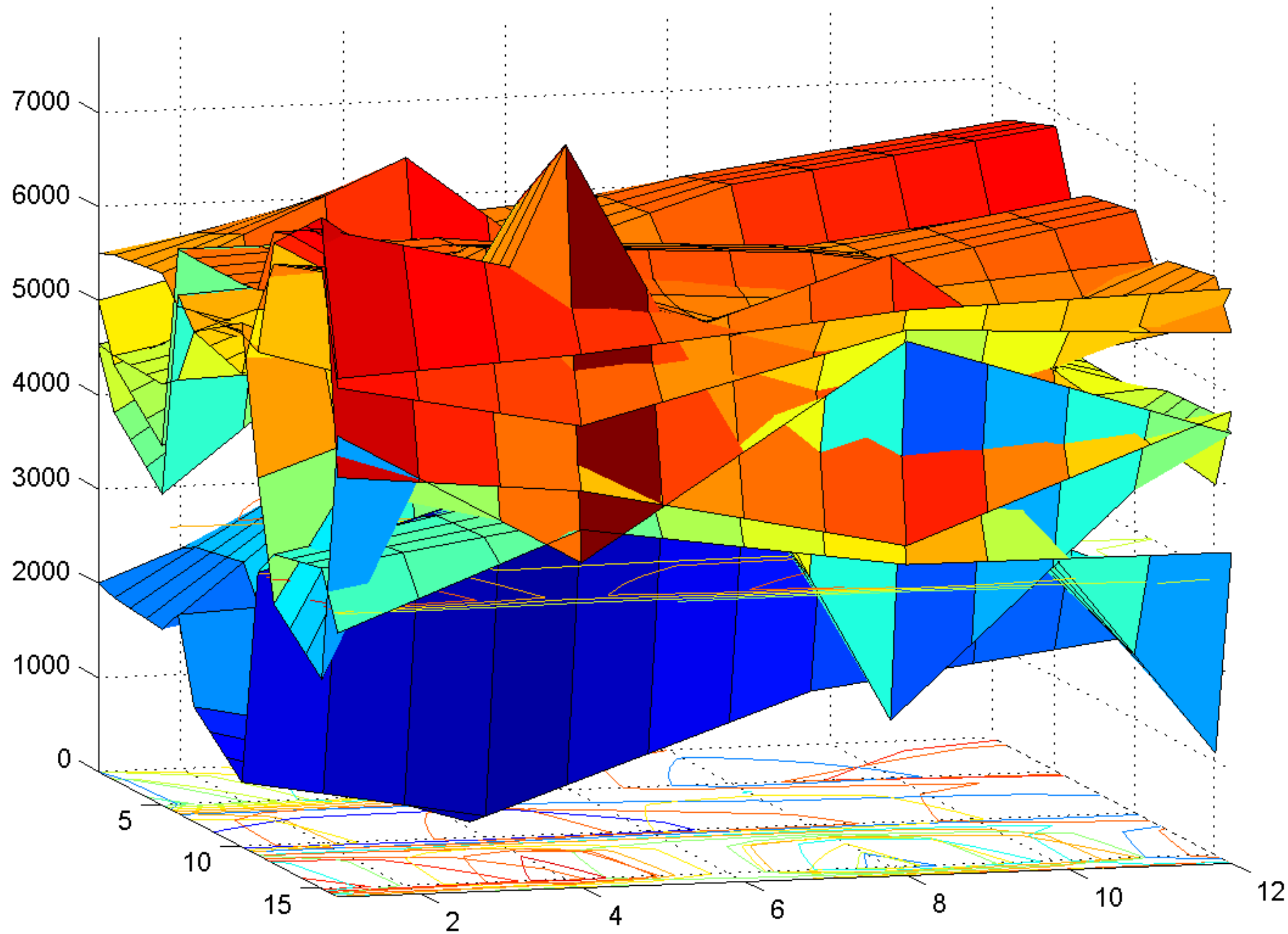

Soil Profiles at the Four Excavated Soil Corners

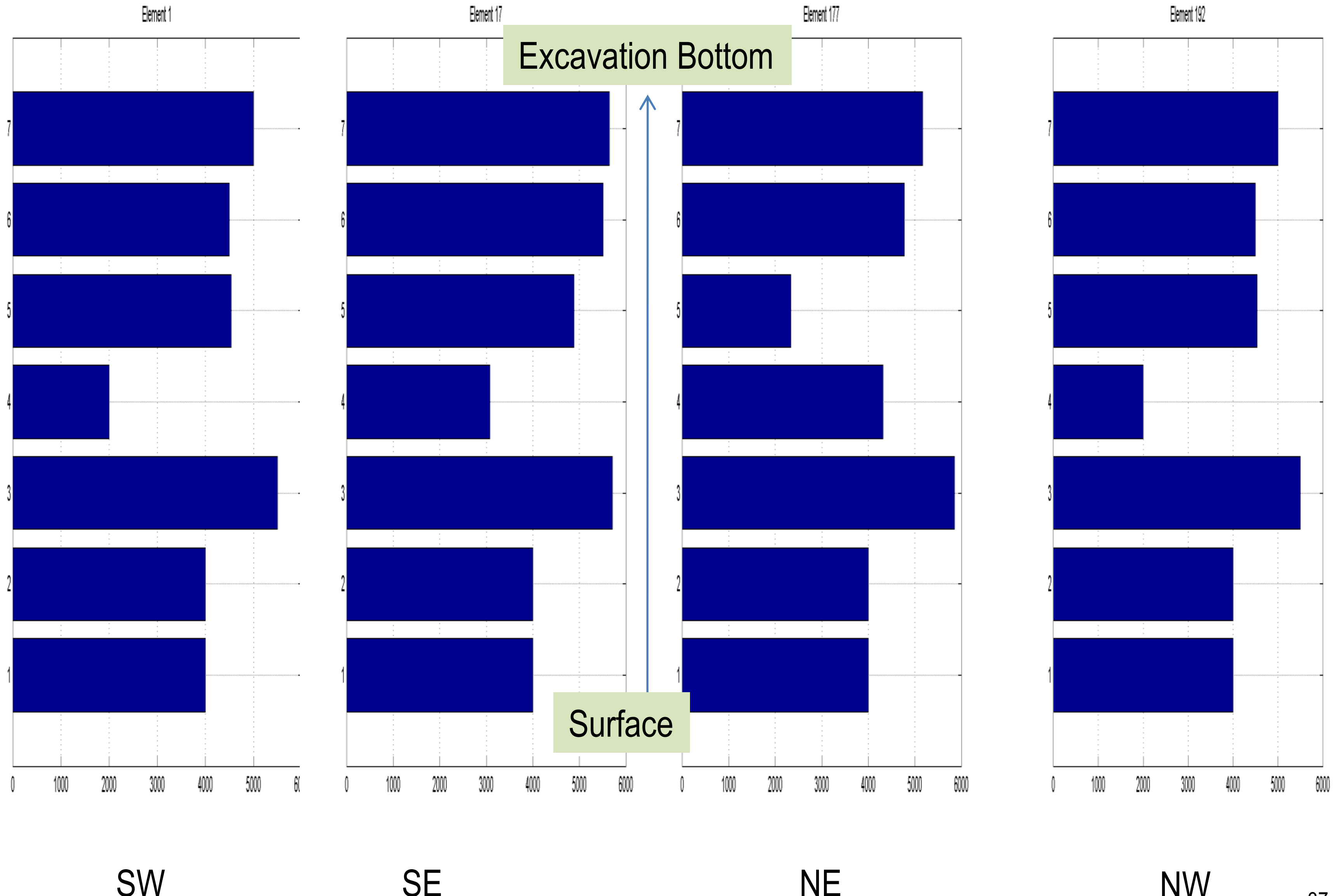

Soil Profiles at Center and Two Excavated Soil Corners

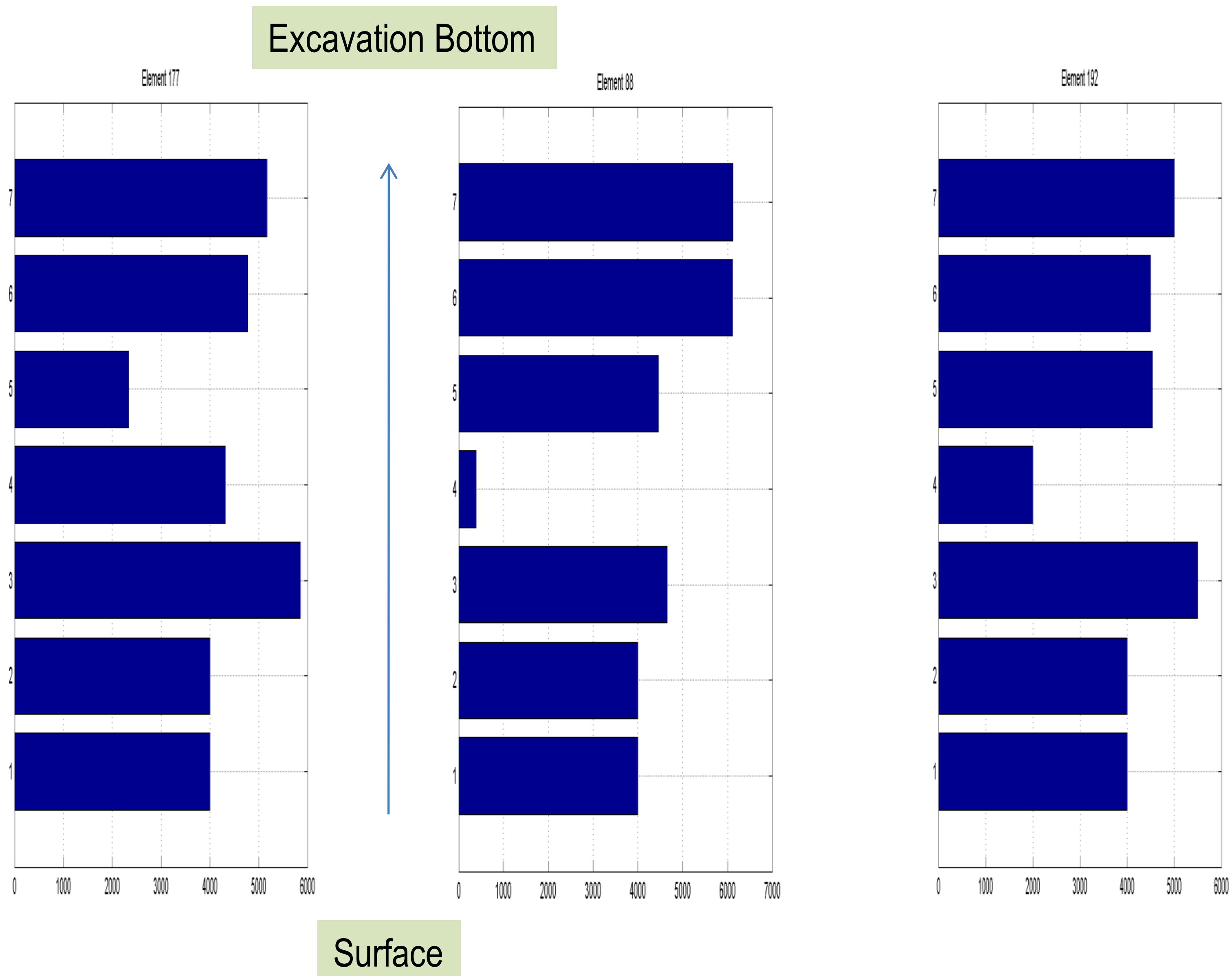

Bottom Corner and Center – SM (FI) vs. MSM (FIT) vs. FV Methods

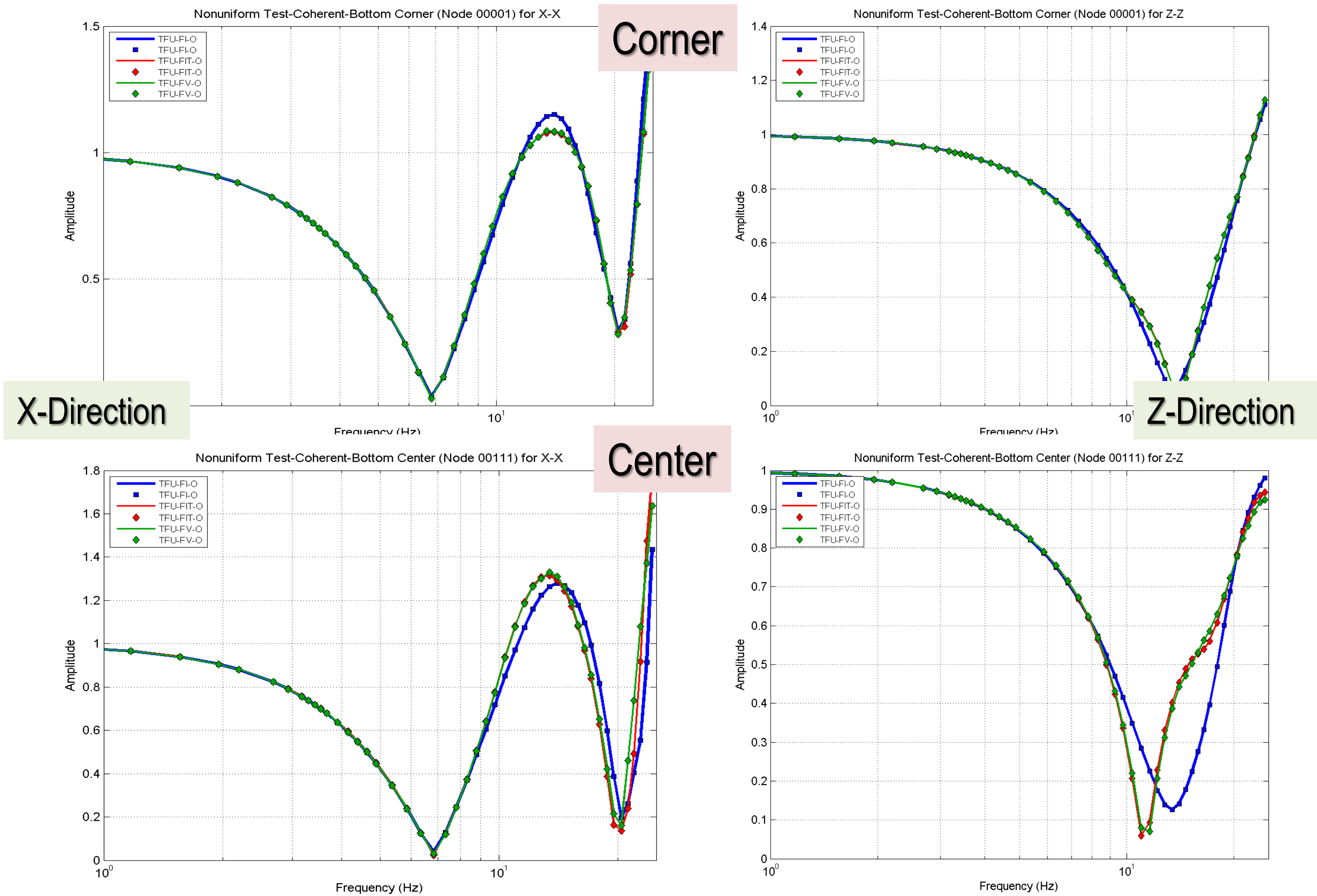

Top Corners - SM (FI) vs. MSM (FIT) vs. FV Methods

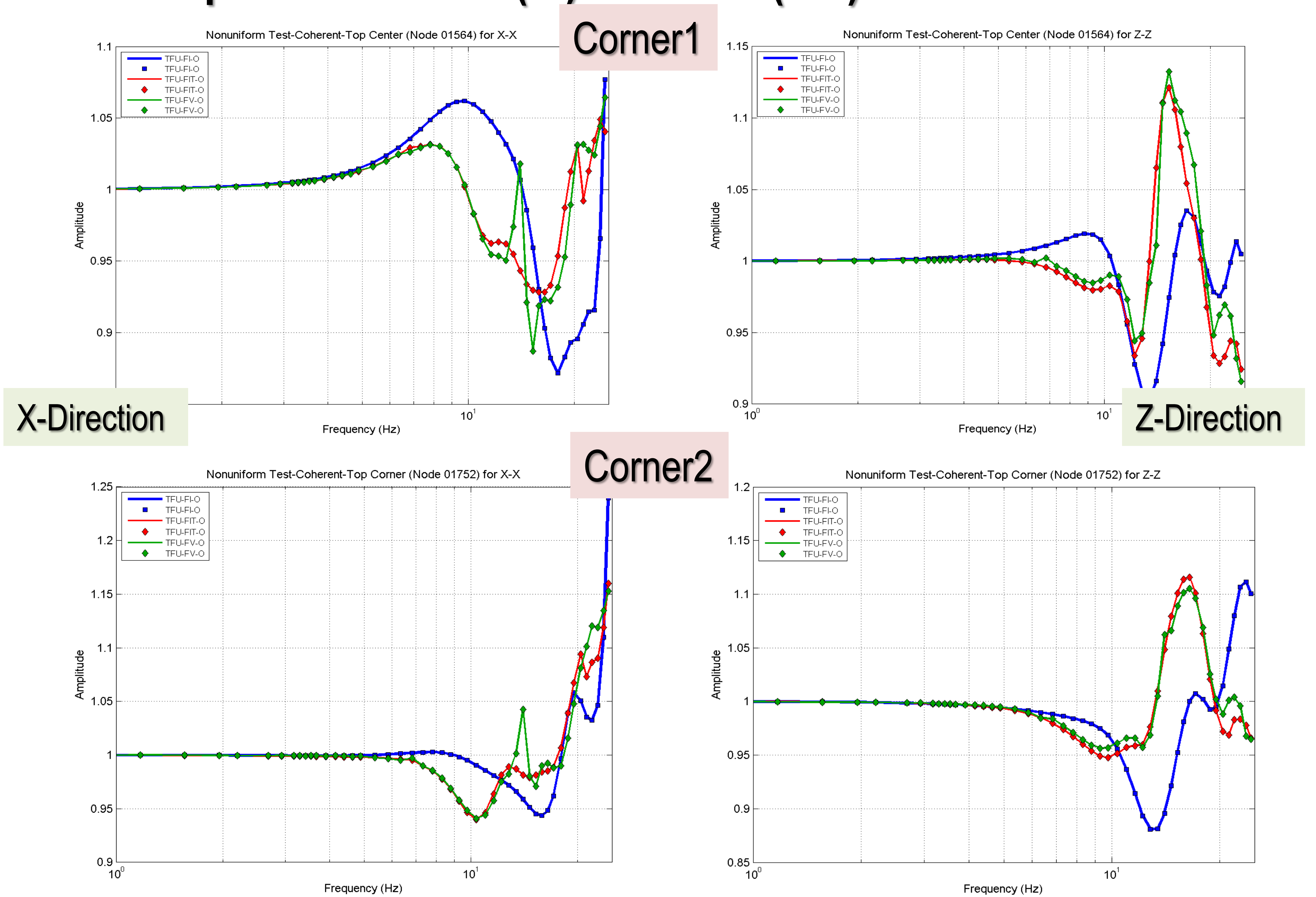

Remarks on SASSI Excavated Soil Modeling

- The MSM approach (interaction nodes on outher surface) is expected not to work well for DES and SMR for high frequencies
- Element size should be sufficiently refined in vertical and horizontal directions to capture highest frequency wave components. Sensitivity studies for horizontal size are recommended.
- The excavated soil mesh should be a regular, uniform mesh to accurately model the wave scattering effects in high-frequency. Need to use transition mesh zones. For regular meshes no need for sensitivity studies on the point load radius size for soil impedance calculations.

3. ACS SASSI Motion Incoherency Modeling

Content:

1) Explanation of Motion Incoherency
2) ACS SASSI Mathematical Modeling and Implementation
3) Typical Application of Incoherent SSI Analysis

1) Explanation of Motion Incoherency

COHERENT

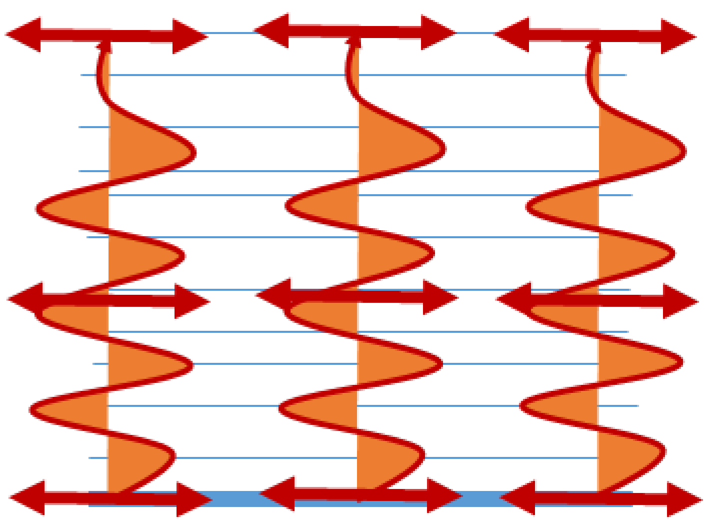

IDEALISTIC MOTION
(1D DETERMINISTIC WAVE MODEL)

Assume vertically propagating S and P Waves in horizontal soil layering

INCOHERENT

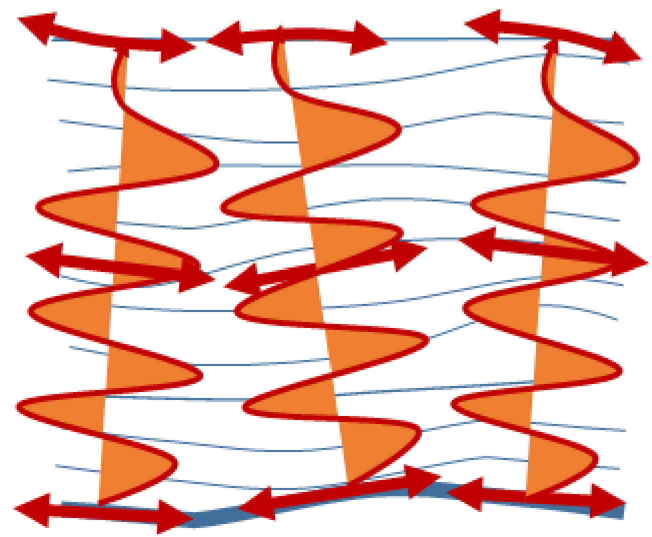

REALISTIC MOTION
(3D RANDOM WAVE MODEL)

Based on stochastic models developed from real record dense array databases (Chiba, Lotung, Pinyon Flat, etc.)

Coherent vs. Incoherent Wave Propagation Models

3D Rigid Body Motion (Idealized)

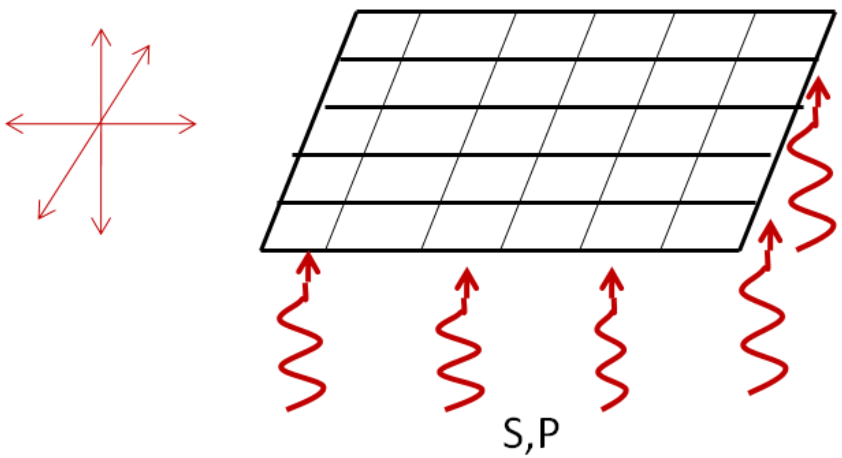

3D Random Wave Field Motion (Realistic)

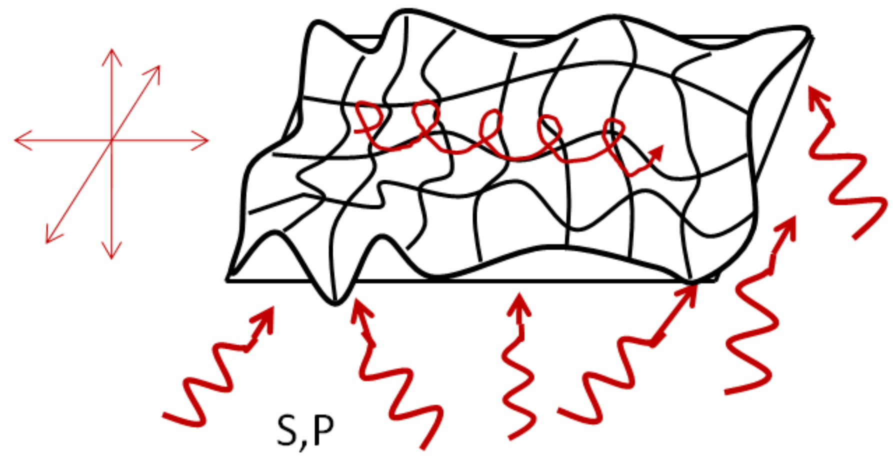

1 D Wave Propagation Analytical Model (Coherent)

- Vertically Propagating S and P waves (1D)

- No other waves types included

- No heterogeneity random orientation and arrivals included

- Results in a rigid body soil motion, even for large-size foundations

3D Wave Propagation Data-Based Model (Incoherent – Database-Driven Adjusted Coherent)

- Includes real field records information, including implicitly motion field heterogeneity, random arrivals of different wave types under random incident angles.

ANIMATIONS

Incoherency Produces Differential Motions

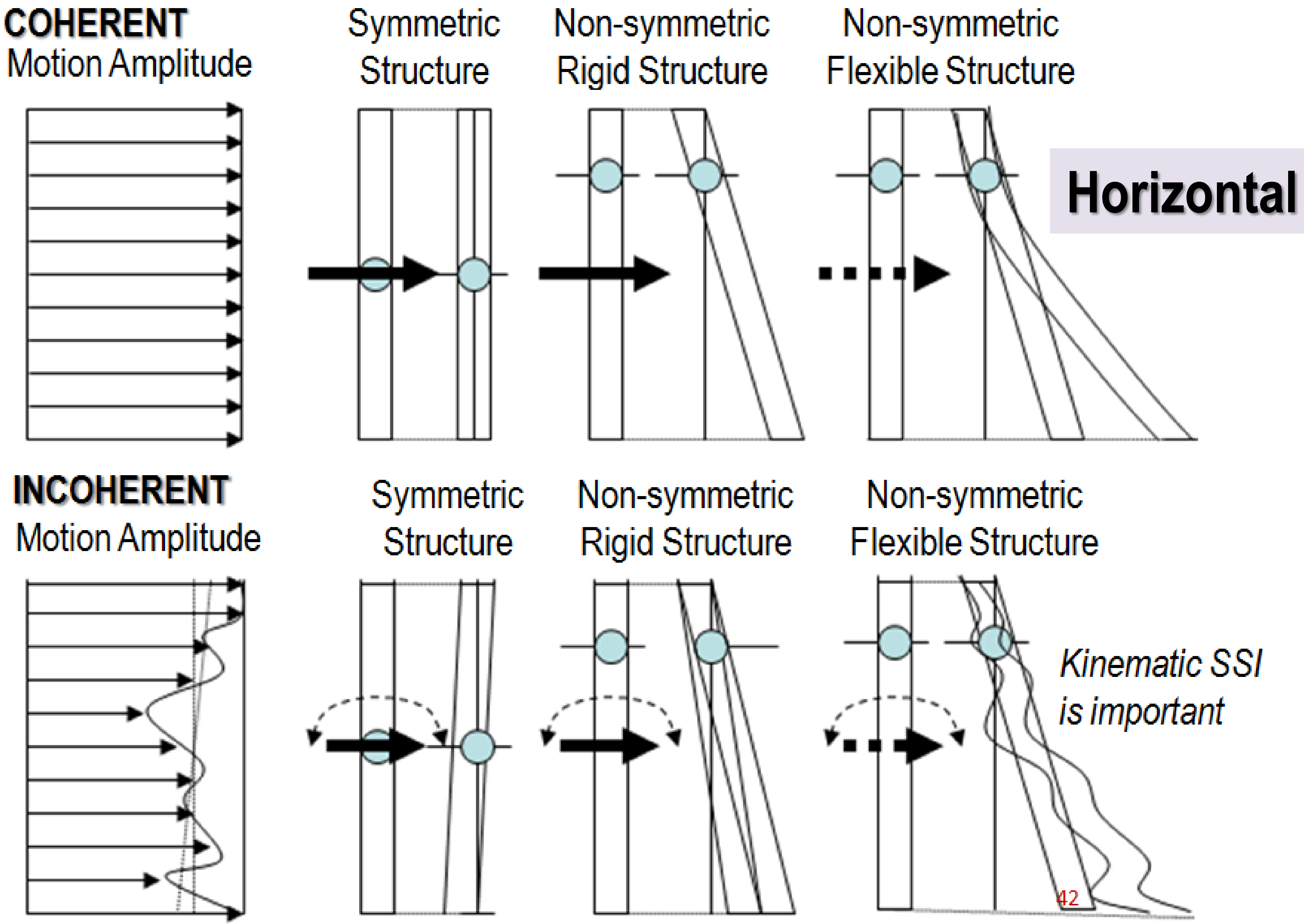

Incoherency Produces Differential Motions

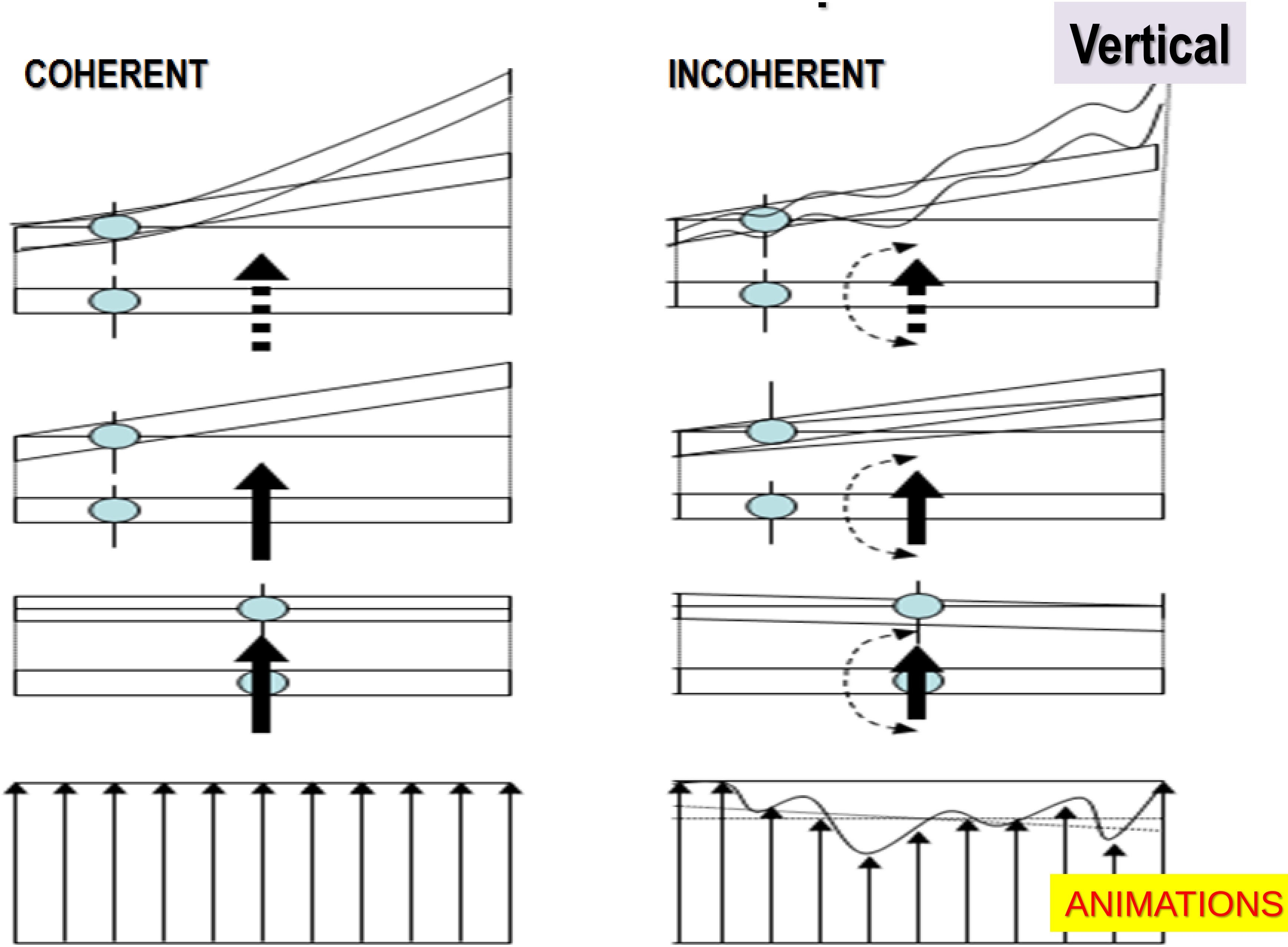

Typical RB Basemat SSI Response for COHERENT Inputs

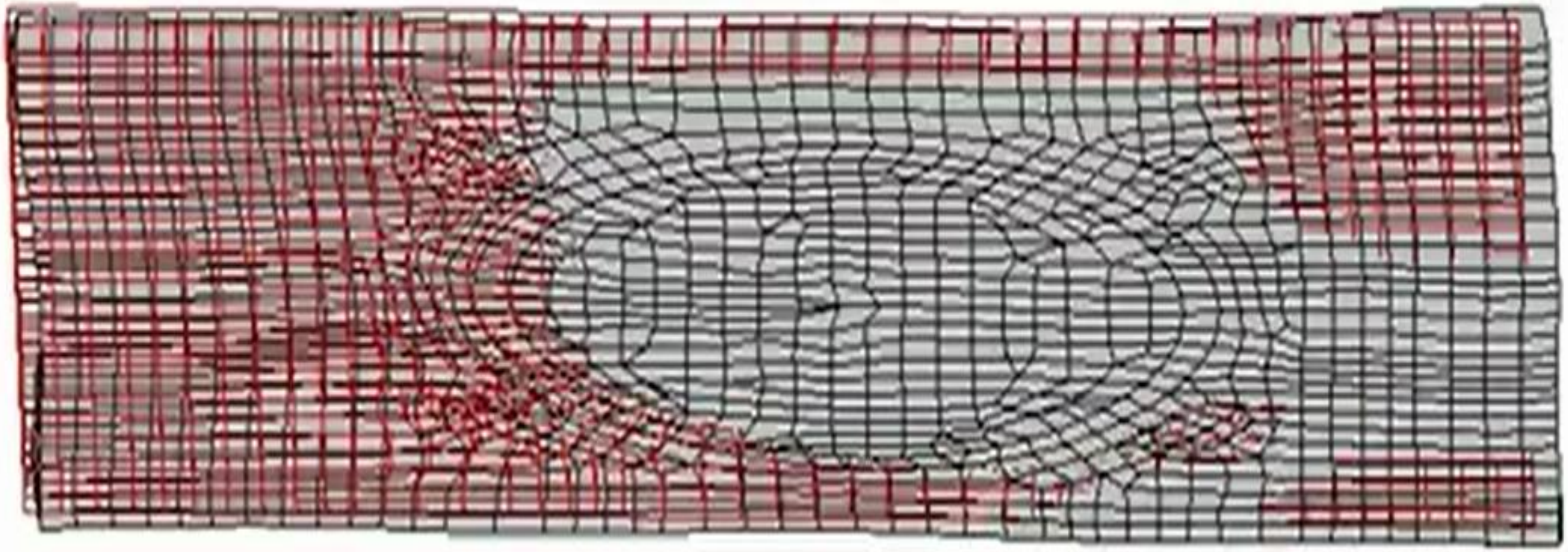

Typical RB Basemat SSI Response for INCOHERENT Inputs

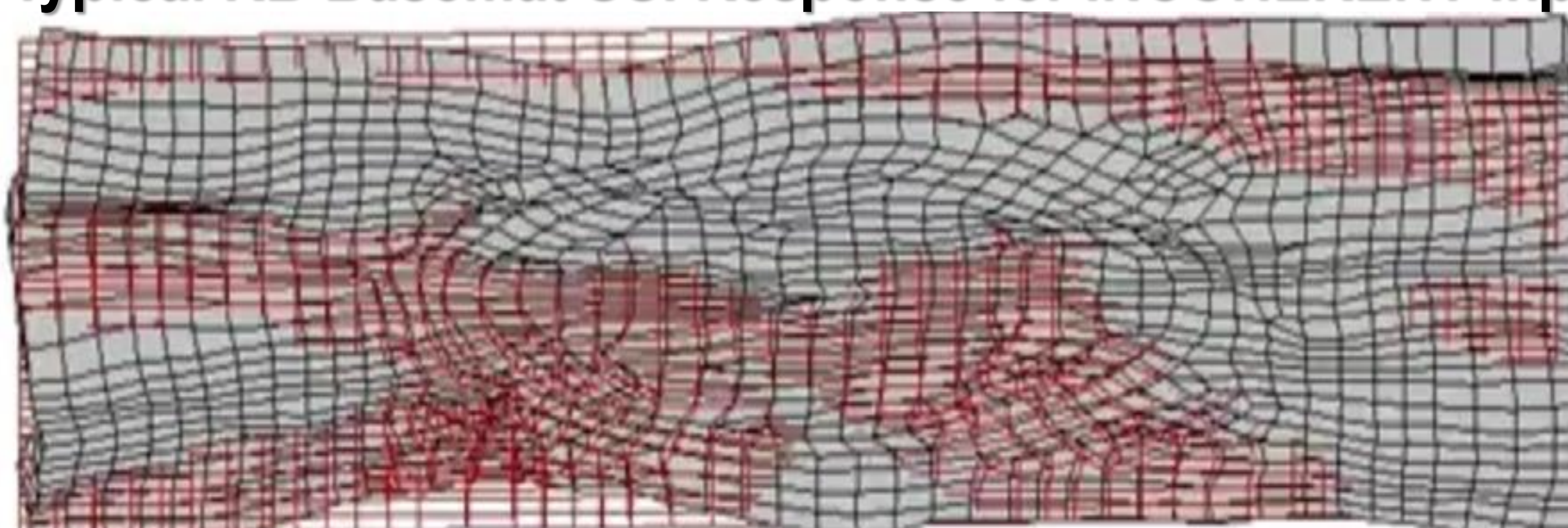

Factors Influencing Motion Incoherency

Spatial incoherency is caused by the complex wave propagation random pattern at the site. The main cause of incoherency observed over distances of tens of meters is caused by wave scattering in the top 500 m of the soil/rock deposit (Abrahamson, 2007)

Influential Factors:

- Soil profile stiffness variation in horizontal directions increases incoherency
- Soil layer inclination, local discontinuities, faults increase incoherency
- Topography features in vicinity could significantly increase incoherency
- Earthquake magnitude is less influential especially for single point source
- For short distances near faults, the multiple wave paths from different parts of fault rupture may drastically increase the spatial variations, both the motion incoherency and wave passage effects
- Focal mechanism and directivity apparently affect less incoherency

Modeling Parameters:

The main parameters for capturing the motion incoherency is its dependence on relative distances between locations and frequency. The latter is stronger.

Motion Incoherency Includes Two Contributing Random Variations; Incoherency & Wave Passage

The motion spatial random variation is a mix of *two components*:

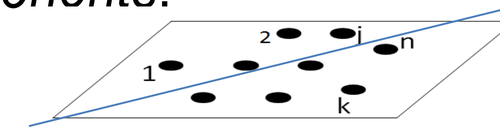

INCOHERENCY (Non-Directional Phenomena):

Measures the lack of similarity of two motions at two separated locations. This lack of similarity is expressed in terms of "correlation coefficient" between the amplitudes of the two motions at each frequency (coherence function).

If relative distance between locations is small, motions are highly correlated.

If relative distance between locations is large, motions are almost uncorrelated.

WAVE PASSAGE (Directional Phenomena):

Produced by the time delay (lag, shift) between two identical motions in a given direction.

If relative time delay locations is small, motions are highly correlated.

If relative time delay is larger, motions are almost uncorrelated.

REMARK: The incoherency and wave passage SSI effects of are qualitatively similar since they both produce lack of spatial correlation between two motions. For NPP structures incoherency is important, for large-span bridges both are important.

Motion Incoherency Includes Two Contributing Random Variations; Incoherency & Wave Passage

INCOHERENCY = lack of similarity after the motions are aligned (no delay)

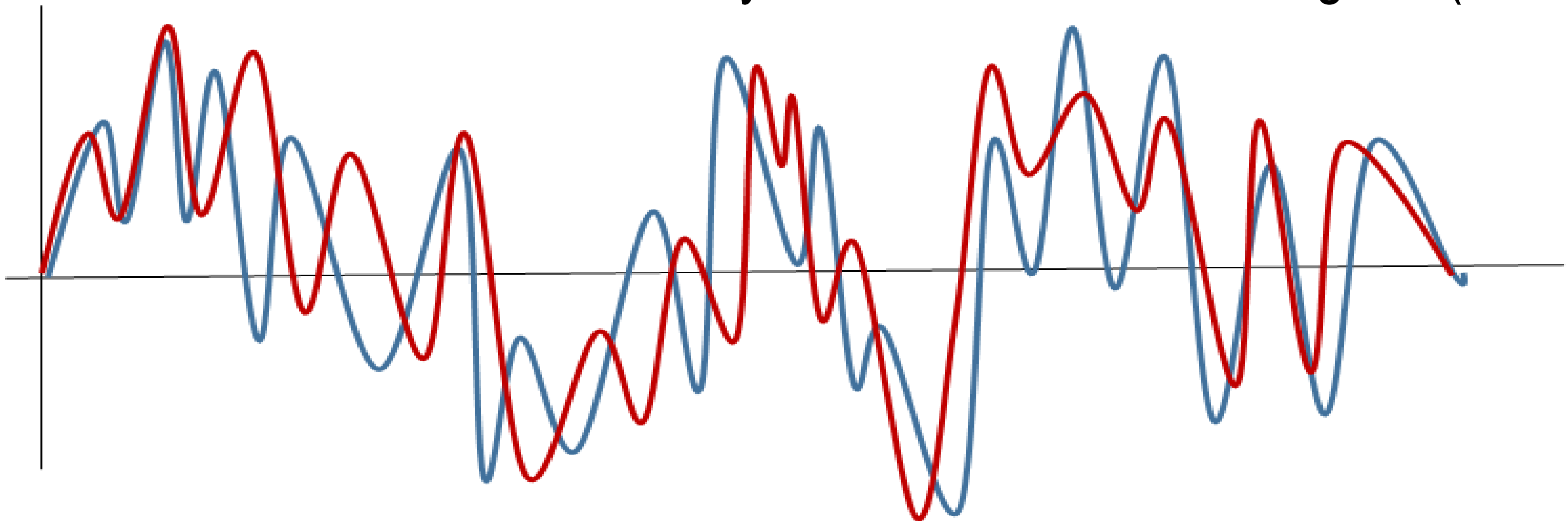

WAVE PASSAGE = systematic delay consistent with wave direction and speed

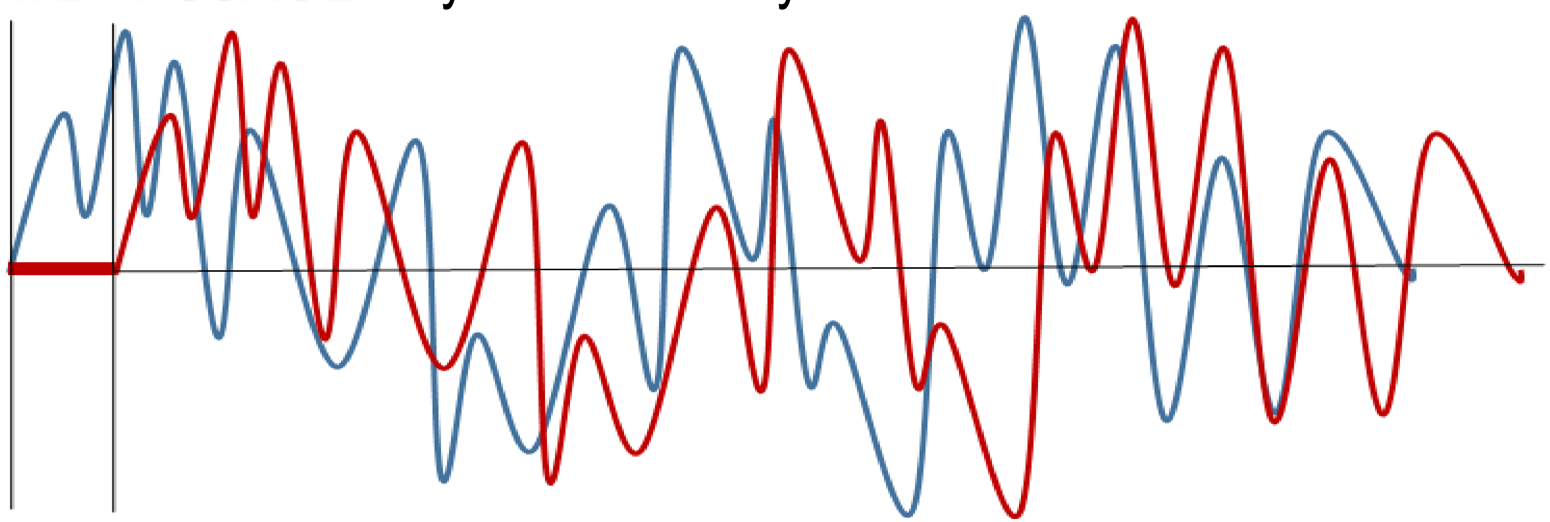

Wave Passage Effects Due to Inclined SV-P Waves

The apparent wave speed Va refers to slight inclination of the SV and P propagating waves, and not to the surface wave speeds.

Median Va values vary in the 2 – 4 km/sec. range (O'Rourke et al., 1982).

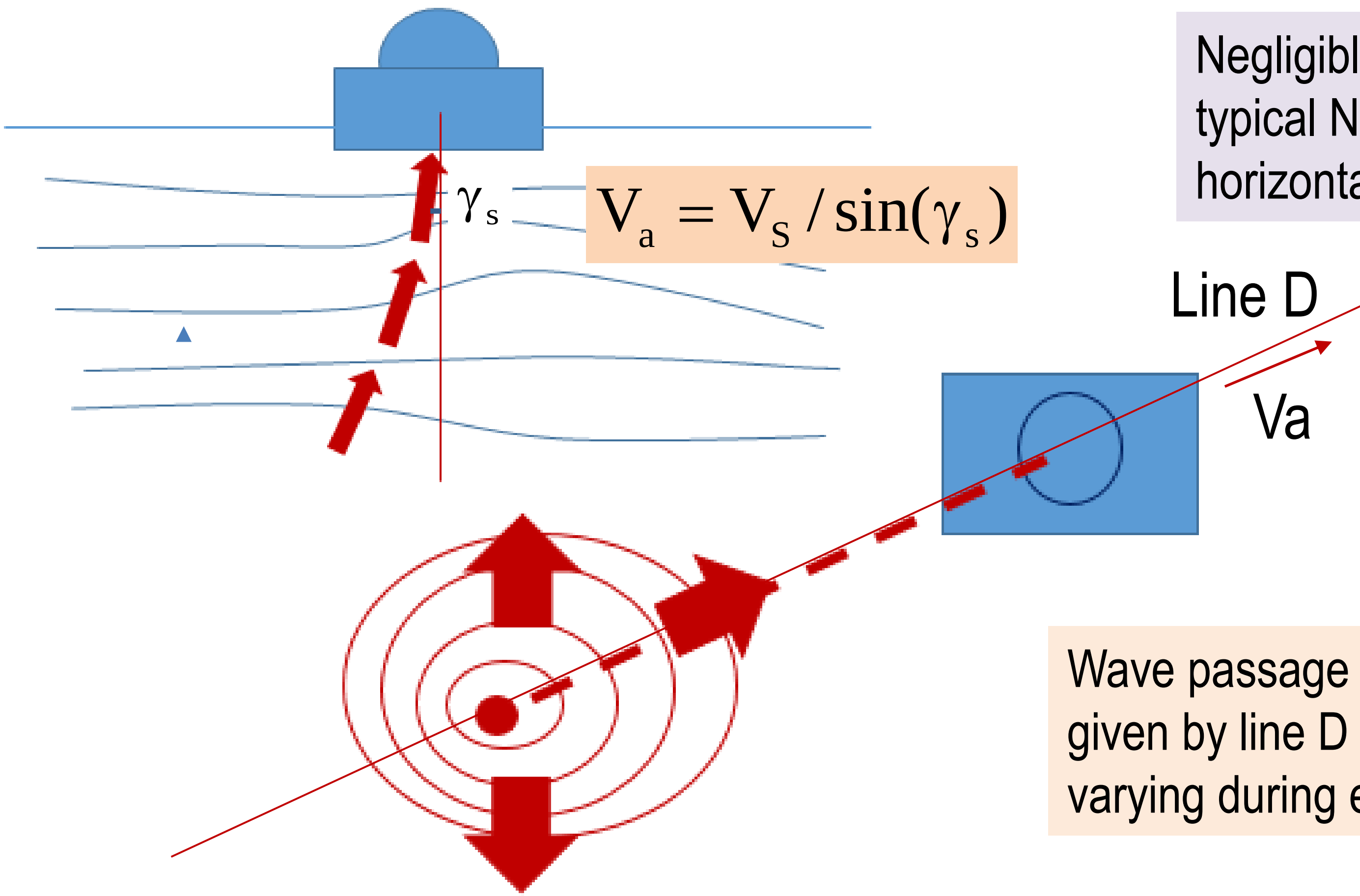

$$V_a = V_S / \sin(\gamma_s)$$

Negligible effects on SSI for typical NPP structures and horizontal soil layering sites

Wave passage direction is given by line D – assumed not varying during earthquake

Example of Motion Incoherency (No Time Lag)

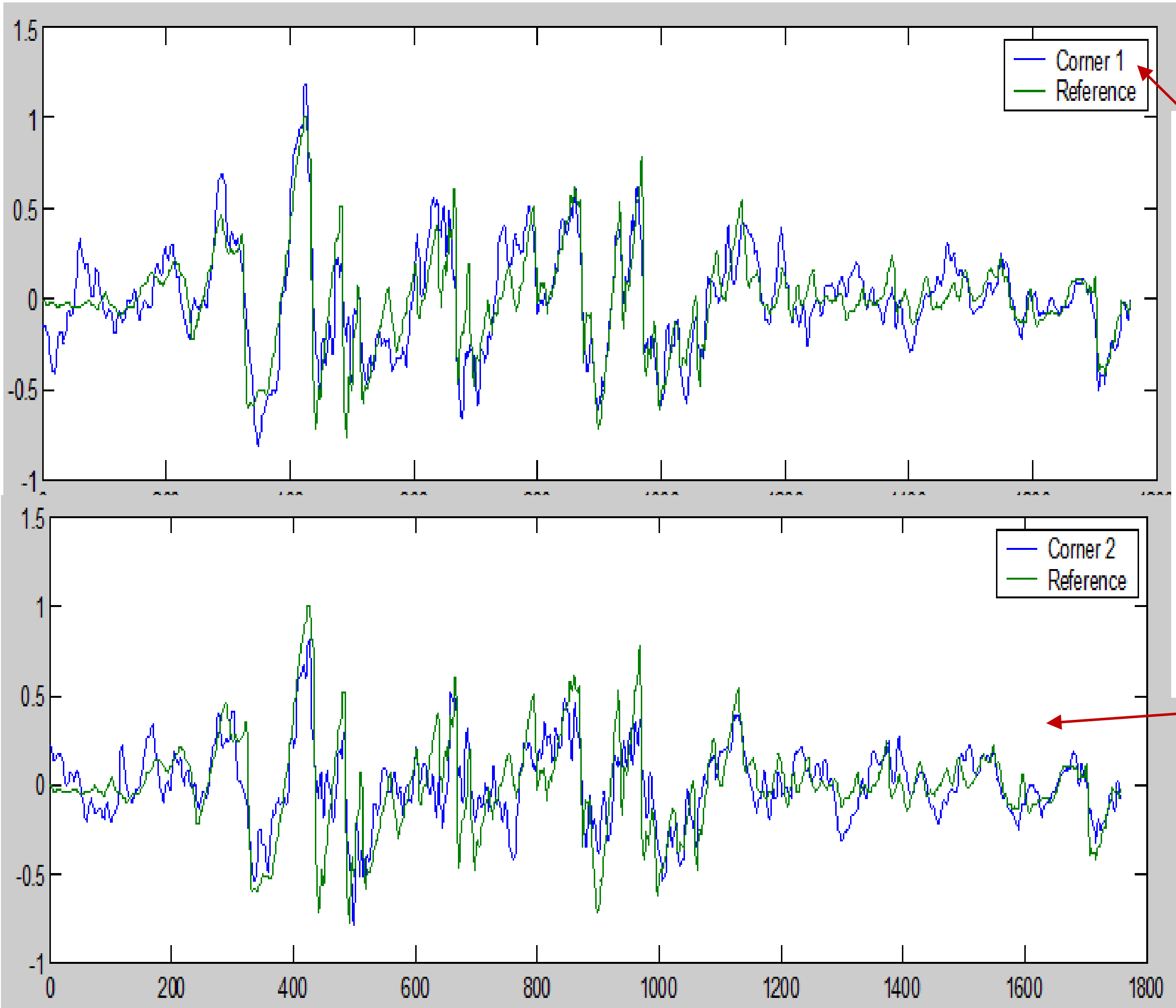

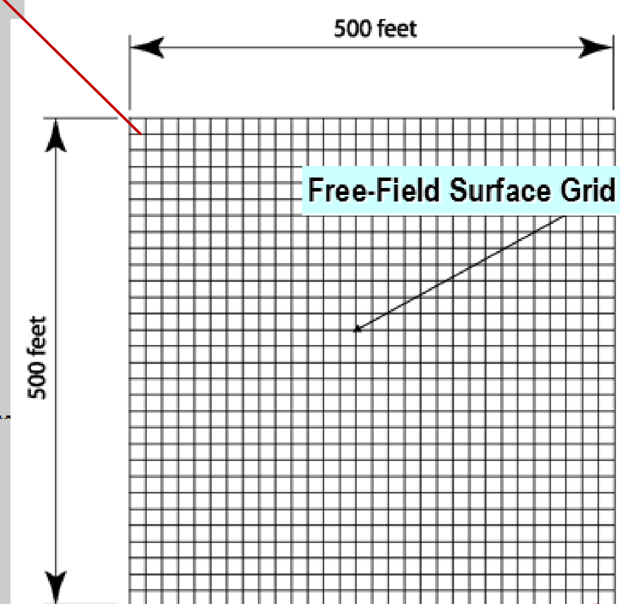

A 500 x 500 ft area was considered for this example.

Incoherent Seismic Wave Field Modeling

- Assuming that motion is a Gaussian vector process, then it is fully defined in frequency domain by

local variability **spatial correlation**

$$S_{Uj,Uk}(\omega) = [S_{Uj,Uj}(\omega) S_{Uk,Uk}(\omega)]^{1/2} \Gamma_{Uj,Uk}(\omega)$$

Thus, for two arbitrary points in horizontal plane, j and k, the coherency spectrum or coherence is defined by

$$\Gamma_{Uj,Uk}(\omega) = \frac{S_{Uj,Uk}(\omega)}{[S_{Uj,Uj}(\omega) S_{Uk,Uk}(\omega]^{1/2}}$$

- The "plane-wave coherency" function for SSI analysis is defined as a complex function (Abrahamson, 1991-2007) including "spatial incoherency" (amplitude) and "wave passage" (phase) effects

$$\Gamma_{U\ Ui,Uk}(\omega) = \Gamma_{PW\,Ui,Uk}(\omega)\ \exp\ [i\omega(X_{D,i} - X_{D,k}) / V_D]$$

amplitude variability **phase shift**

3D Stochastic Model for Incoherent Motion Wave Field

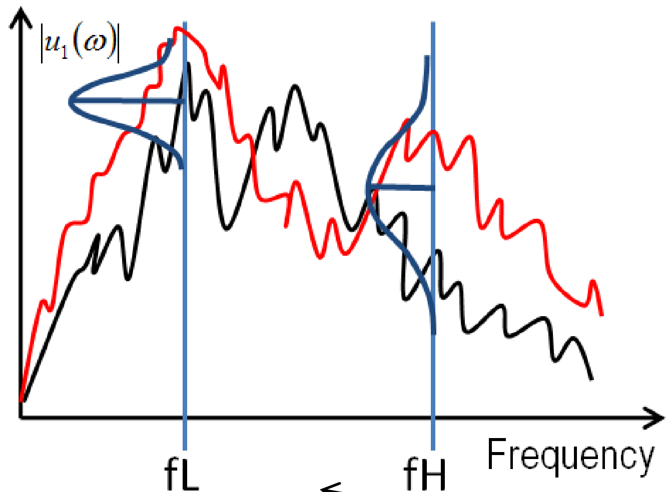

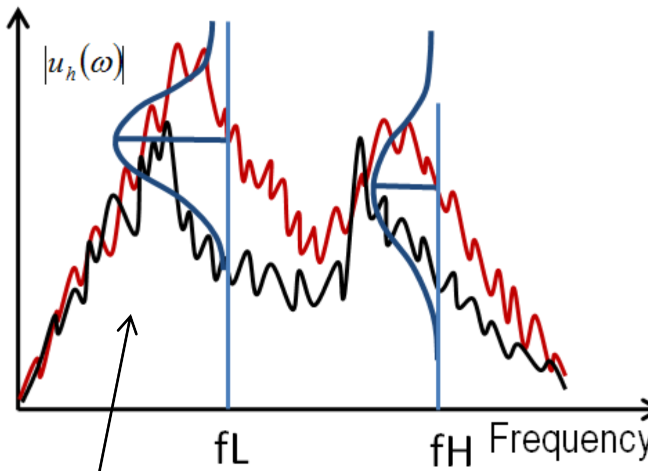

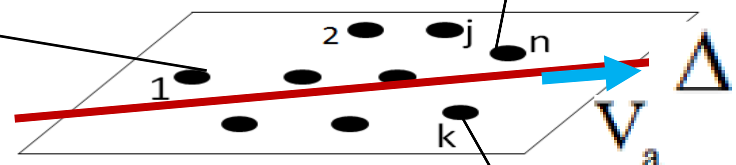

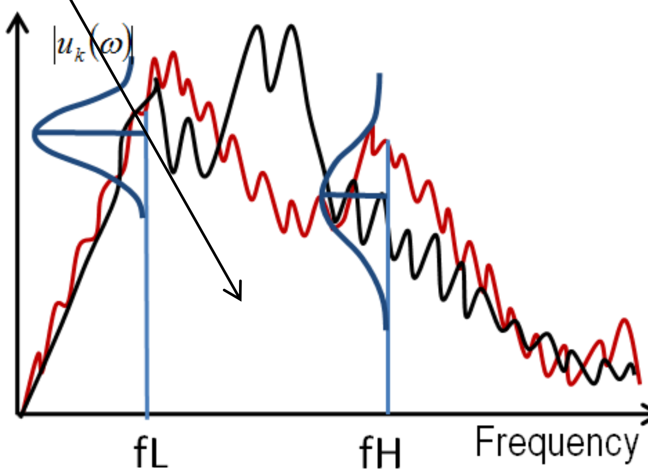

Coherence Function

$$\Gamma_{Uj,Uk}(\omega) = \frac{S_{Uj,Uk}(\omega)}{[S_{Uj,Uj}(\omega) S_{Uk,Uk}(\omega)]^{1/2}}$$

$$\Gamma_{U\,Ui,Uk}(\omega) = \Gamma_{L\,Ui,Uk}(\omega) \exp\left[i\omega(X_{D,i} - X_{D,k})/V_D\right]$$

$$\gamma_{ij}(\omega) = \frac{E\left[|u_i(\omega)||u_j(\omega)|\right]}{E\left[|u_i^2(\omega)|\right]^{1/2} E\left[|u_j^2(\omega)|\right]^{1/2}} \exp\left(i\omega \frac{\Delta_{ij}}{V_a}\right)$$

$$\rho_{X,Y} = \mathrm{corr}(X,Y) = \frac{\mathrm{cov}(X,Y)}{\sigma_X \sigma_Y}$$

Coherence Function Definition for Two Time Series

Cross-Spectral Density (CSD):

$$S_{XY}(\omega) = \frac{2\left|X^*(\omega)Y(\omega)\right|}{2\pi T} = \frac{2}{2\pi T}\sum_{j=1}^{K}\left|\mathrm{Conj}\left[\sum_{t_j=T_{j-1}+dt}^{T_j} W(t_j - T_{j-1})X(t_j)e^{-i\omega t_j}\right]\sum_{t_j=T_{j-1}+dt}^{T_j} W(t_j - T_{j-1})Y(t_j)e^{-i\omega t_j}\right|$$

=

Power Spectral Density (PSD):

$$S_X(\omega) = \frac{2\left|X^*(\omega)X(\omega)\right|}{2\pi T} = \frac{2\left|X(\omega)\right|^2}{2\pi T} = \frac{2}{2\pi T}\sum_{j=1}^{K}\left|\sum_{t_j=T_{j-1}+dt}^{T_j} W(t_j - T_{j-1})X(t_j)e^{-i\omega t_j}\right|^2$$

The quality of the coherence spectrum estimates deteriorate inversely proportional with its value between from 0 to 1.

Coherence Function is defined by:

$$\gamma_{X,Y}(\omega) = \frac{S_{X,Y}(\omega)}{S_X(\omega)S_Y(\omega)}$$

(Ghiocel, ICASP, Paris, 1996)

Lagged Coherence Function Estimates Using Different Smoothing Bandwidths of Hamming Window

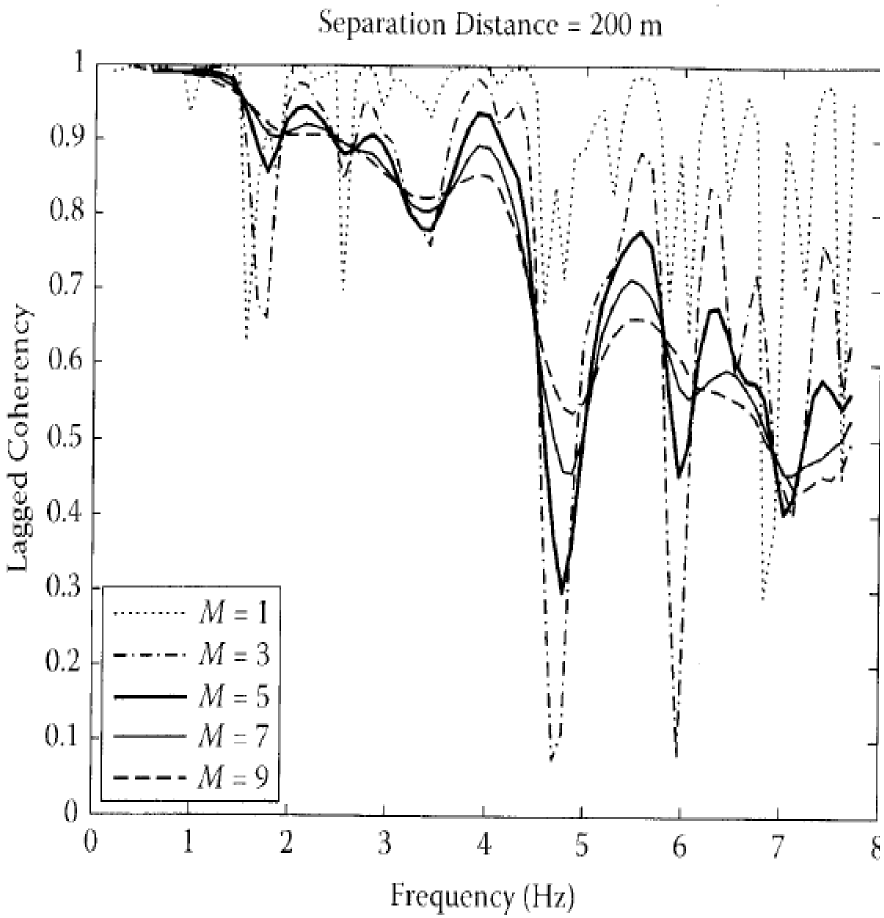

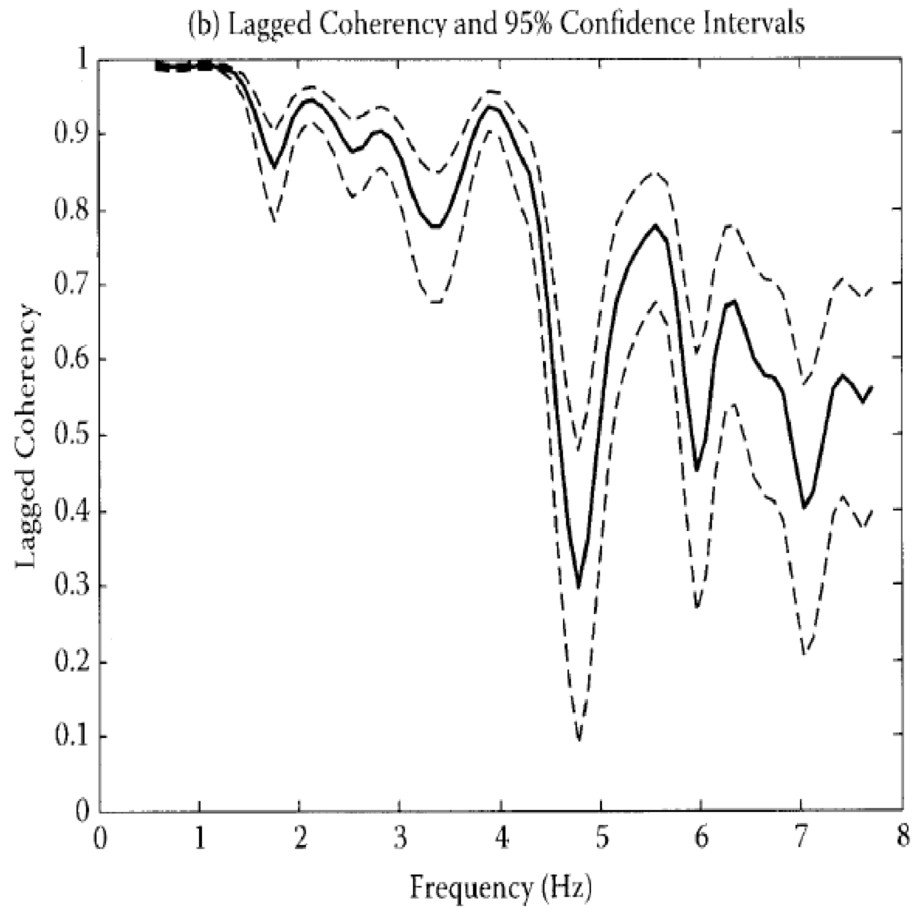

(Zerva, 2008)

Abrahamson recommends using 11-point Hamming window (M=5)

Lagged and Plane-Wave Coherence Functions

Unlagged and Lagged Coherence Functions:

$$\gamma(\omega, x, x') = |\gamma(\omega, x, x')| \exp(i\phi(\omega, x, x'))$$

Plane-Wave (P-W) Coherence Function is defined by

$$\gamma_{PW}\left(\omega, \xi_{x,x'}, \xi^{pw}_{x,x'}\right) = \left|\gamma\left(\omega, \xi_{x,x'}\right)\right| \alpha\left(\omega, \xi^{pw}_{x,x'}\right) \exp\left(-\omega \xi^{pw}_{x,x'} / V_{pw}\right)$$

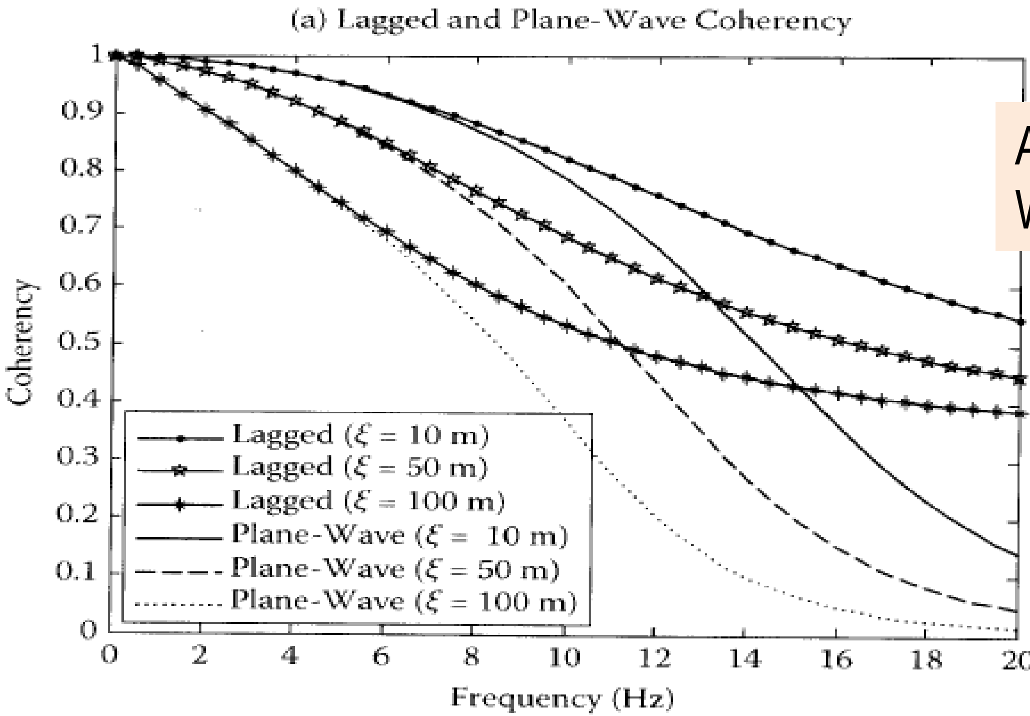

Abrahamson Lagged and Plane-Wave Coherence Functions

(Abrahamson, 1991, Zerva, 2008)

P-W Coherency Functions for Different Soil Sites

Coherence Function from many records in different dense arrays:

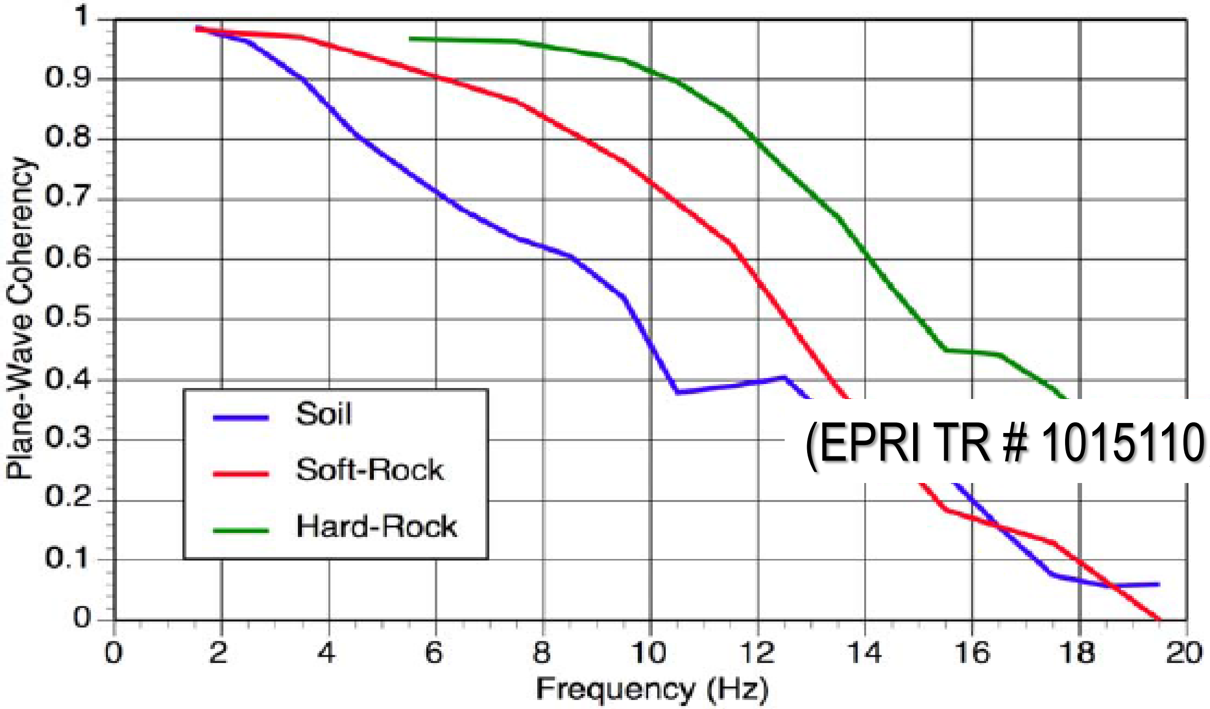

(EPRI TR # 1015110, December 2007)

Abrahamson Coherence Function (Fitted) Analytical Form:

$$\gamma_{pw}(f,\xi)=\left[1+\left(\frac{f\ \ Tanh(a_3\xi)}{a_1 f_c(\xi)}\right)^{n1(\xi)}\right]^{-1/2}\left[1+\left(\frac{f\ \ Tanh(a_3\xi)}{a_2}\right)^{n2}\right]^{-1/2}$$

Abrahamson Generic Coherence Functions for Rock & Soil Sites

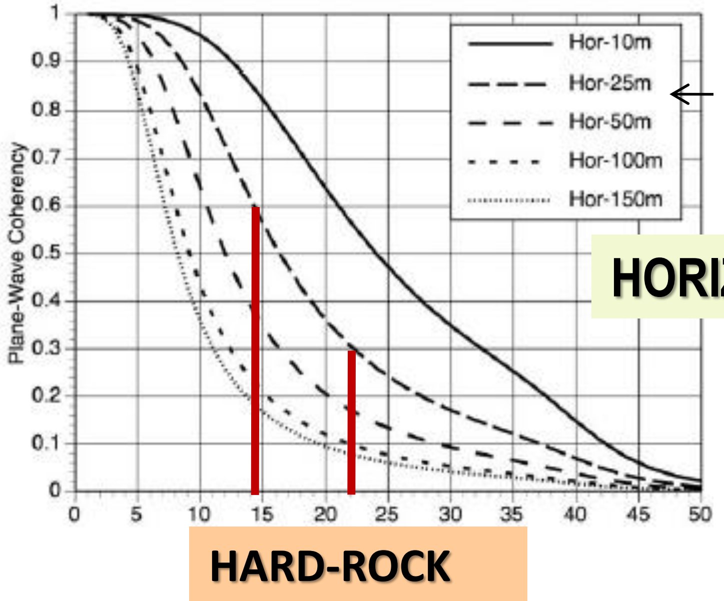

Figure 6-1
Plane-Wave Coherency for the Horizontal Component

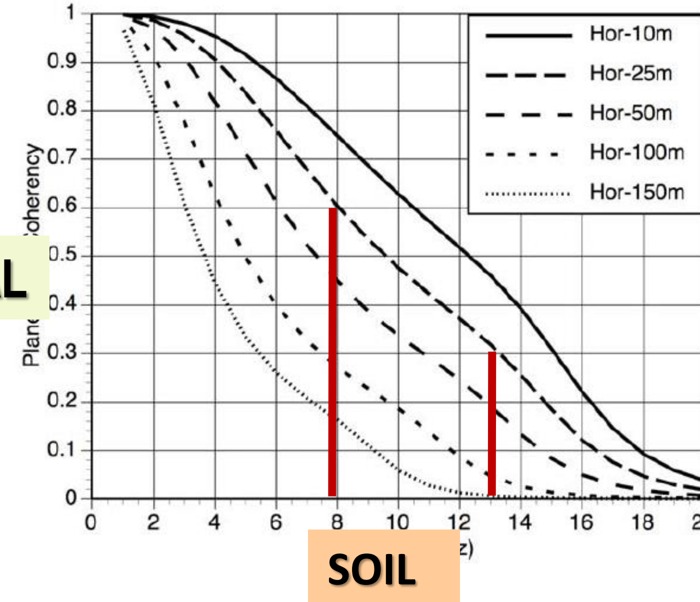

Figure 7-1
Plane-Wave Coherency for the Horizontal Component for Soil Sites

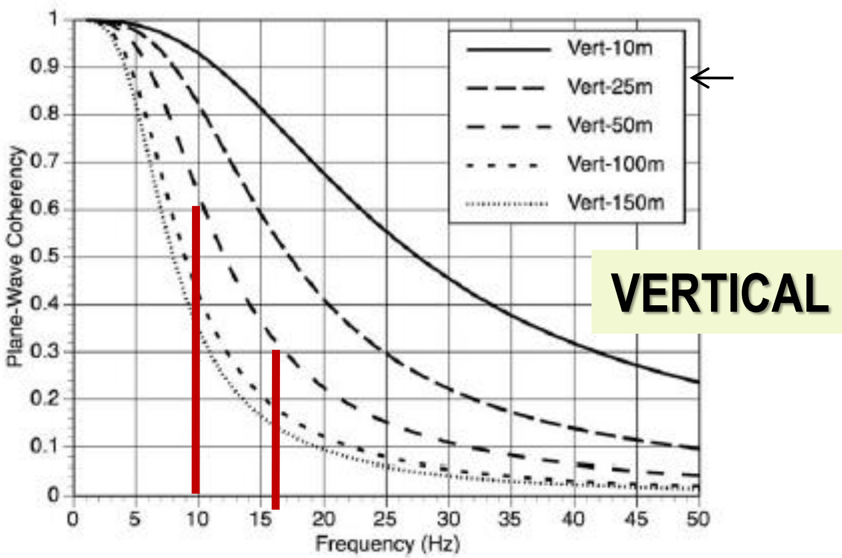

Figure 6-2
Plane-Wave Coherency for the Vertical Component

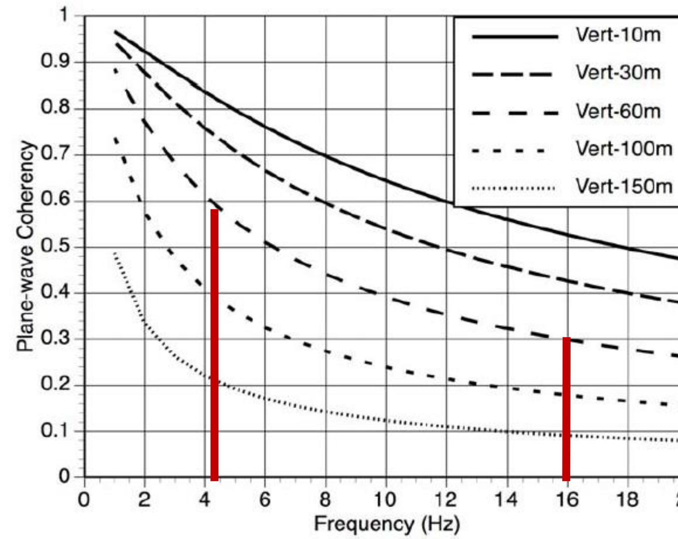

Figure 7-2
Plane-Wave Coherency for the Vertical Component for Soil Sites

(EPRI TR # 1015110, December 2007)

ACS SASSI Motion Coherency Models

There are several plane-wave incoherency models (with wave passage effects):

1) 1986 Luco-Wong model (theoretical, unvalidated, geom anisotropic)
2) 1993 Abrahamson model for all sites and surface foundations
3) 2005 Abrahamson model for all sites and surface foundations
4) 2006 Abrahamson model for all sites and embedded foundations
5) 2007 Abrahamson model for hard-rock sites and all foundations (NRC)
6) 2007 Abrahamson model for soil sites and surface foundations
7) User-Defined Plane-Wave Coherency Functions for X, Y and Z

Motion Incoherency Models

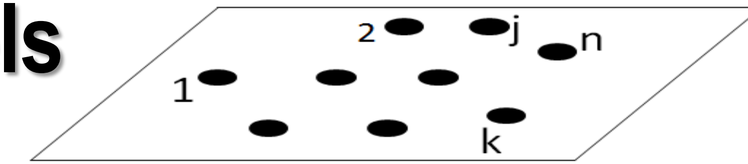

Radial/Non-Directional/Isotropic Variation Models.

Incoherency depends only on the *relative distances* between different locations, but not on the location position or orientation.

For equal relative distances between paired locations, dij, the coherency/ correlation at all frequencies is the same for all paired locations.

$\gamma(\omega, \Delta)$, where $\Delta = \sqrt{(\Delta x^2 + \Delta y^2)}$ - circular correlation – extended to ellipse.

The effect of directionality is lost. Generic Abrahamson coherency models.

Directional/Anisotropic Variation Models

Incoherency depends only on the *relative distances between different locations, but also on the location positions and orientation*.

For equal relative distances between paired locations, dij, the coherency/ correlation at all frequencies is different for the paired locations.

$\gamma(\omega, \Delta x, \Delta y, x, y)$ - more general model

The effect of directionality is NOT lost. Site-specific coherency models. More refined and realistic (if site-specific soil layering data is available)

Radial and Directional Incoherency Using Isotropic and Geometric Anisotropic Models

RADIAL

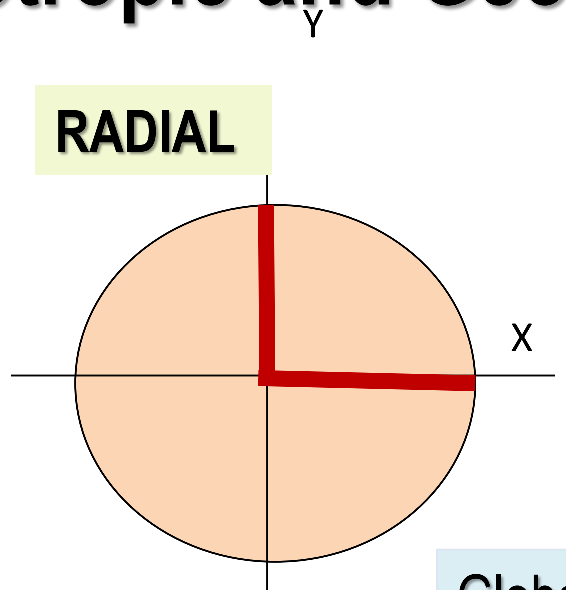

DIRECTIONAL

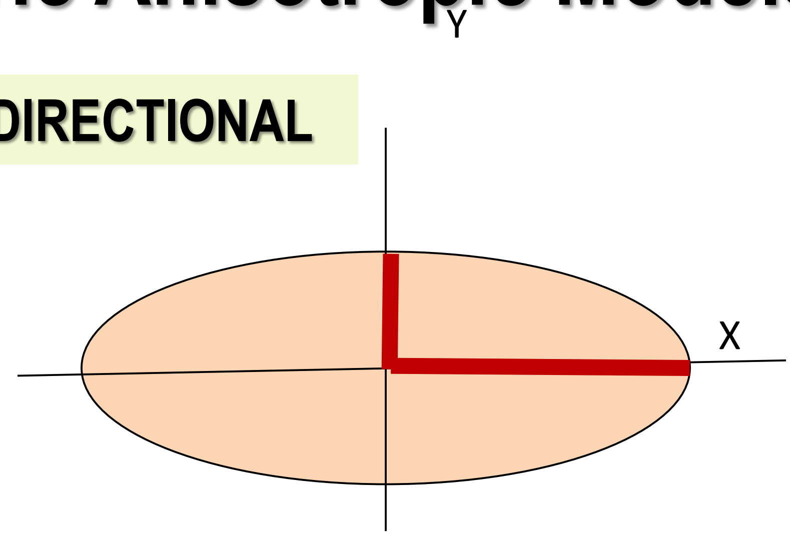

Global Coordinate Axes

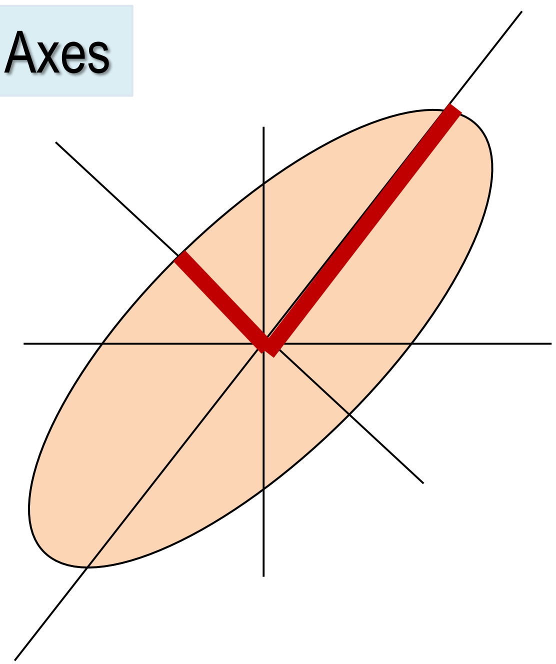

$$D^2 = 2[(1-\alpha)Dx^2 + \alpha Dy^2]$$

Local Coordinate Rotated Axes

P-W Coherence Function for Different Models

Coherence Function Radial Model

Coherence Functions for Same Distance, Different Directions

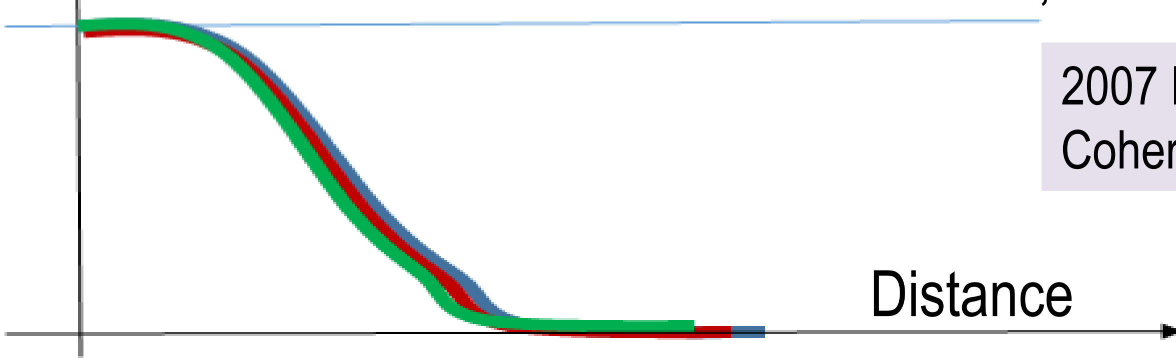

2007 EPRI Studies Limited to Coherency Radial Models

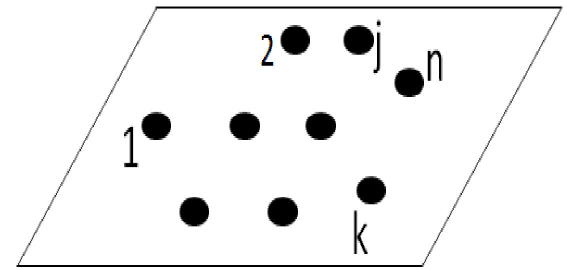

Coherence Function Directional Model

Coherence Functions for Same Distance, Different Directions

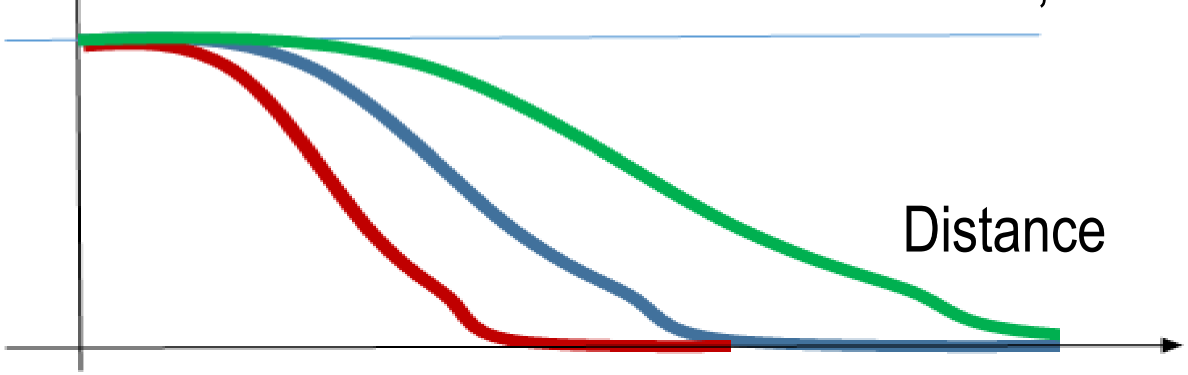

EPRI AP1000 NI Stick Model Incoherency Directivity Study

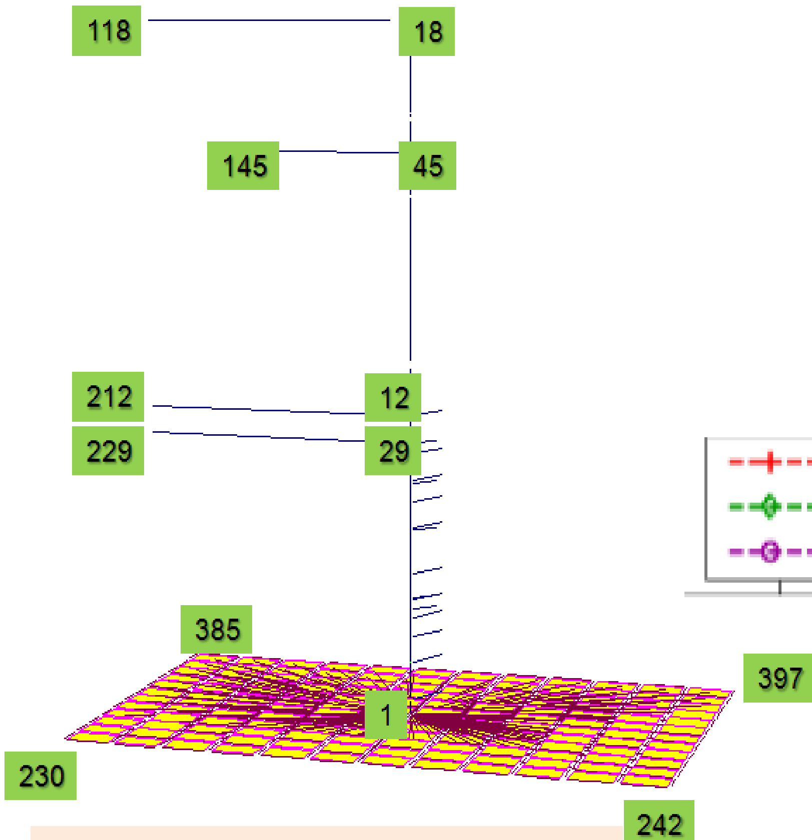

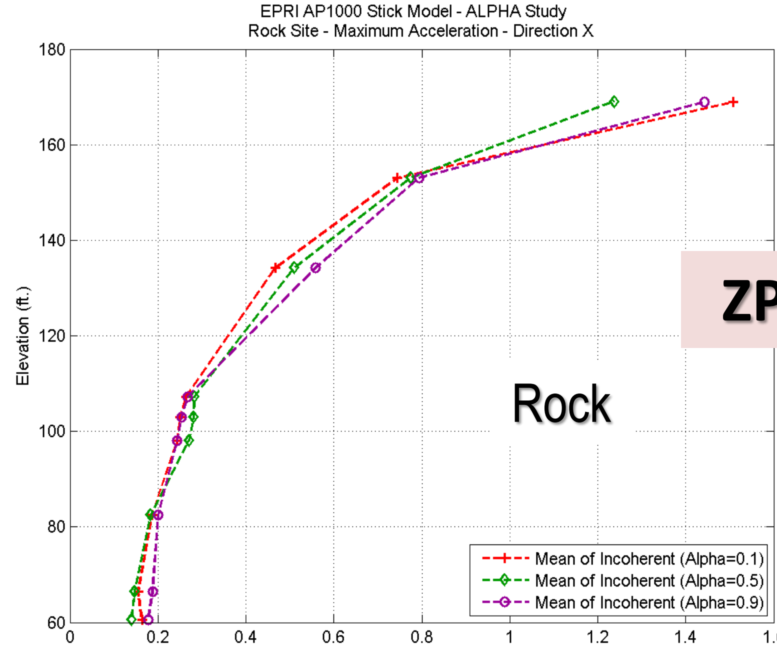

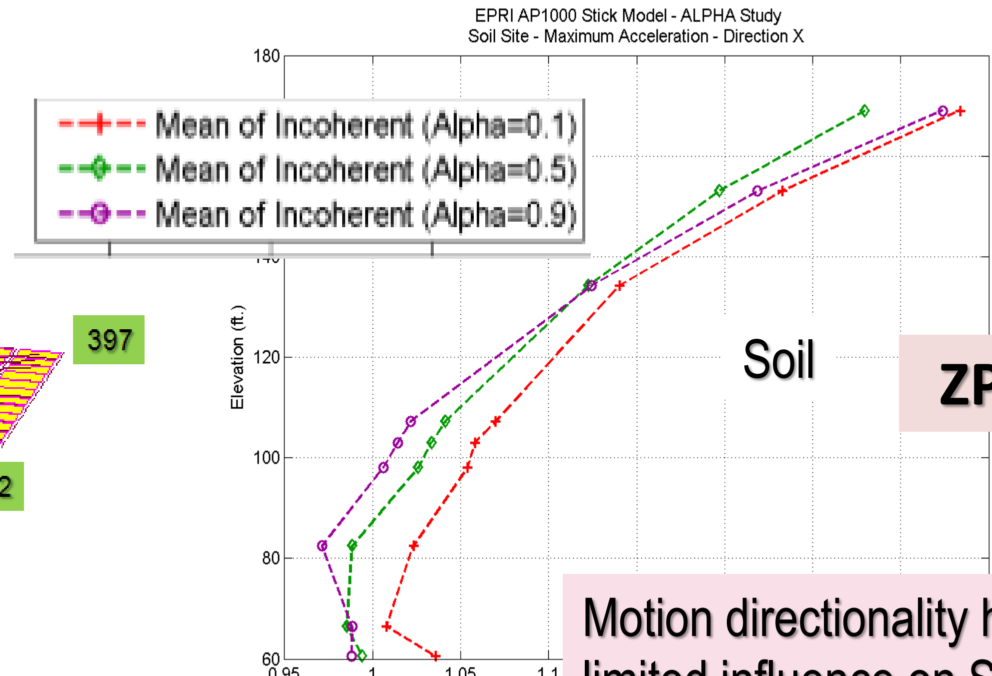

- Soil Site, Vs = 1,000 fps, CSDRS, AB2007Soil
- Rock Site, Vs = 6,000 fps, EPRIRockRS, AB2007Rock

Motion directionality has limited influence on SSI

Incoherent Motion Directionality Effects on ISRS for Large-Size RB Complex W/ Zeroing Phase

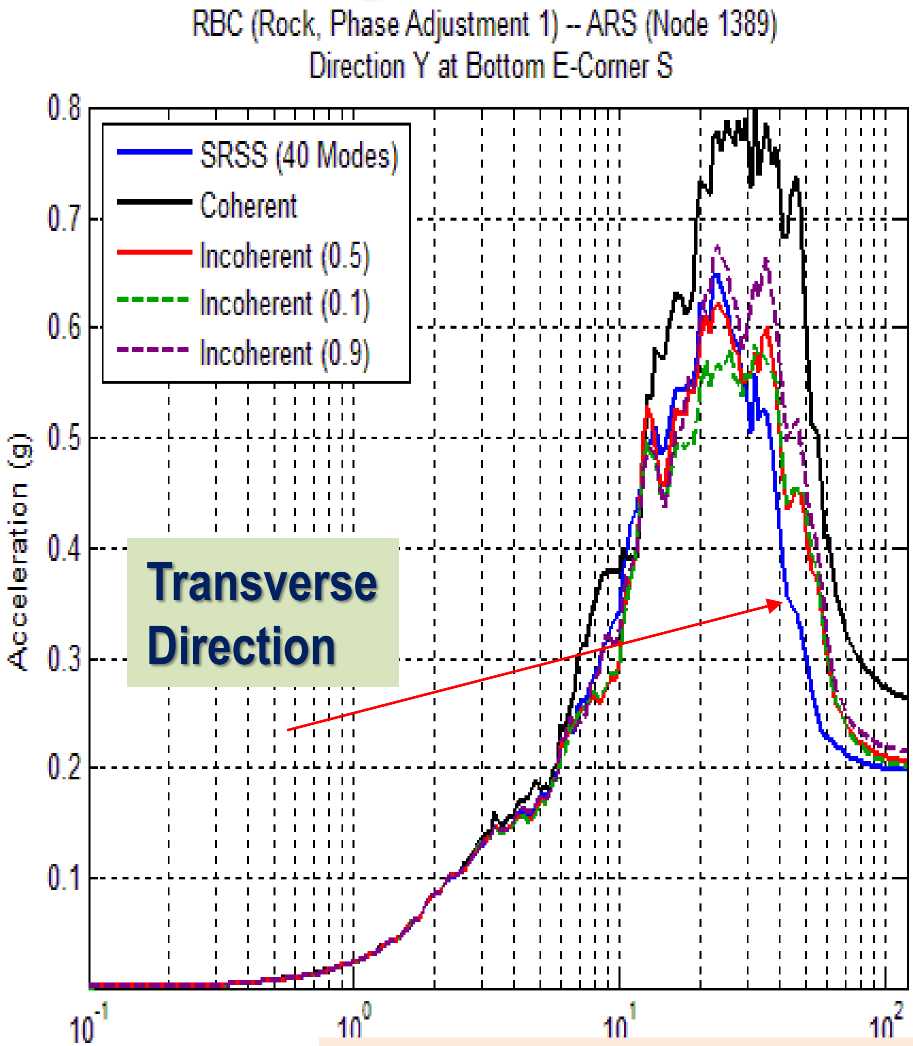

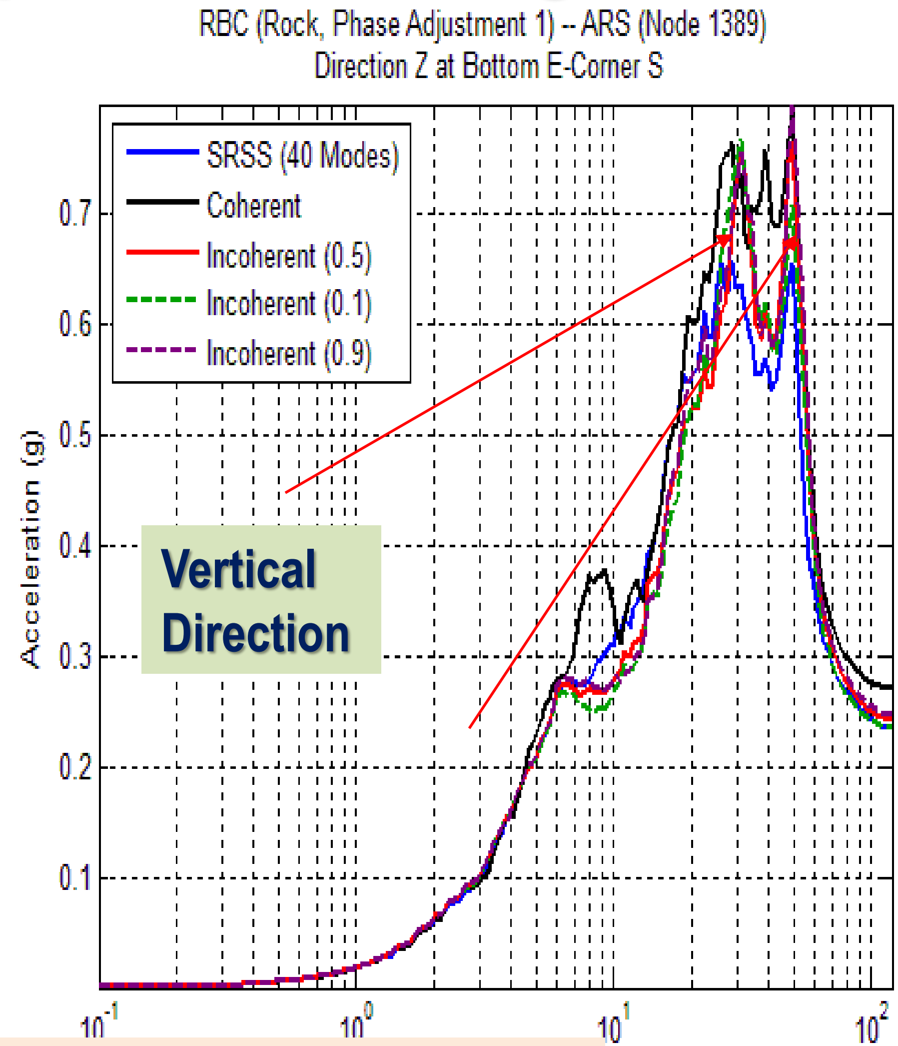

Bottom Basemat Corner

 Ghiocel, DOE NPH SSI Workshop, October 18-19, 2016

“Site-Specific” Plane-Wave Incoherency Models

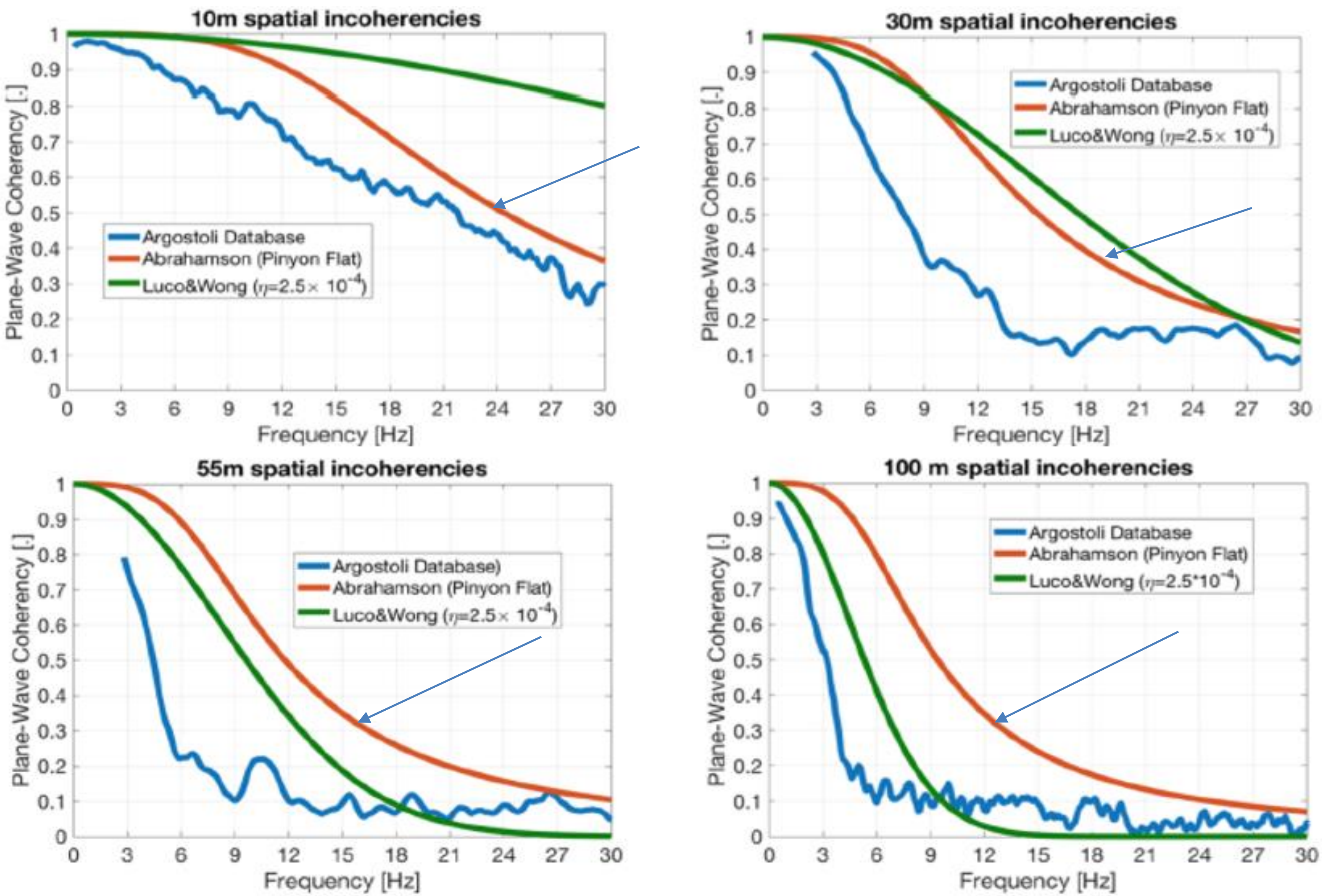

Site-Specific Coherence Function for Argostoli Site (after Svay et al., 2016, EDF)

Developing Site-Specific Coherency Function Models for NPP Site Using 2D/2V Probabilistic Soil Profiles (Vs, D)

Horizontal Mean Soil Layering (2D/2V Homogeneous Correlated Fields)
>>> Generic Coherency Models, Statistical, as Abrahamson, Luco

Slopped Mean Soil Layering (2D/2V NonHomogeneous Correlated Fields)
>>> Site-Specific Coherency Models, Physics-based Modeling

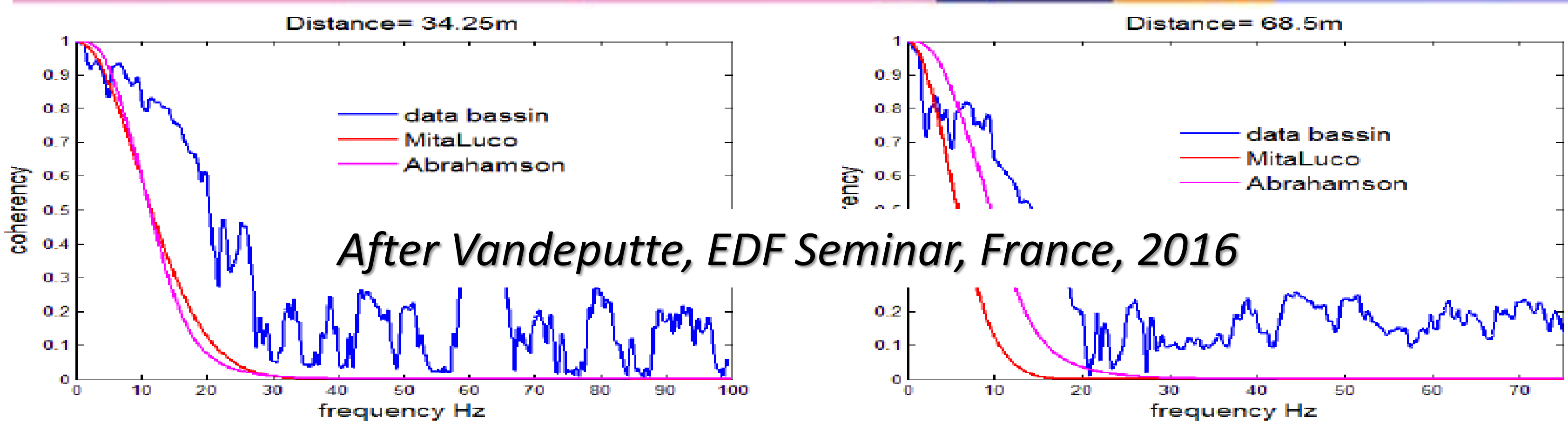

After Vandeputte, EDF Seminar, France, 2016

Simulated Vs and D Profiles for Uniform Deep Soil

Vs and D Simulated Profiles for Correlation Lengths of 60m x 10m (EDF site)

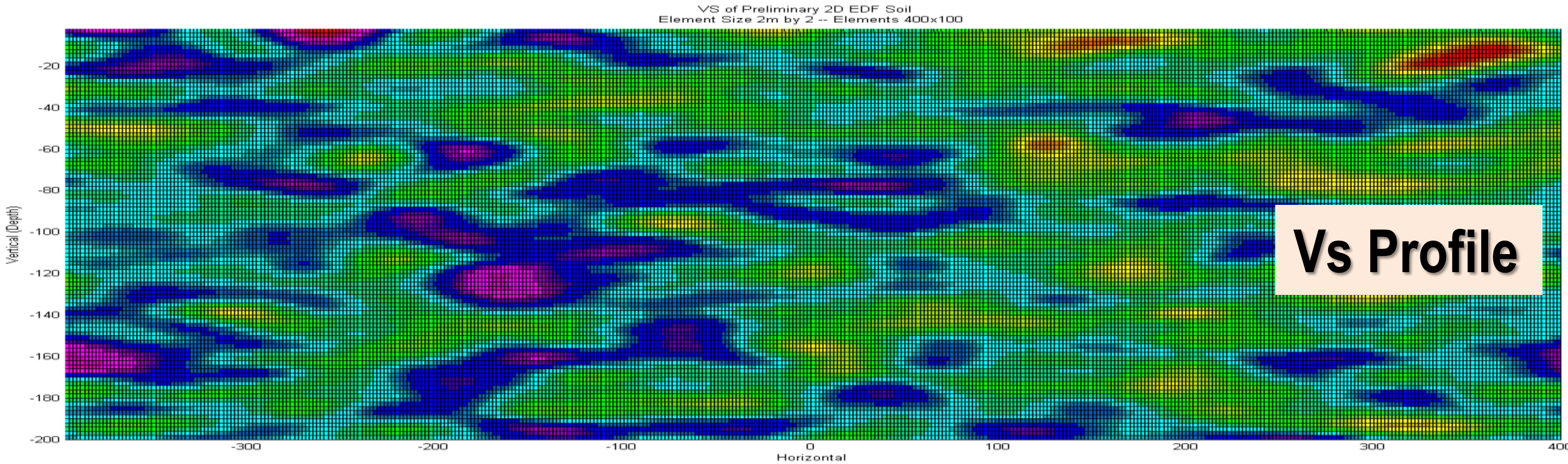

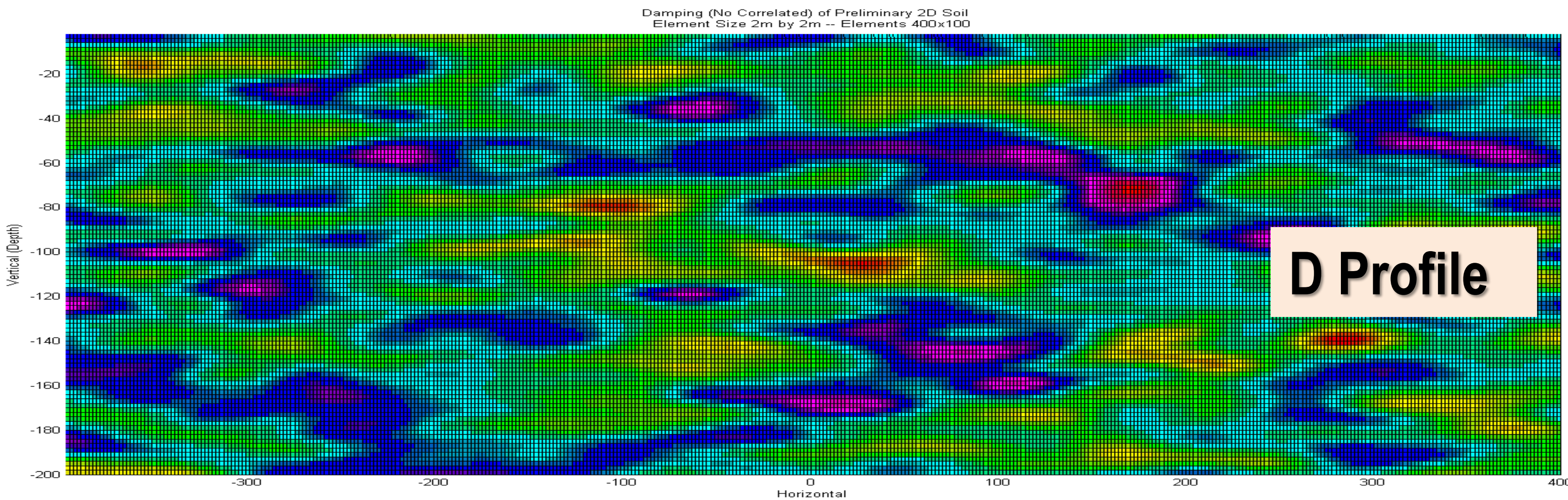

Armenian NPP Project Used 2D Probabilistic Soil Models

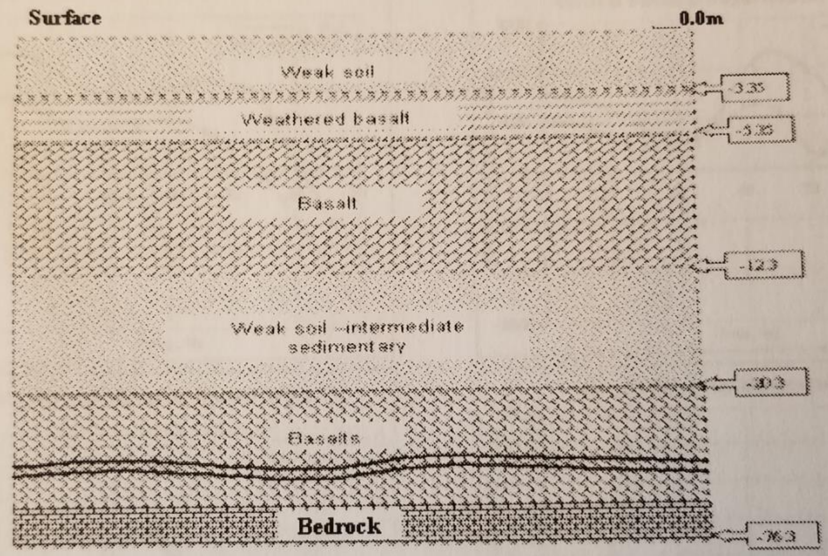

Figure 6. Layered soil profile under the Armenian Nuclear Power Plant (ANPP)

Spatially Correlated Vs Profiles. BNL Report 2006 (Simos and Costantino, 2007).

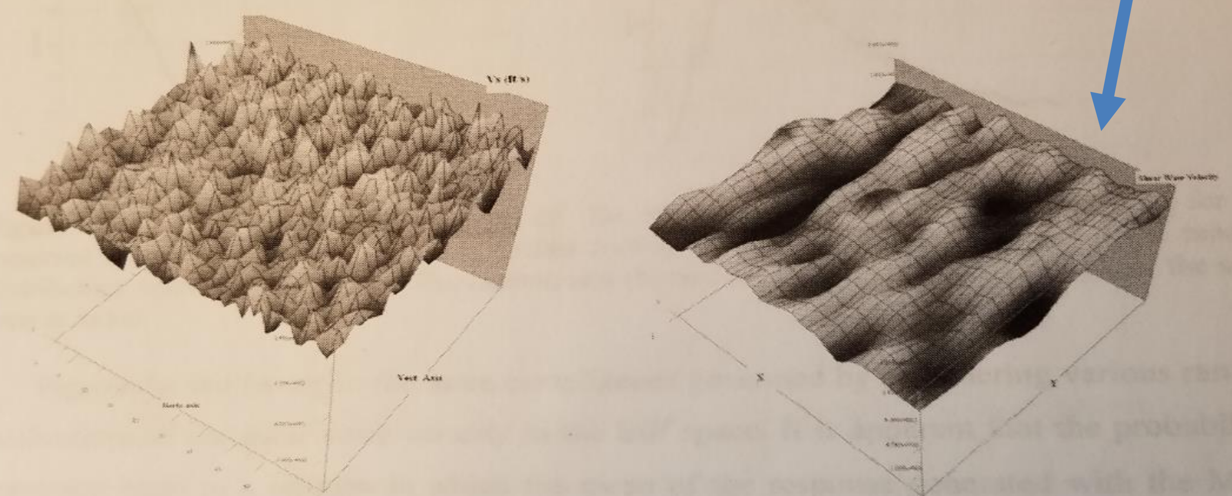

Figure 3. (a) Randomized shear wave velocity in half space domain of Figure 2 without special correlation and (b) resulting shear wave spatial distribution after cross-correlation procedures have been introduced in the randomized field shown in (a).

Probabilistic Simulation of Soil Layering As 2D/2v Stochastic Field Models

Spatial Correlation:

$$R_U[u(\mathbf{x}),u(\mathbf{x}')] = \sum_{n=0}^{\infty} \lambda_n \Phi_n(\mathbf{x}) \Phi_n(\mathbf{x}')$$

In engineering applications, usually, independent correlation structures for horizontal and vertical directions Can be assumed.

Karhunen-Loeve Expansion:

$$u(\mathbf{x},\theta) = \sum_{i=0}^{n} \sqrt{\lambda_i}\, \Phi_i(\mathbf{x}) z_i(\theta)$$

Can be used to identify the Zi random variable simulation values based on available measurements. Applicable to Gaussian and non-Gaussian stochastic fields.

$$z_i(\theta) = \frac{1}{\sqrt{\lambda_i}} \int_D \Phi_n(\theta)\, u(\mathbf{x},\theta)\, d\mathbf{x}$$

Spatial correlation coefficient for non-Gaussian soil profiles:

$$\rho_{yi,yj} = \frac{1}{\sigma_{yi}\sigma_{yj}} \int_{-\infty}^{\infty}\int_{-\infty}^{\infty} [F_i^{-1}\Phi(x_i) - \mu_{yi}][F_i^{-1}\Phi(x_j) - \mu_{yj}]\phi(x_i, x_j) dx_i dx_j$$

(Ghiocel, 2004)

2D Probabilistic Nonlinear Site Response (ACS SASSI New Option PRO) for Site-Specific Coherency Models

1D Mean/BE Soil Profile Model
Generic Coherency Models, Statistical

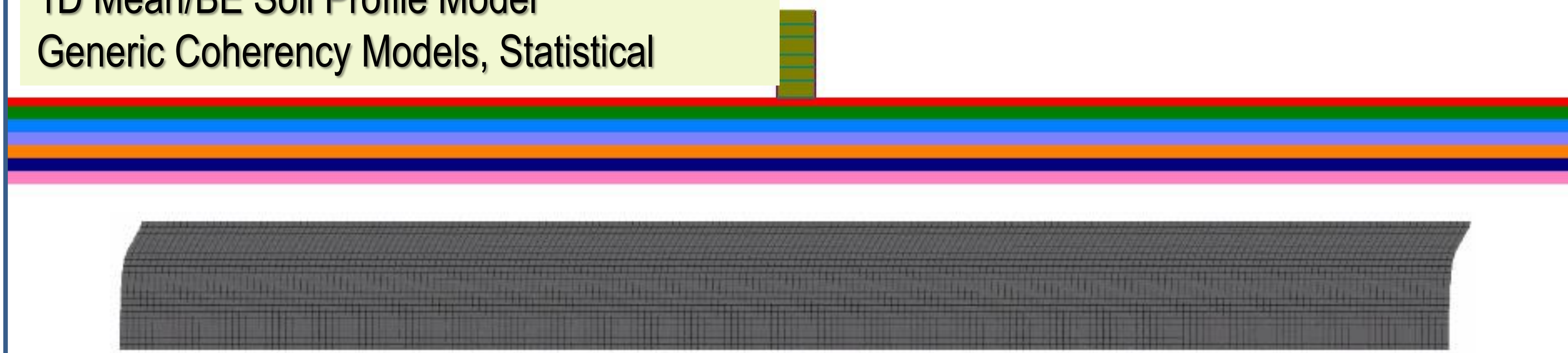

2D Mean/BE Soill Profile Model
Site-Specific Coherency Models,
Physics-Based

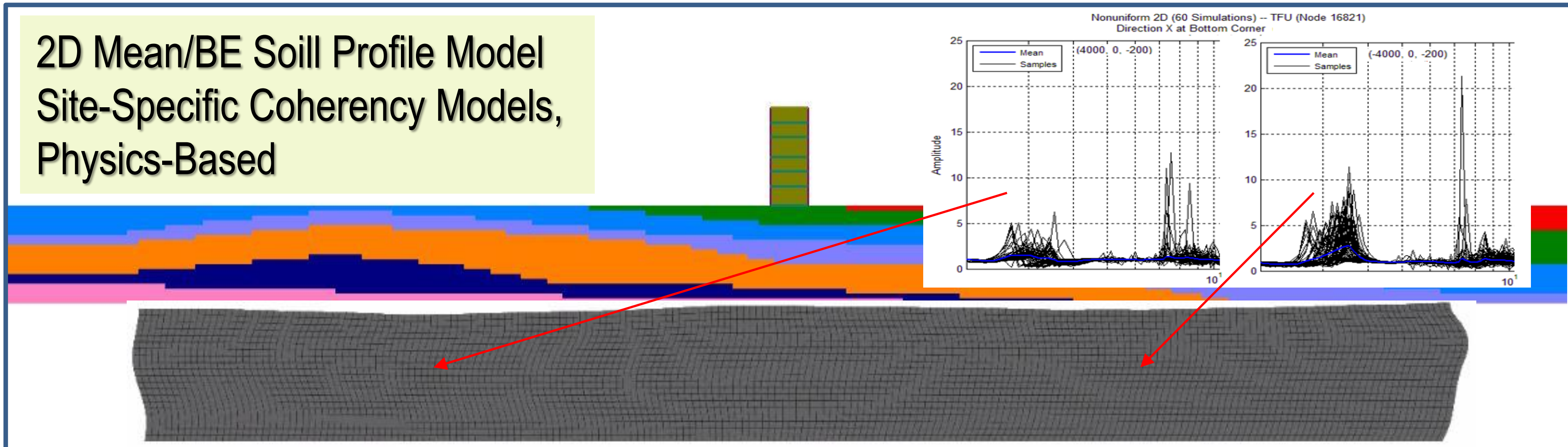

Application of 2D Probabilistic Soil Model Simulations for 1D Pinyon Flat Rock Site Layering Model

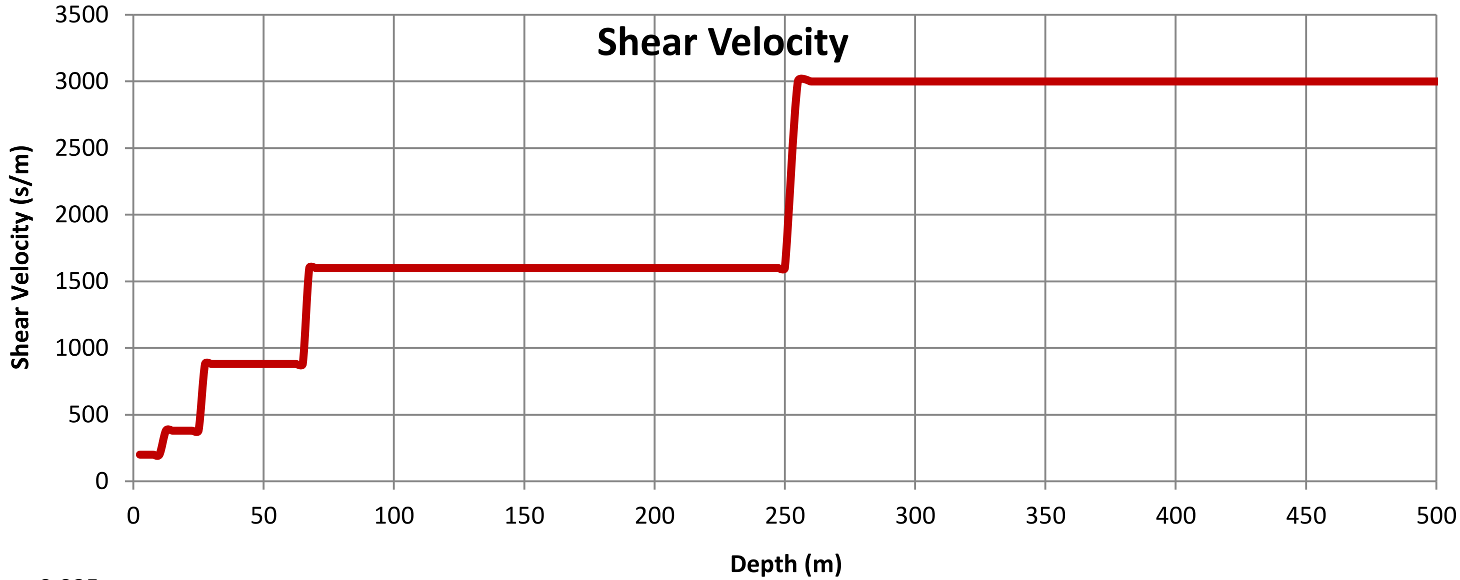

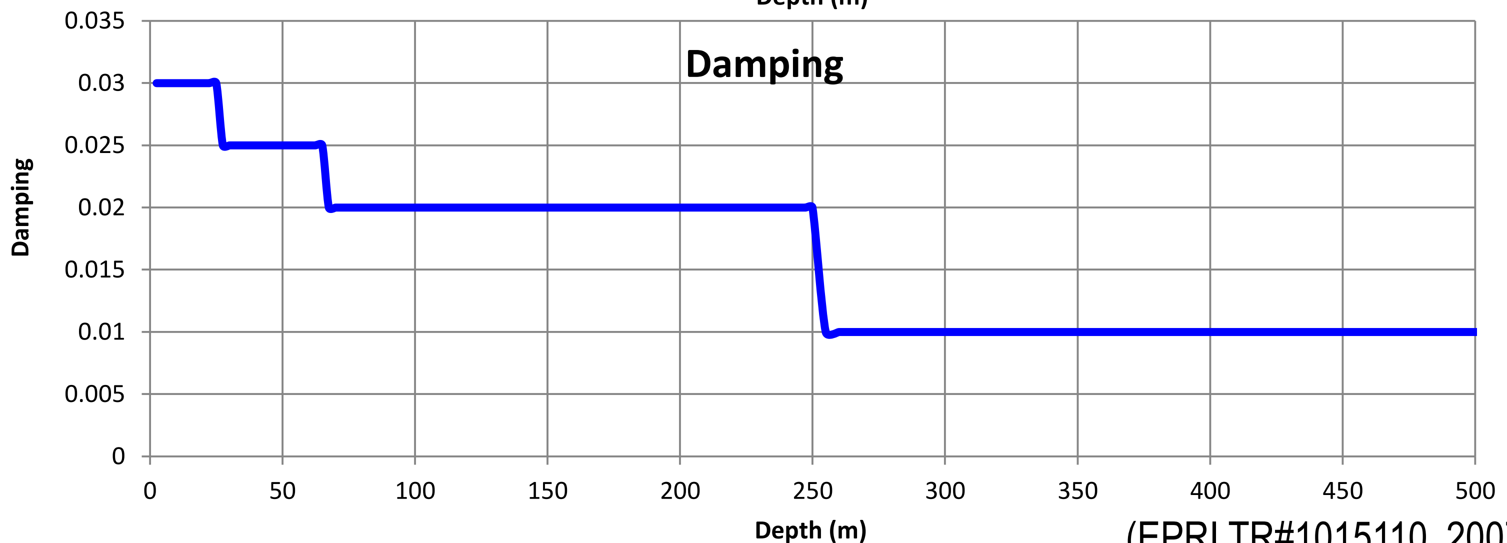

(EPRI TR#1015110, 2007)

Simulated Vs and D Soil Profiles for Pinyon Flat Site (Stochastic Field for 1000m H x 500m V Area)

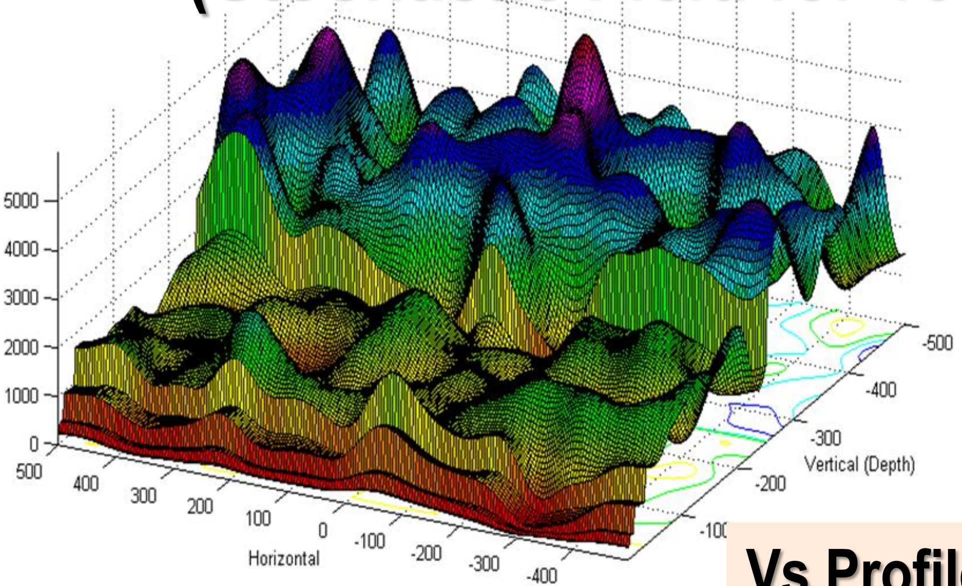

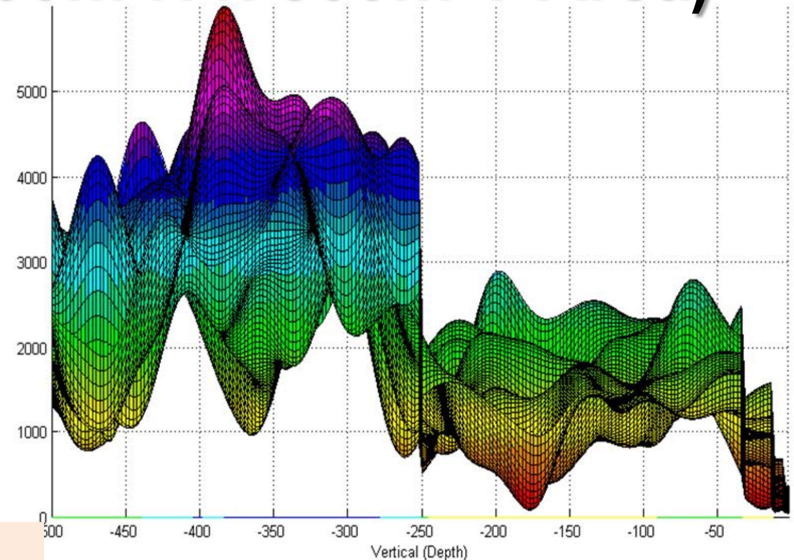

Vs Profile

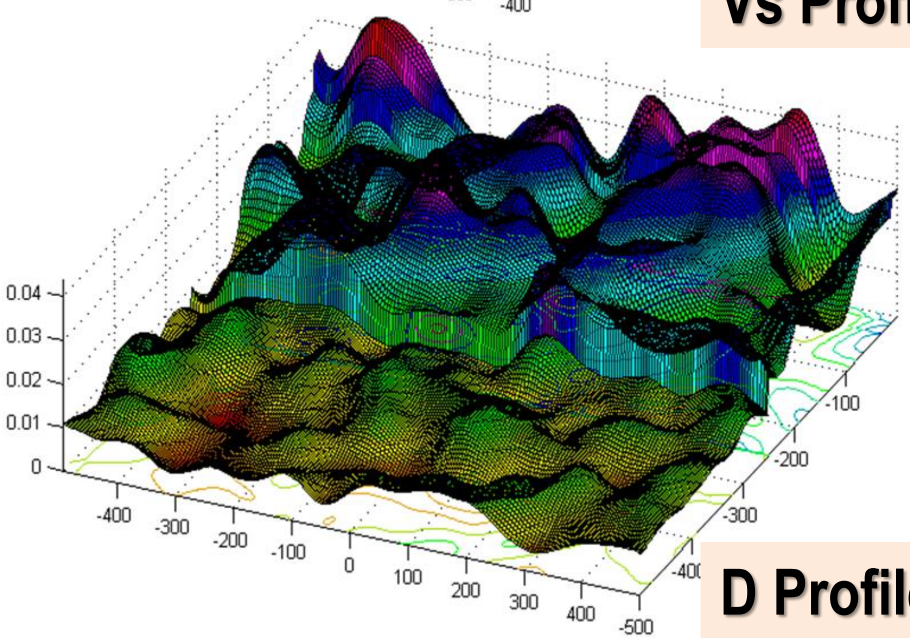

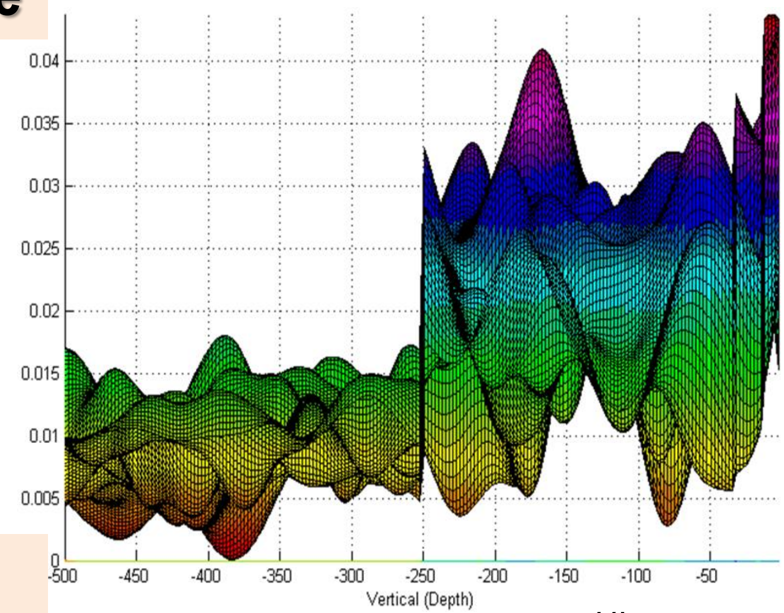

D Profile

Estimation of Site-Specific Coherence Functions for Pinyon Flat Site

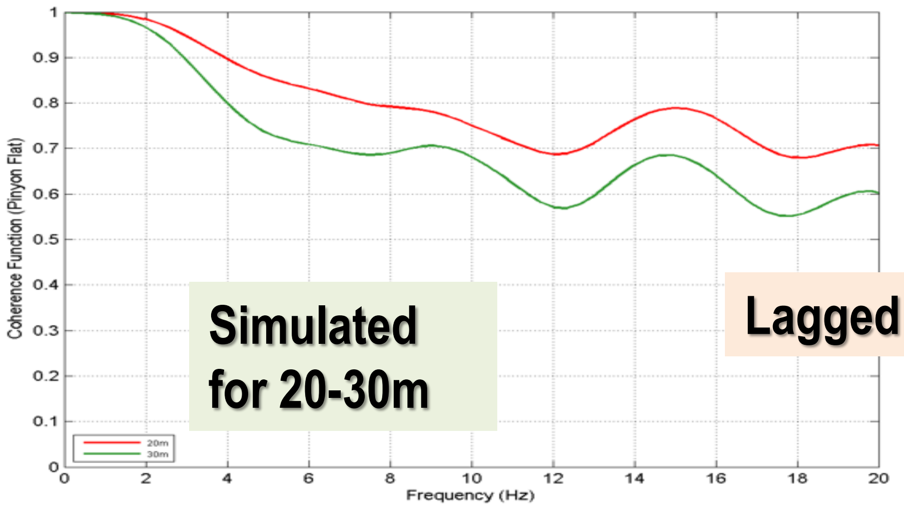

Lagged Coherence

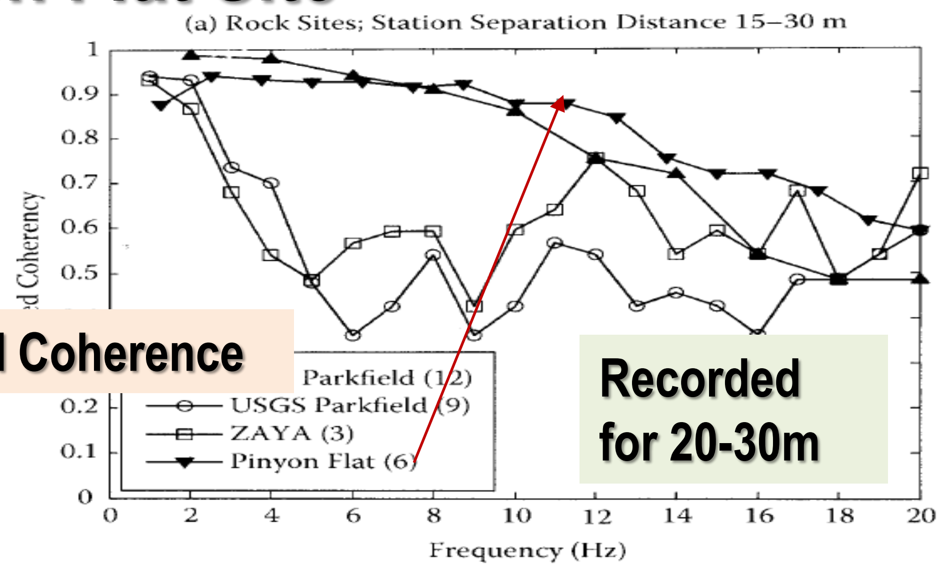

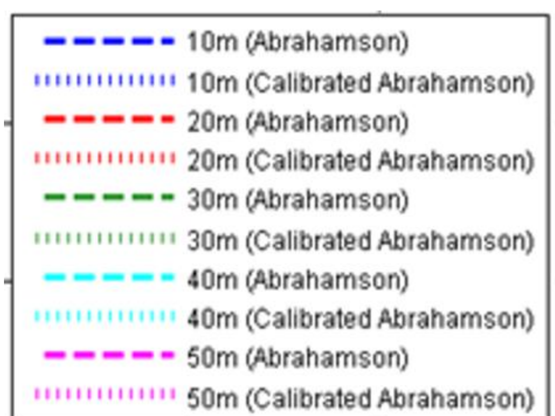

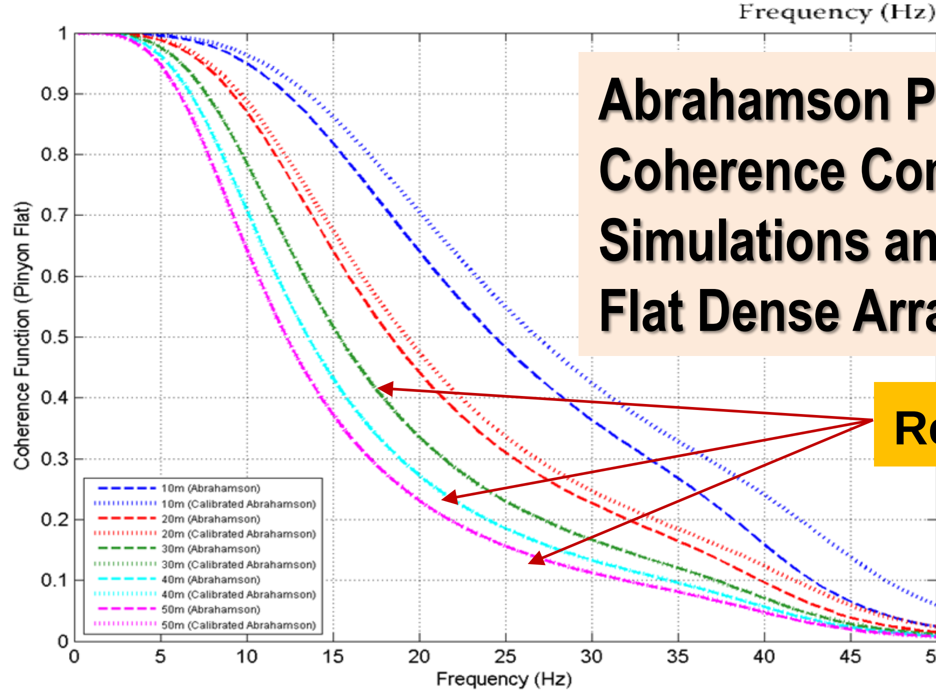

Abrahamson Plane Wave Coherence Computed from Simulations and Pinyon Flat Dense Arrays Records

Results overlap

Site-Specific Coherence Functions for *EDF Digital Site* with An Uniform Soil with Vs=818m/s

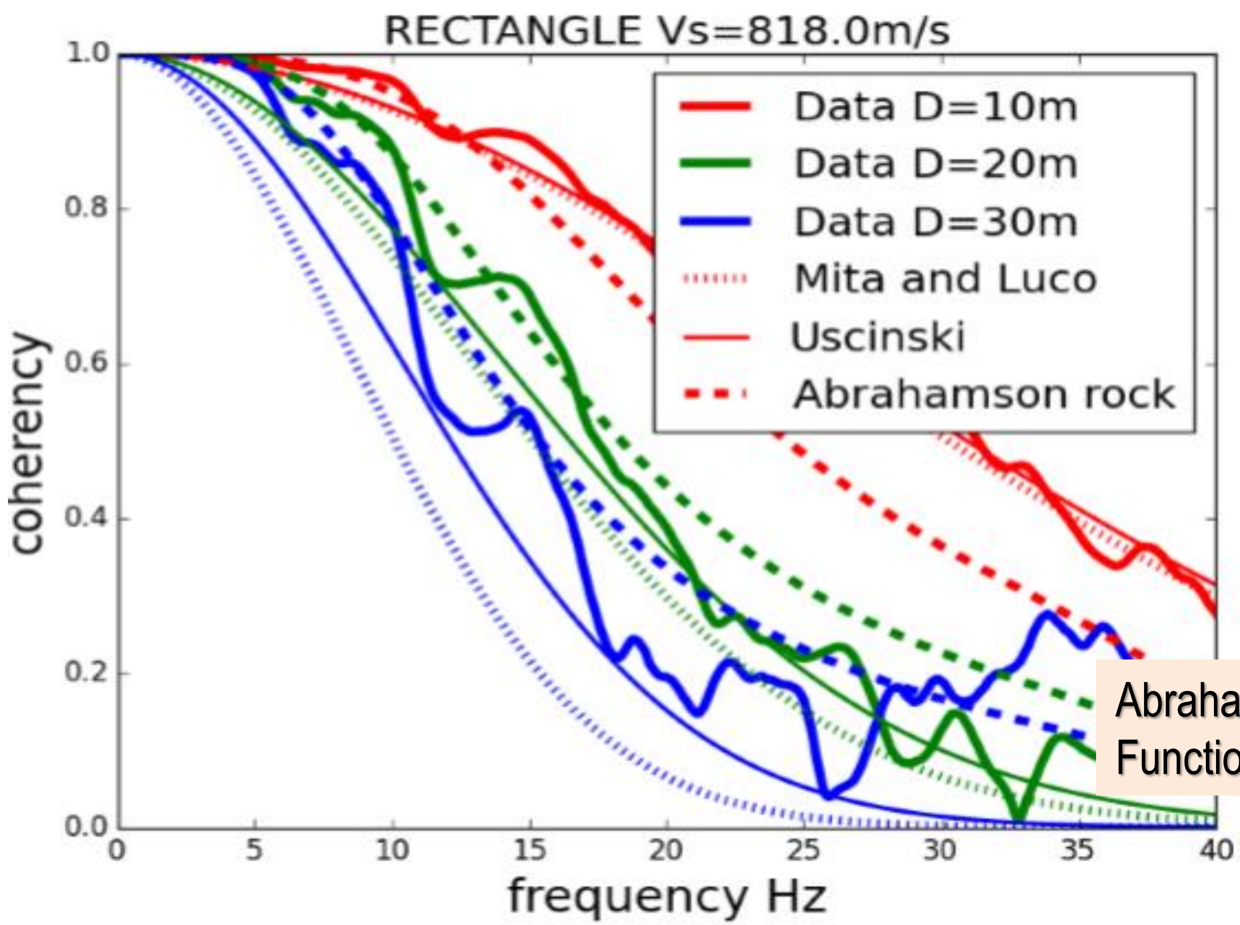

Abrahamson P-W coherence Function significantly different

Zentner, 2016

Site-Specific Coherence Functions Computed for *EDF Digital Site* with An Uniform Soil with Vs=818m/s

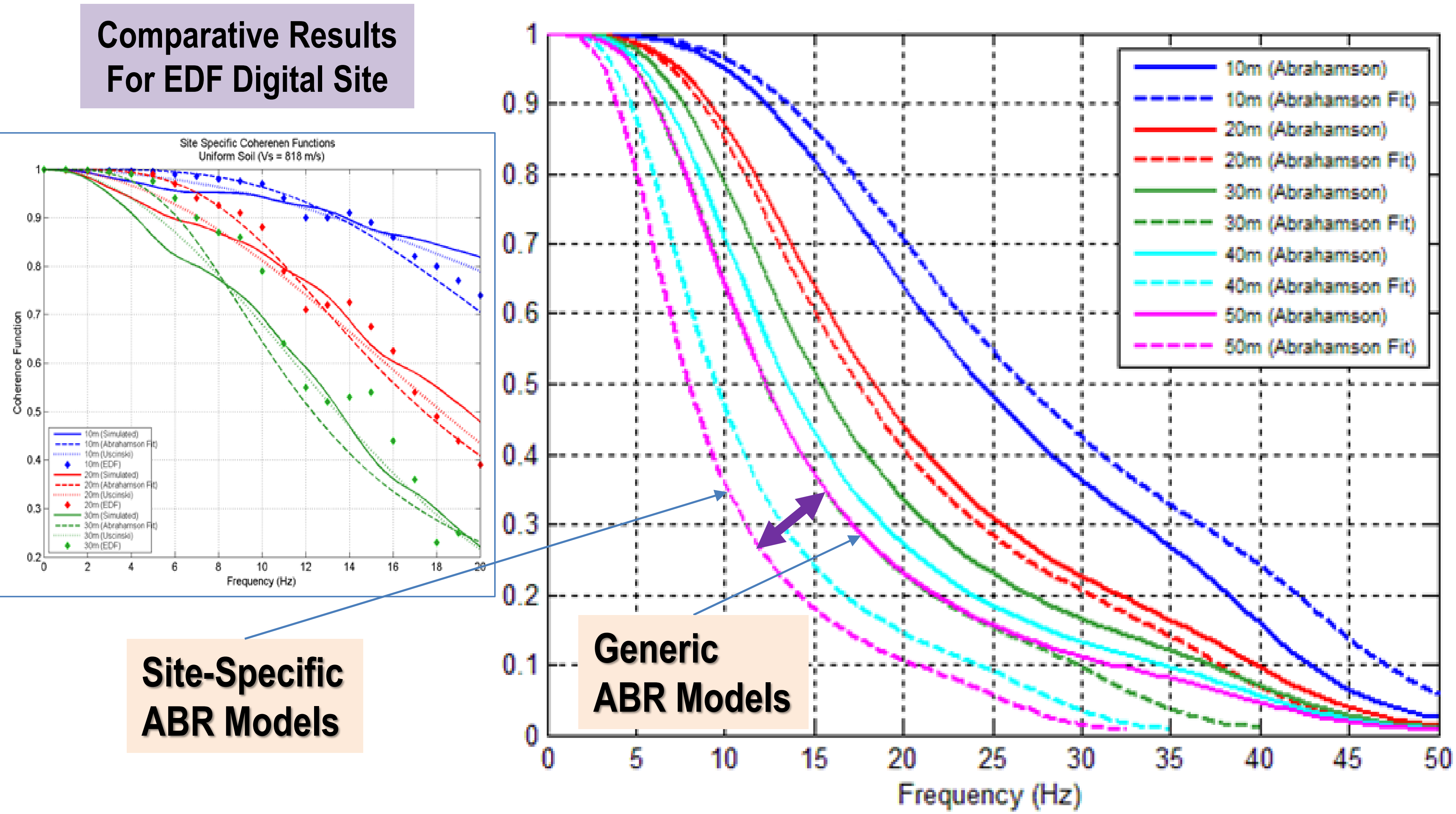

2) ACS SASSI Mathematical Modeling and Implementation for Incoherent SSI Analysis

Mathematical Modeling of Motion Incoherency

The seismic incoherent wave random field is represented by a space-time varying stochastic process or a time-varying stochastic field with zero-mean and Gaussian probability distribution that is completely described by its cross-spectral density function (CSD).

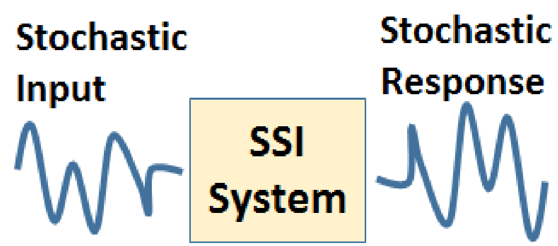

Incoherent SSI Approaches:

Since the simulated seismic input accelerations are non-stationary, non-Gaussian space-time stochastic processes, the most accurate approach to compute the stochastic SSI responses is the *stochastic simulation* (SS) approach based on the Monte Carlo simulation. ACS SASSI include also simplified *deterministic approaches* validated by EPRI (TR 1015111) for simple stick models with rigid basemat.

Incoherent SSI Analysis in ACS SASSI

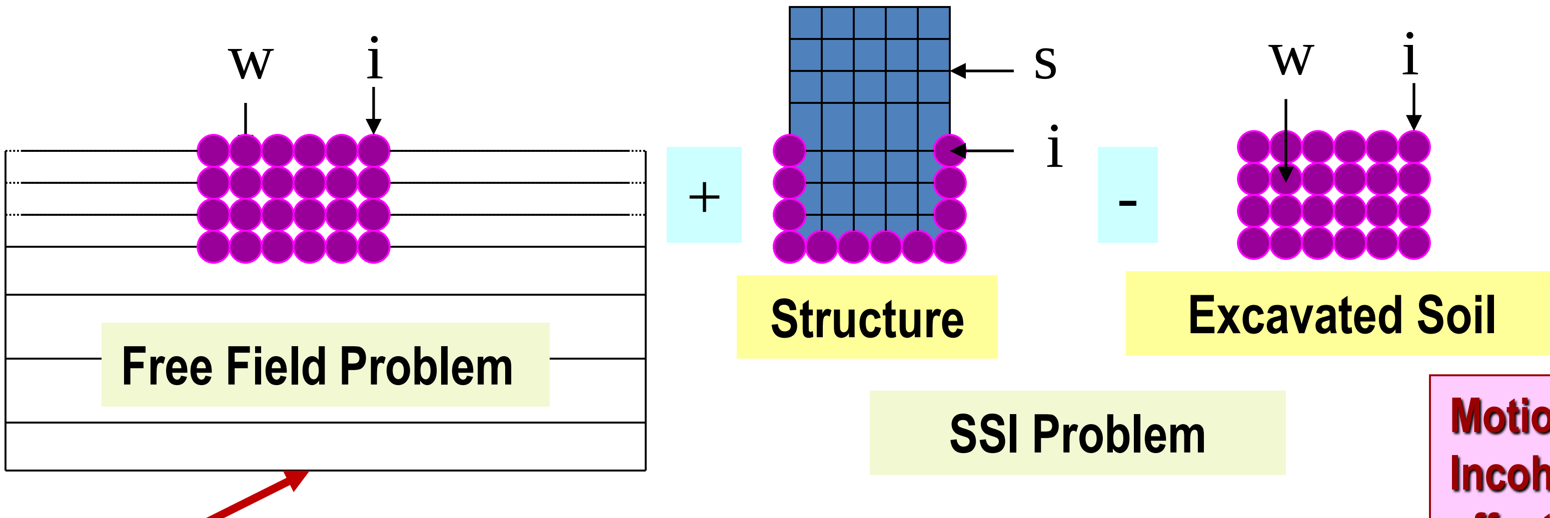

Motion Incoherency affects free-field motion at interaction nodes

Flexible Volume Method (using all excavated volume nodes)

$$\begin{bmatrix} C^e_{ii} - C^e_{ii} + X_{ii} & -C^e_{iw} - X_{iw} & C^s_{is} \\ -C^e_{wi} + X_{wi} & -C^e_{ww} + X_{ww} & 0 \\ C^s_{si} & 0 & C^s_{ss} \end{bmatrix} \begin{Bmatrix} U_i \\ U_w \\ U_s \end{Bmatrix} = \begin{Bmatrix} X_{ii} U'_i + X_{iw} U'_w \\ X_{wi} U'_i + X_{ww} U'_w \\ 0 \end{Bmatrix}$$

Flexible Interface Methods (using boundary volume nodes)

$$\begin{bmatrix} C^e_{ii} - C^e_{ii} + X_{ii} & -C^e_{iw} & C^s_{is} \\ -C^e_{wi} & -C^e_{ww} & 0 \\ C^s_{si} & 0 & C^s_{ss} \end{bmatrix} \begin{Bmatrix} U_i \\ U_w \\ U_s \end{Bmatrix} = \begin{Bmatrix} X_{ii} U'_i \\ 0 \\ 0 \end{Bmatrix}$$

$$\boxed{C(\omega) U(\omega) = Q(\omega)}$$

where $C(\omega) = K - \omega^2 M$

Incoherent SSI Analysis in Complex Frequency

The complex frequency response is computed as follows:

- Coherent SSI response:

Structural transfer function given input at interaction nodes

Coherent ground transfer function at interface nodes given control motion

$$U_s(\omega) = H_s(\omega) * H_g^c(\omega) * U_{g,0}(\omega)$$

Complex Fourier transform of control motion

- Incoherent SSI response:

Incoherent ground transfer function given coherent ground motion and coherency model (random spatial variation in horizontal plane)

$$U_s(\omega) = H_s(\omega) * S_g^i(\omega) * H_g^c(\omega) * U_{g,0}(\omega)$$

$$S_g(\omega) = [\Phi(\omega)][\lambda(\omega)]\{\eta_\theta\}$$

Complex Fourier transform of relative spatial variations of soil motion at interaction nodes = stochastic wave field

Eigen**modes** of coherency kernel (deterministic part)

Random **phases** (stochastic part)

Incoherent SSI Analysis in Complex Frequency

Coherent SSI Response

$$U_i^{s,c}(\omega) = \sum_{k=1}^{N} H_{i,k}^{s}(\omega) U_k^{g,c}(\omega) = \sum_{k=1}^{N} H_{i,k}^{s}(\omega) H_k^{g,c}(\omega) U_0^{g}(\omega)$$

Incoherent SSI Response

$$U_i^{s,i}(\omega) = \sum_{k=1}^{N} H_{i,k}^{s}(\omega) U_k^{g,i}(\omega) = \sum_{k=1}^{N} H_{i,k}^{s}(\omega) [\sum_{j=1}^{M} \Phi_{j,k}(\omega) \lambda_j(\omega) \eta_{\theta j}(\omega)]\, H_k^{g,c}(\omega) U_0^{g}(\omega)$$

(Ghiocel, 2009, 2013)

How Many Modes Should Be Considered for SRSS Approaches? SS Considers All!

Low Frequency/Large Wavelengths/Only Few Low Order Incoherency Modes

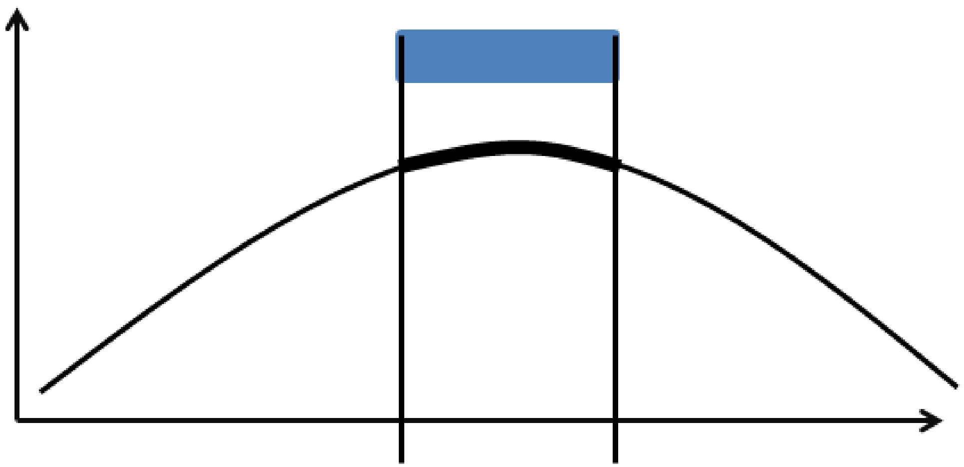

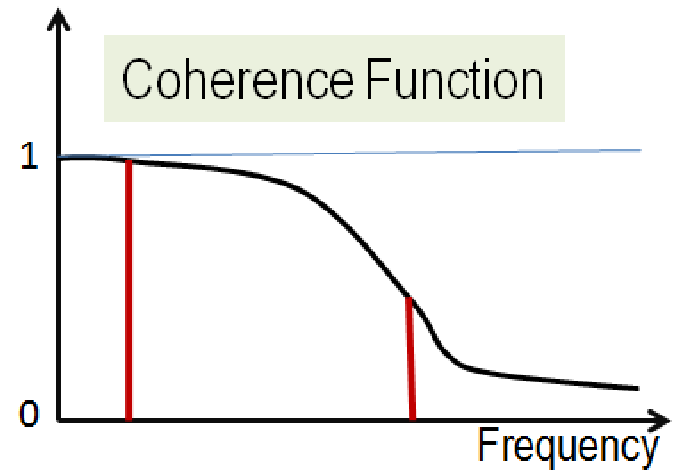

High Frequency/Short Wavelengths/Low and High Order Incoherency Modes

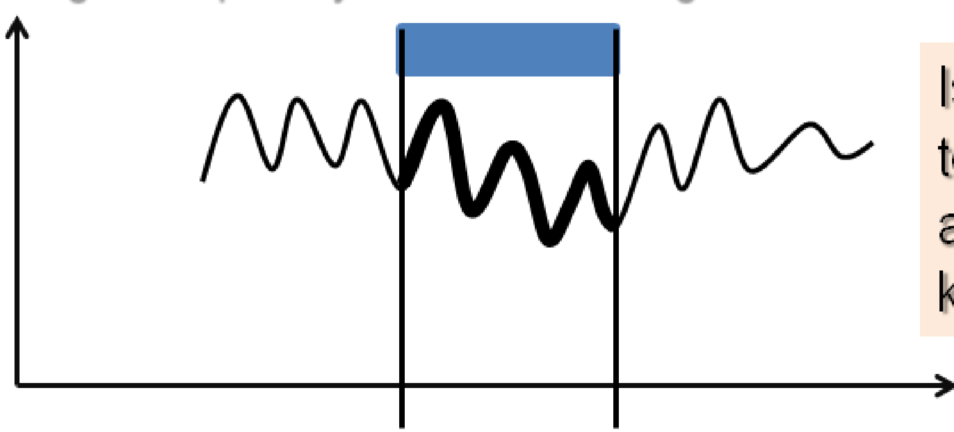

Is the foundation sufficiently rigid
to neglect high order modes
at high frequency due to
kinematic interaction effects?

Spectral Factorization of Coherency Matrix Using Limited Number of Incoherency Modes

Spectral factorization uses the diagonal eigenvalue matrix and the eigenvector matrix of coherency matrix at any given frequency

$$\mathbf{\Sigma}(\omega) = \mathbf{\Phi}(\omega)\mathbf{\Lambda}^2(\omega)\mathbf{\Phi}^T(\omega)$$

To check the eigen-expansion convergence the norm of the trace of the eigen-value matrix $\mathbf{\Lambda}^2$ that is equal to the original matrix $\mathbf{\Sigma}$.

$$\sum_{j=1}^{N}\lambda_j^2 = N \quad \text{or} \quad \sum_{j=1}^{N}\frac{\lambda_j^2}{N}100 = 100\%$$

For m < N eigen-modes their cumulative contribution to the total variance of the motion amplitude should be greater than 90% (similar criterion with 90% cumulative modal mass in dynamics)

$$\sum_{j=1}^{m}\upsilon_j = \sum_{j=1}^{m}\frac{\lambda_j^2}{N}100 > 90\%$$

Stochastic simulation includes all incoherency modes! Exact!

Free-Field Covariance Matrix Convergence

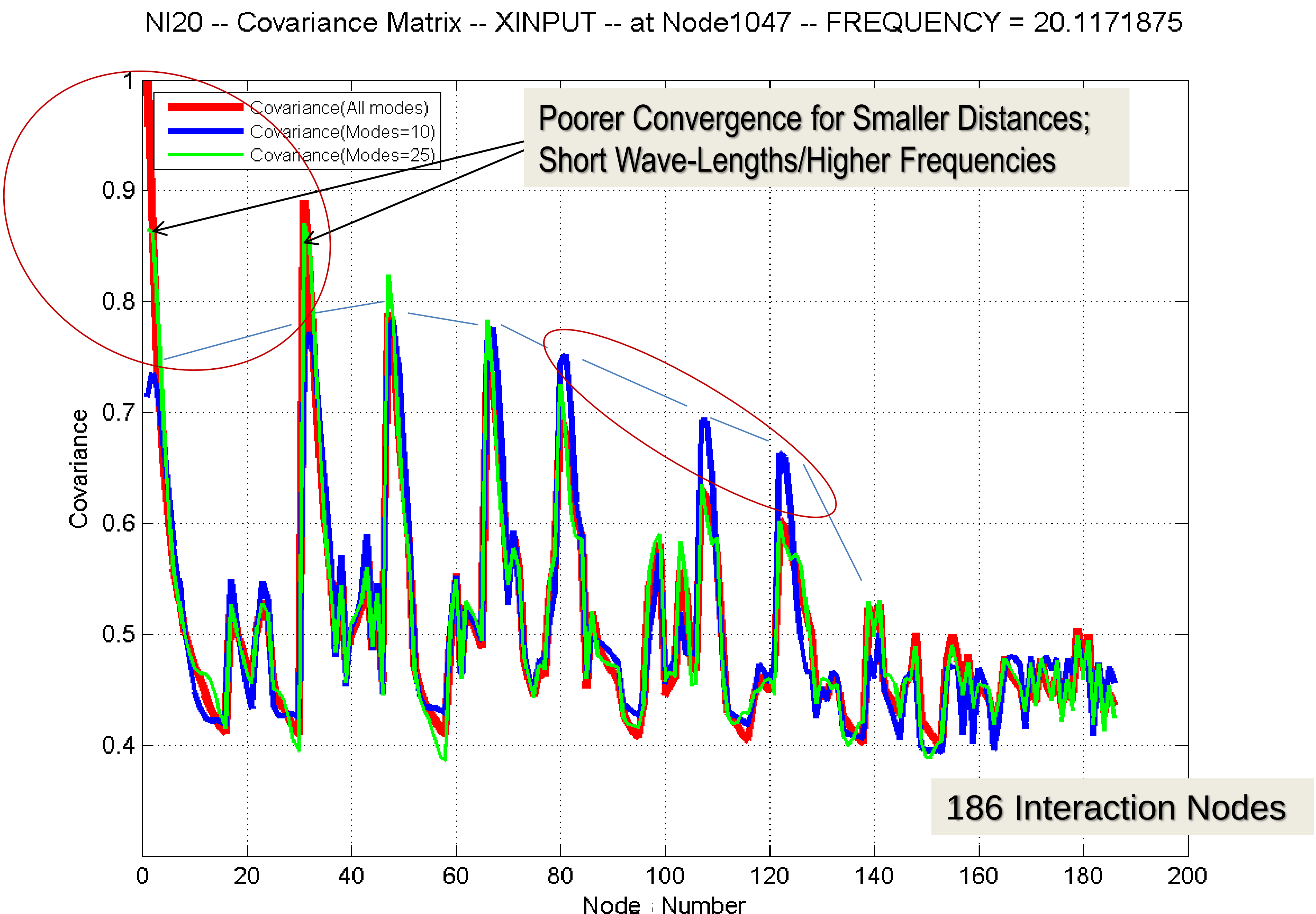

Cumulative Modal Contribution for 10 Modes

2007 Abrahamson Rock Site Model

*** CUMULATIVE MODAL MASS/VARIANCE(%) ***

Frequency =	0.098	Horizontal =	100.00%	Vertical =	100.00%
Frequency =	1.562	Horizontal =	100.00%	Vertical =	99.97%
Frequency =	3.125	Horizontal =	99.94%	Vertical =	99.75%
Frequency =	4.688	Horizontal =	99.69%	Vertical =	99.20%
Frequency =	6.250	Horizontal =	98.90%	Vertical =	98.09%
Frequency =	7.812	Horizontal =	97.01%	Vertical =	96.00%
Frequency =	9.375	Horizontal =	93.55%	Vertical =	92.59%
Frequency =	10.938	Horizontal =	88.54%	Vertical =	87.93%
Frequency =	12.500	Horizontal =	82.47%	Vertical =	82.46%
Frequency =	14.062	Horizontal =	75.90%	Vertical =	76.67%
Frequency =	15.625	Horizontal =	69.31%	Vertical =	70.92%
Frequency =	17.188	Horizontal =	63.02%	Vertical =	65.45%
Frequency =	18.750	Horizontal =	57.20%	Vertical =	60.37%
Frequency =	20.312	Horizontal =	51.92%	Vertical =	55.74%
Frequency =	21.875	Horizontal =	47.19%	Vertical =	51.55%
Frequency =	23.438	Horizontal =	42.99%	Vertical =	47.79%
Frequency =	25.000	Horizontal =	39.26%	Vertical =	44.40%
Frequency =	26.562	Horizontal =	35.96%	Vertical =	41.37%
Frequency =	28.125	Horizontal =	33.04%	Vertical =	38.65%
Frequency =	29.688	Horizontal =	30.42%	Vertical =	36.20%
Frequency =	31.250	Horizontal =	28.04%	Vertical =	34.00%
Frequency =	32.812	Horizontal =	25.81%	Vertical =	32.01%
Frequency =	34.375	Horizontal =	23.63%	Vertical =	30.21%
Frequency =	35.938	Horizontal =	21.37%	Vertical =	28.57%
Frequency =	37.500	Horizontal =	18.93%	Vertical =	27.09%
Frequency =	39.062	Horizontal =	16.31%	Vertical =	25.74%

Comparative 20 vs. 40 Incoherent Mode Solution Using SRSS Deterministic Approach

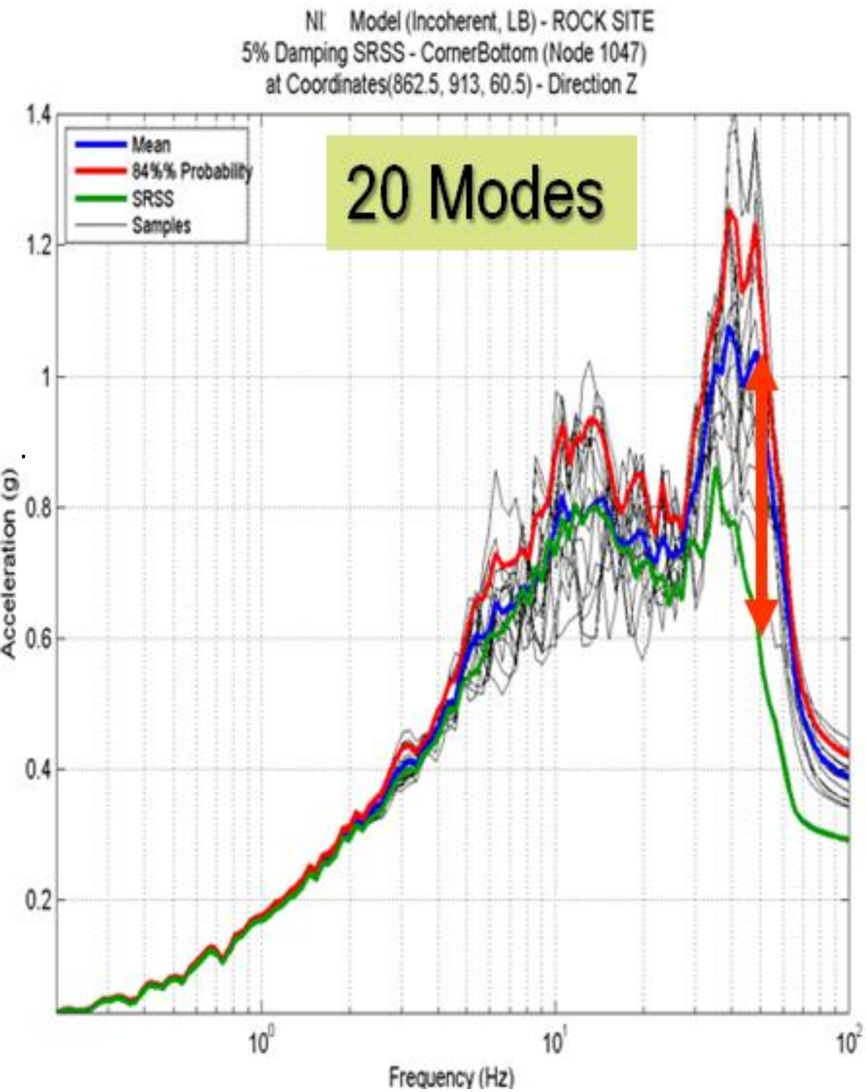

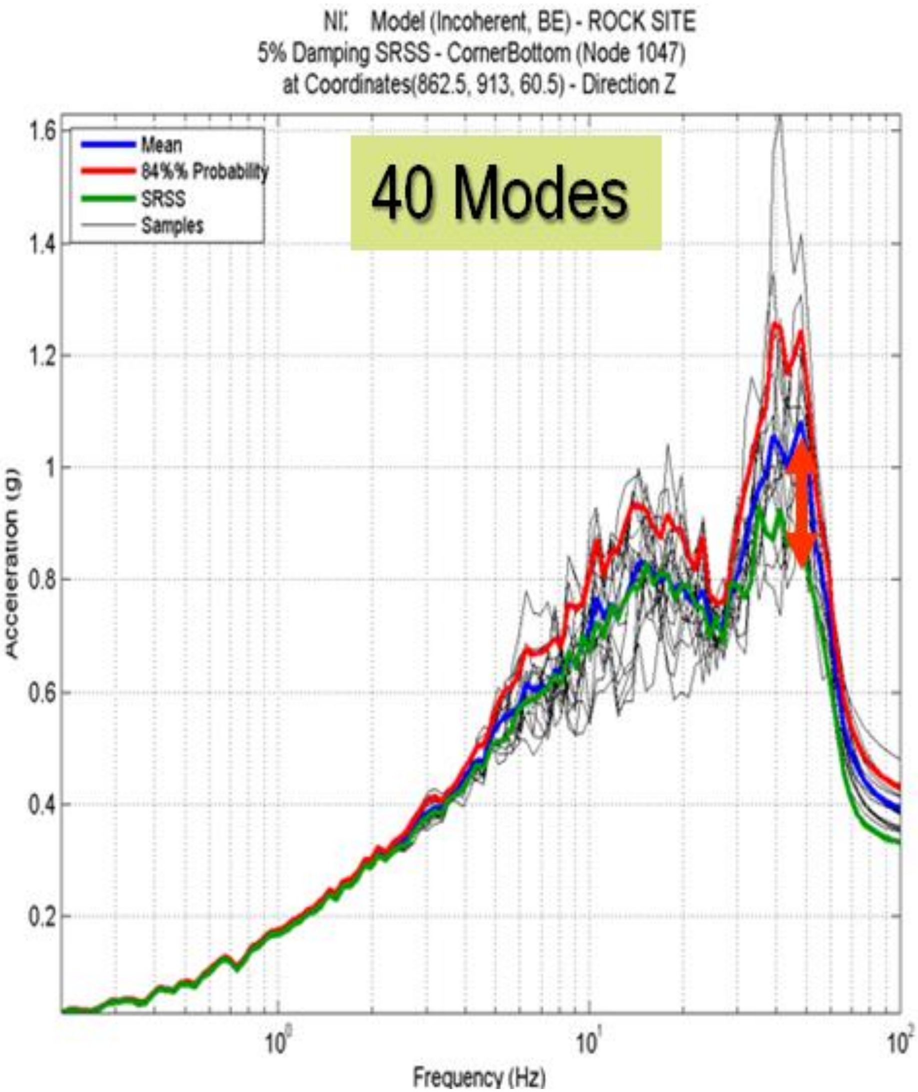

Comparative 20 vs. 40 Incoherent Mode Solution Using SRSS Deterministic Approach

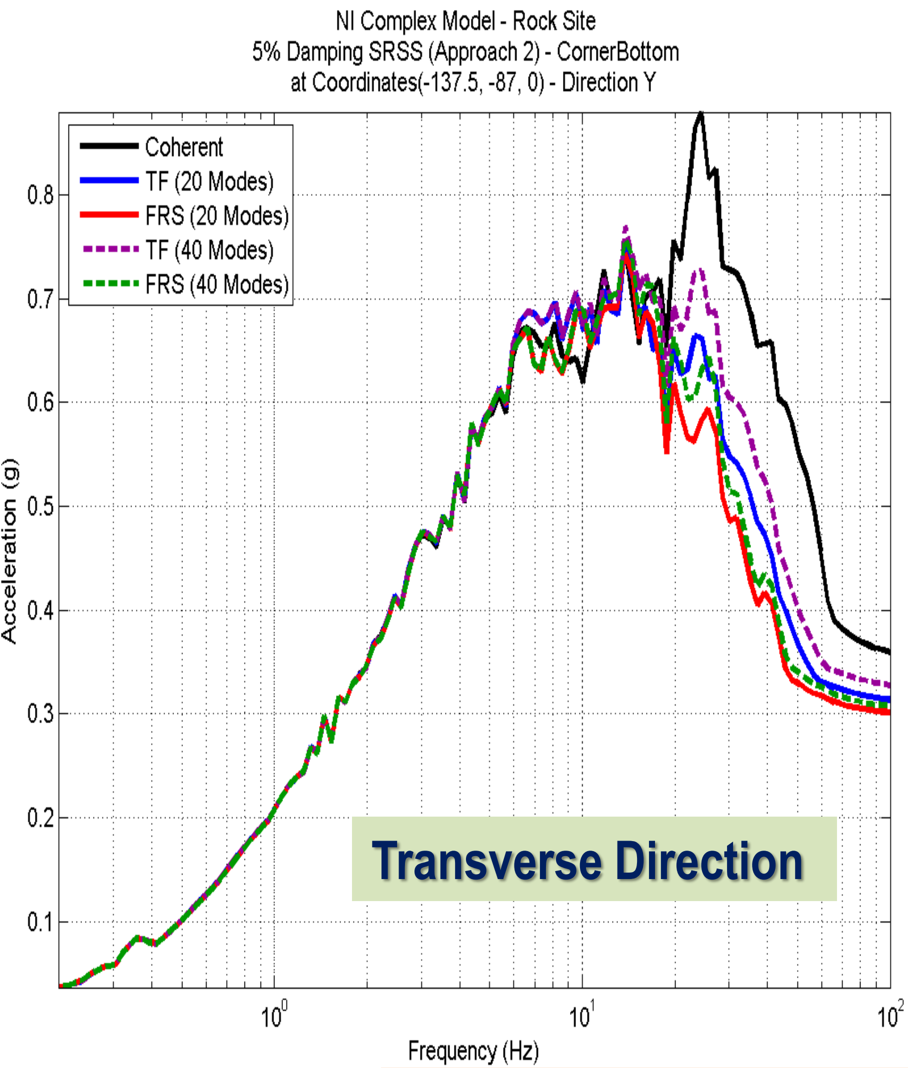

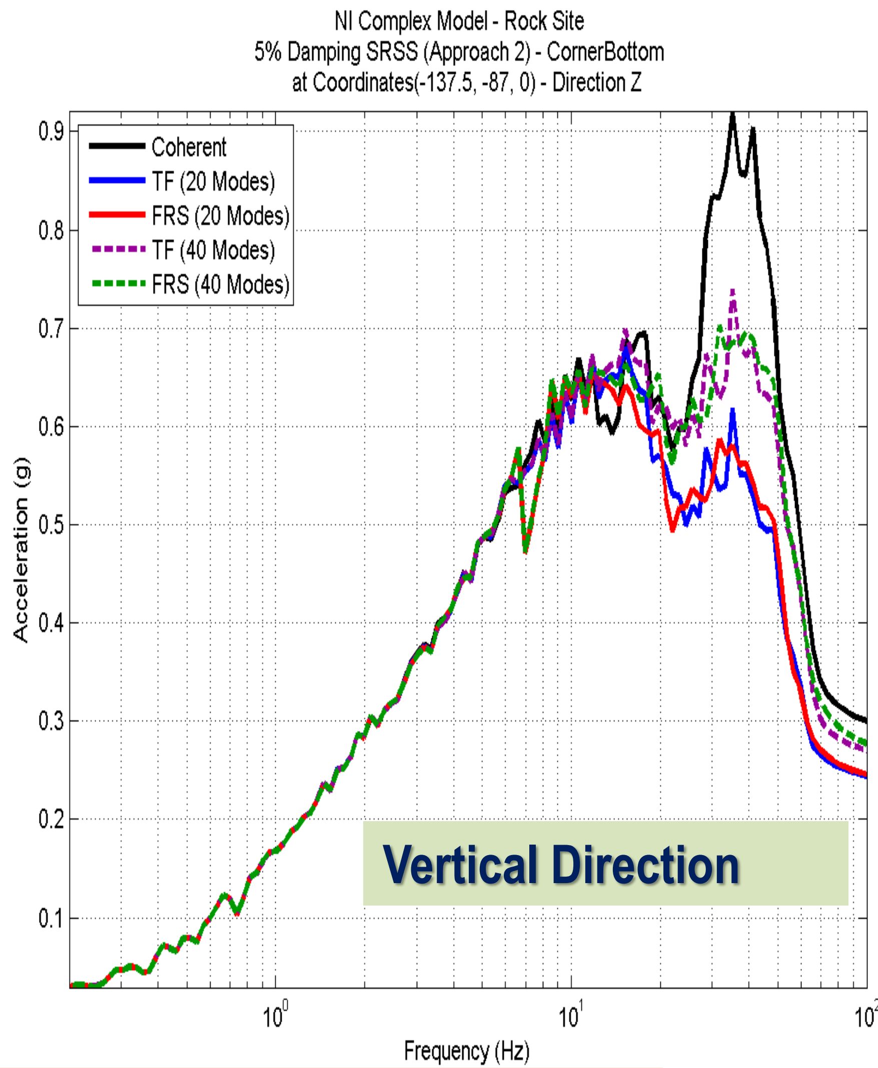

Basemat Corner ISRS of NI Complex with 50m Width

Basemat Flexibility Effects on RB Complex ISRS

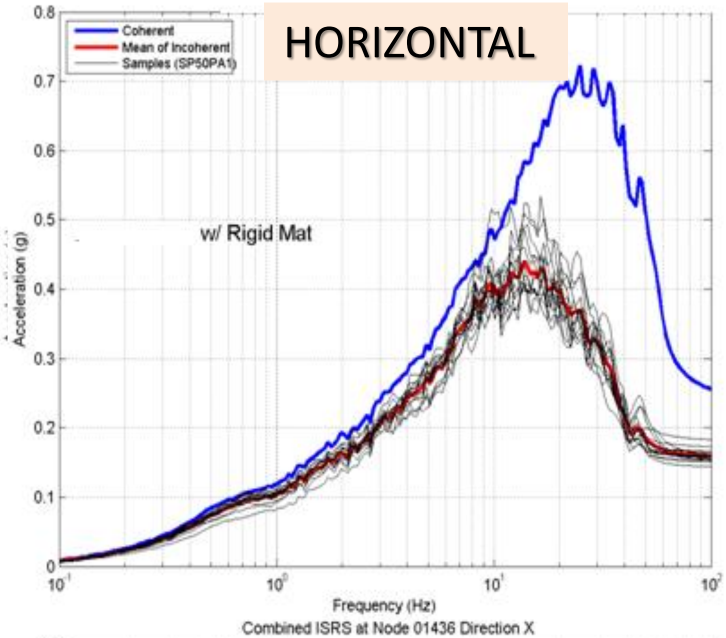

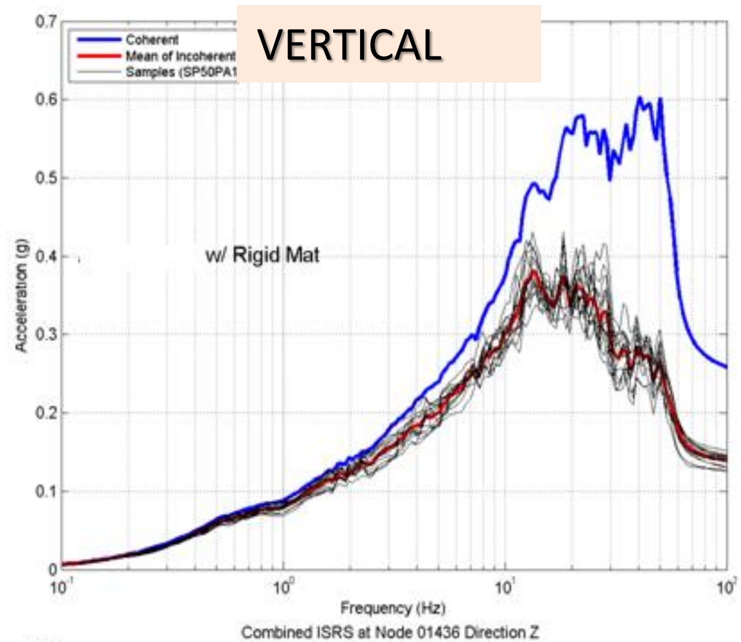

Elastic
is 20%
up for
horizonta

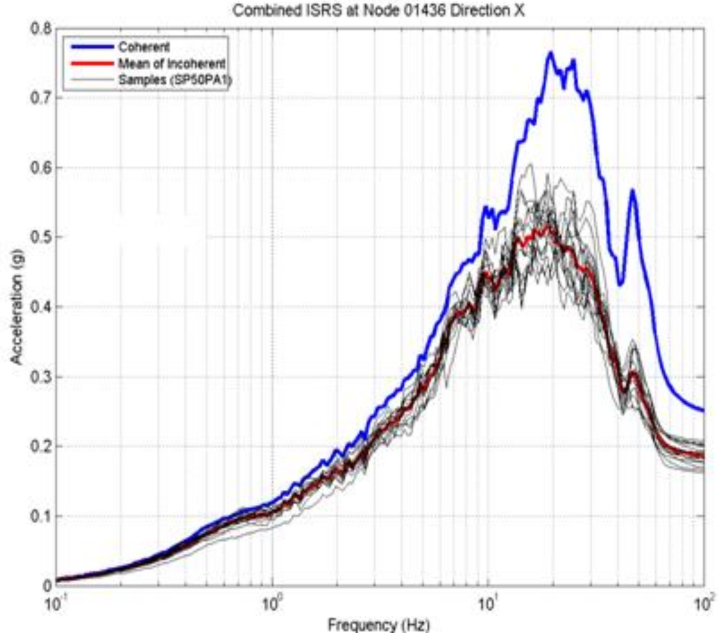

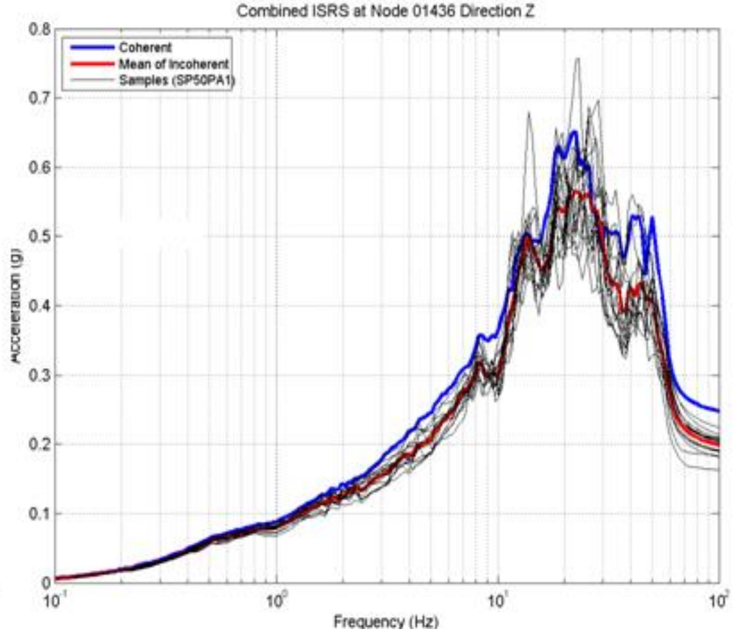

lastic
s 65% (!)
p for
ertical

2007 EPRI Validation Study on Seismic Incoherent SSI Approaches

(EPRI Report # 1015111)

EPRI AP1000 Stick Model: 3 Stick Models with A Common Rigid Basemat

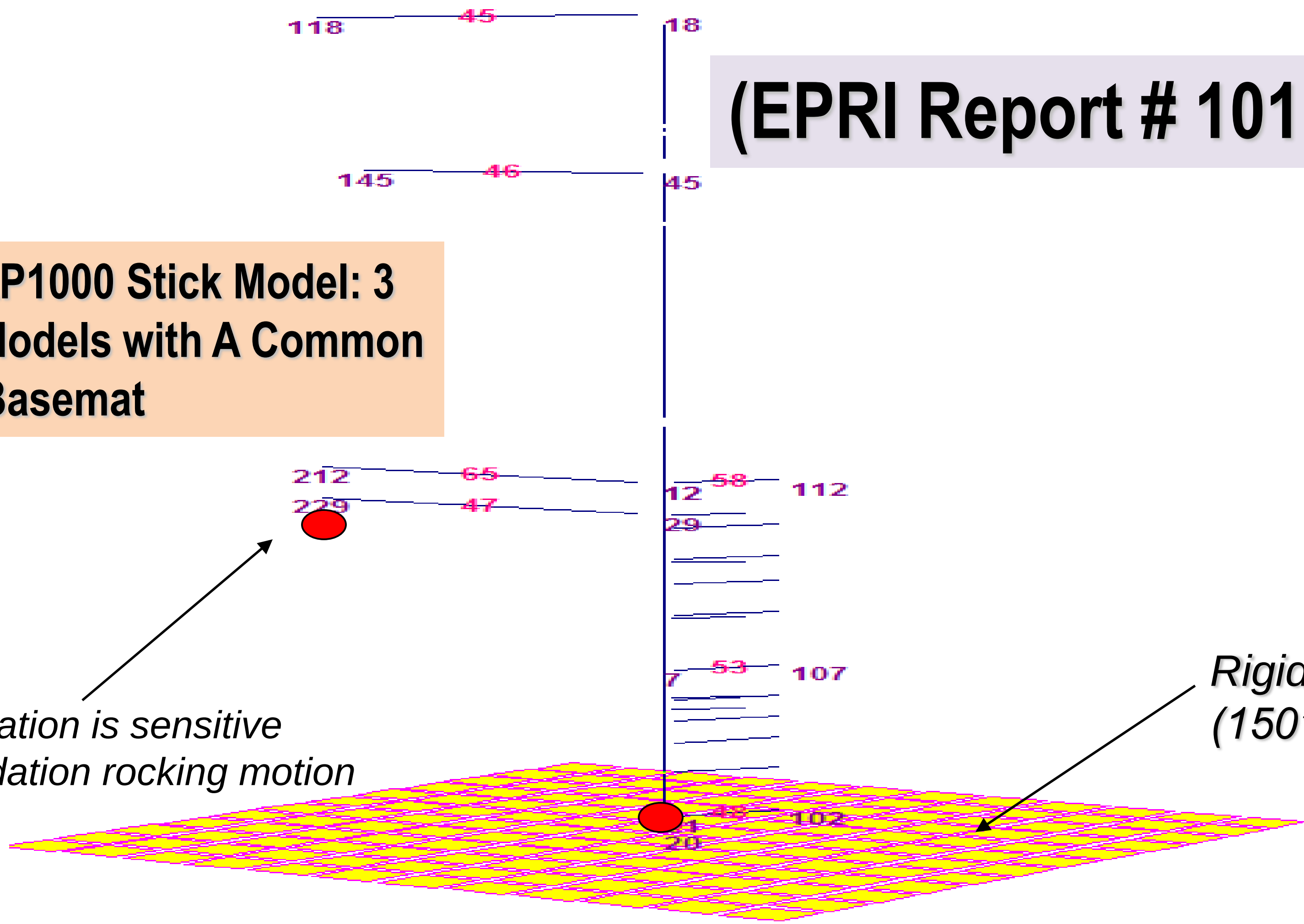

Z translation is sensitive to foundation rocking motion

Rigid Mat (150'x150')

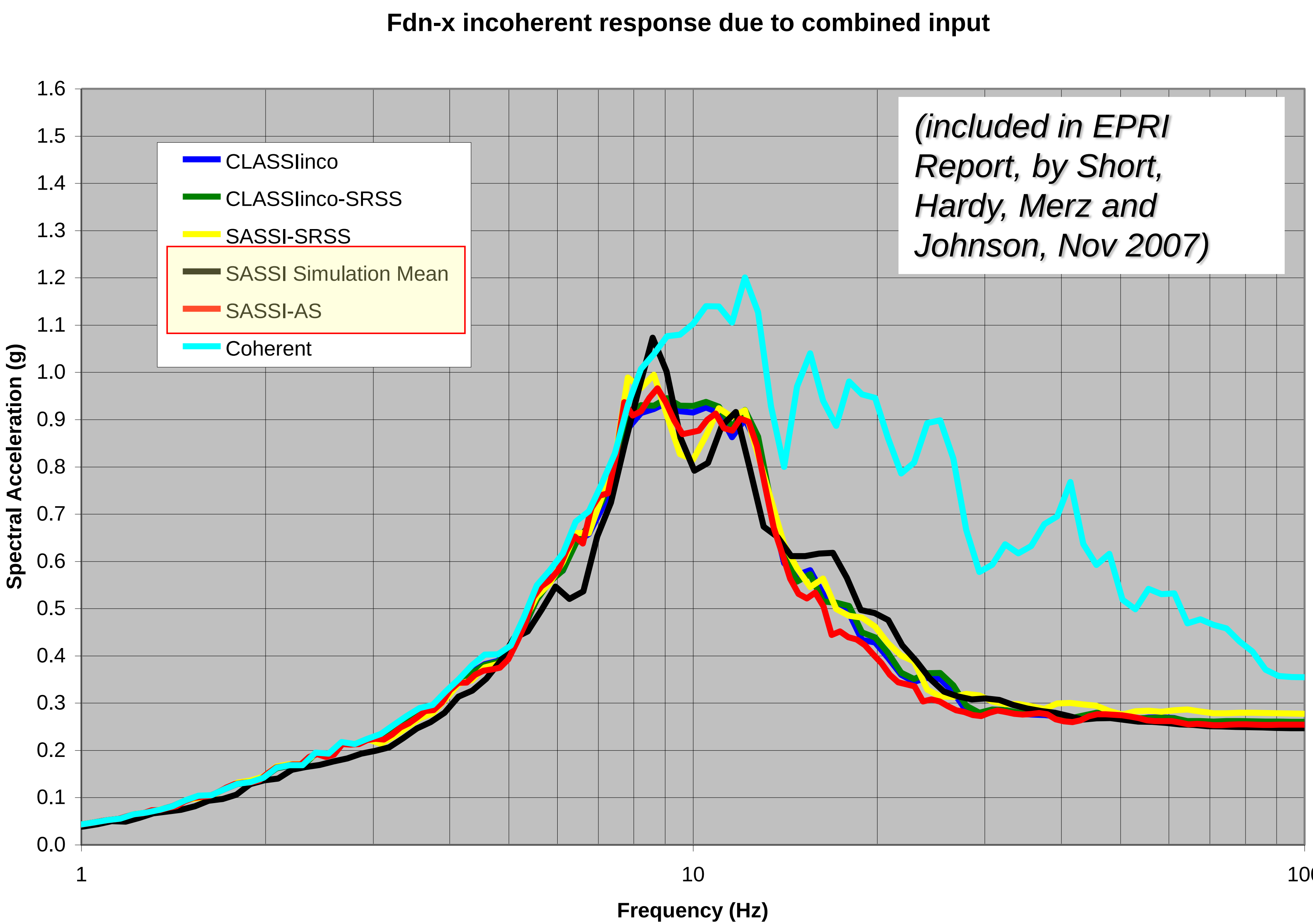

Center of Foundation (Node 1) Response Spectra – X Direction
CLASSIinco, CLASSIinco-SRSS, Bechtel SASSI-SRSS, ACS SASSI Simulation Mean and AS

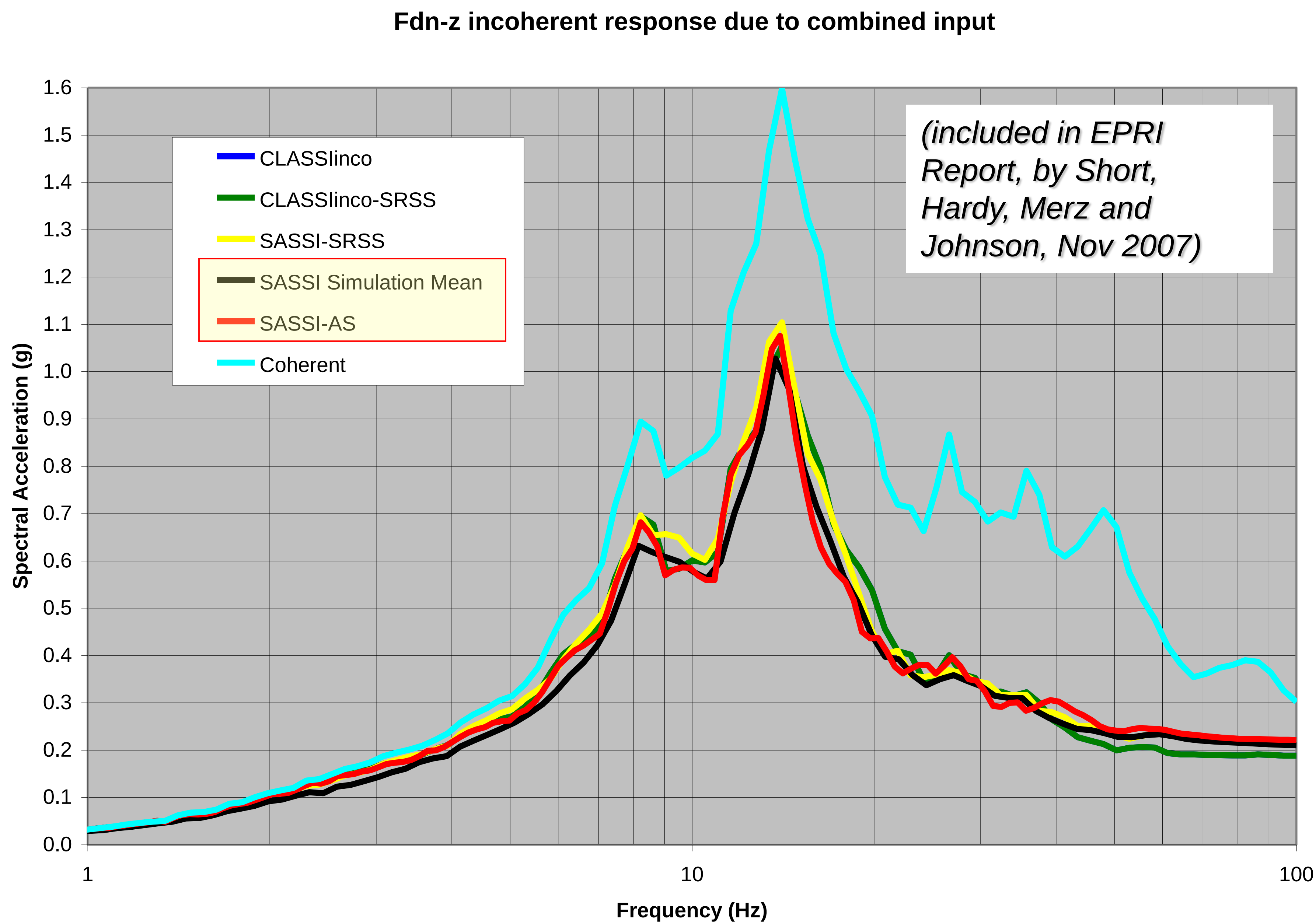

Center of Foundation (Node 1) Response Spectra – Z Direction

CLASSIinco, CLASSIinco-SRSS, Bechtel SASSI-SRSS, ACS SASSI Simulation Mean and AS

EPRI Conclusions on Incoherency Effects Based on AP1000 Stick Model (EPRI Report # 1015111, Nov 30, 2007)

The qualitative effects of motion incoherency effects are:

i) for horizontal components, there is a reduction in excitation translation concomitantly with an increase of torsion and a reduction of foundation rocking

ii) for vertical components, there is a reduction in excitation translation concomitantly with an increase of rocking excitation.

Benchmarked SASSI-Based "Consensus" Approaches:

1) Stochastic Simulation – As reference approach (*with phase adjustment*)
2) SRSS TF Approach (with ATF zero-phases and includes 10 modes)
3) AS Approach (with phase adjustment)

Other remarks:

- No evaluation of the effects of zeroing the ATF phases
- No guidance for flexible or embedded foundations
- No guidance for the piping/equipment multiple history analysis with incoherent inputs
- No specific guidance is provided for evaluation of incoherent structural forces

Motion Incoherency Differential Phasing Effects

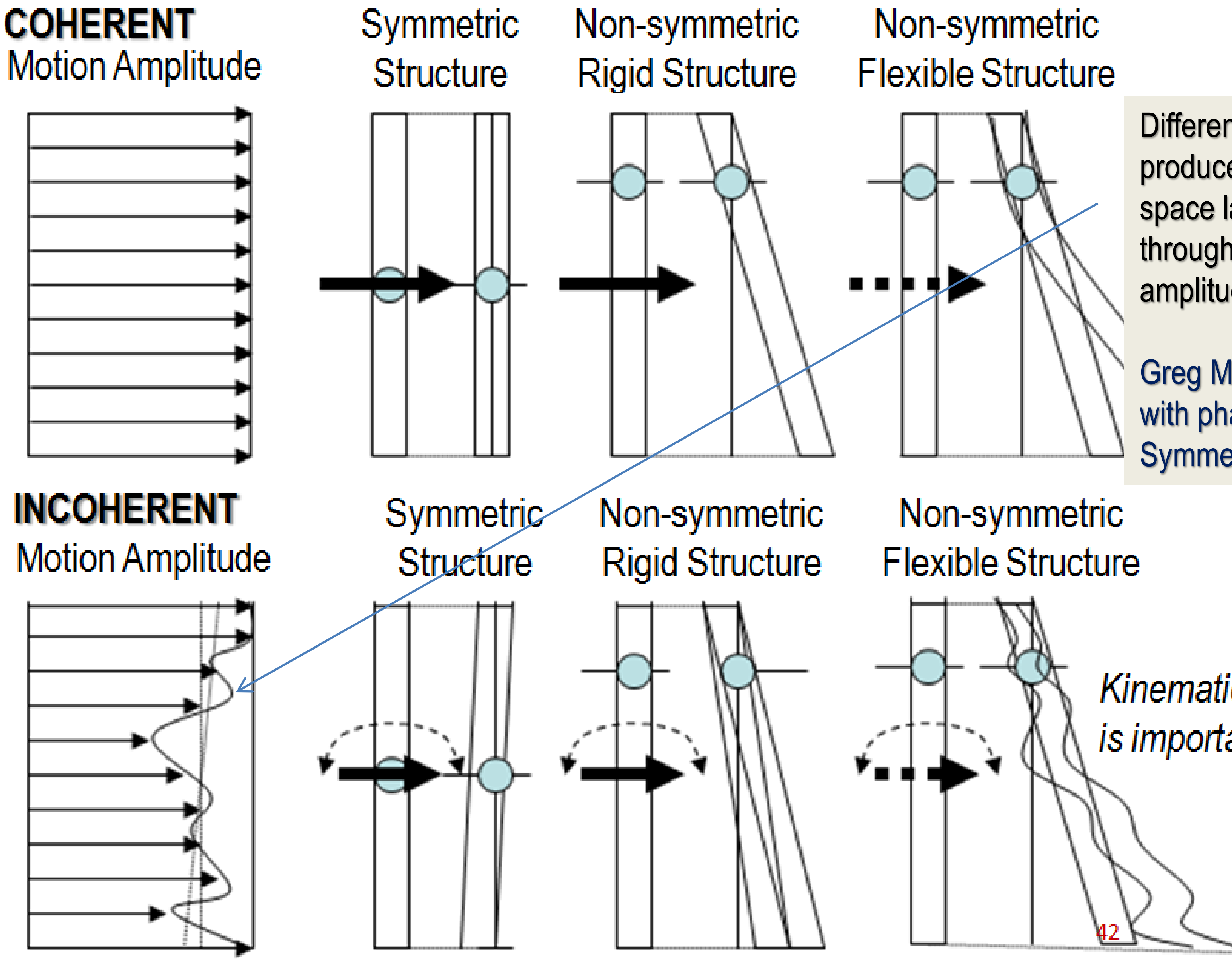

Differential phasing produces time and space lags and through these, amplitude variations

Greg Mertz's example with phasing effect on Symmetric beam

Differential Phasing Effects for Same Harmonic Inputs at Supports with Zero and Nonzero Time Lags

Symmetric Structure Subjected to Harmonic Inputs at Supports

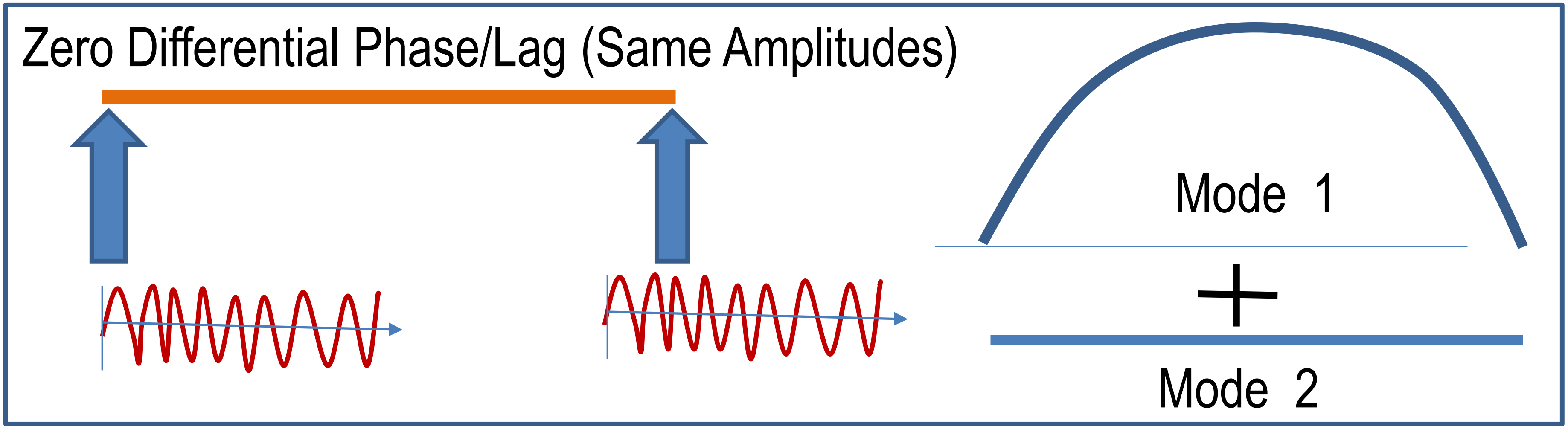

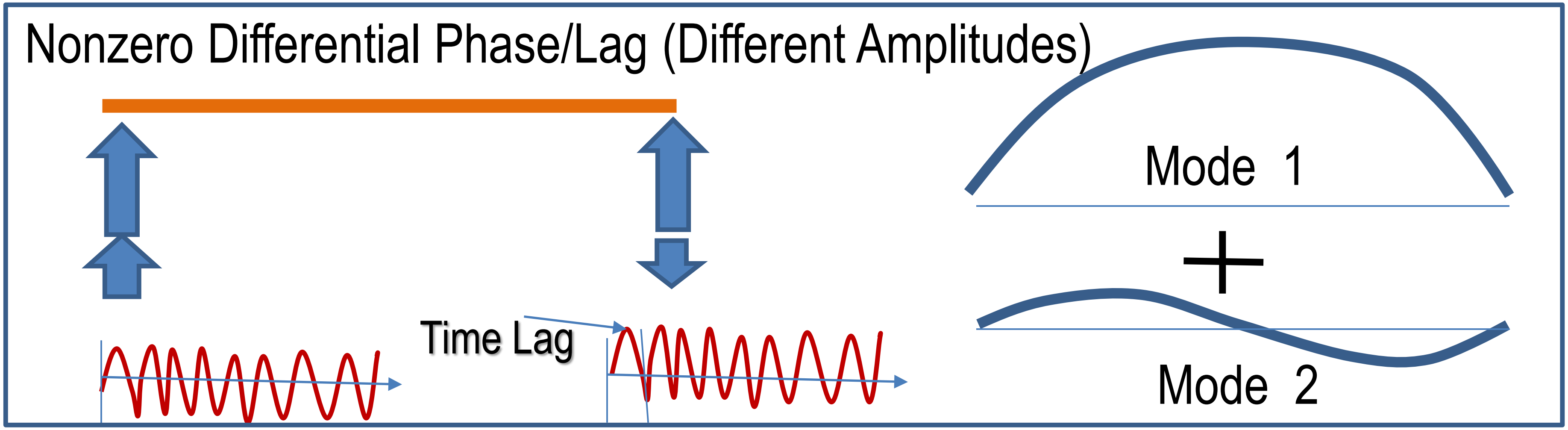

Effect of Zeroing Phases for Low-Mid Frequencies

For dominant single mode situations (in lower frequency range), the *neglect of the (differential) phases* that produce random amplitude variations in frequency space, *basically changes the problem and departs from reality.*

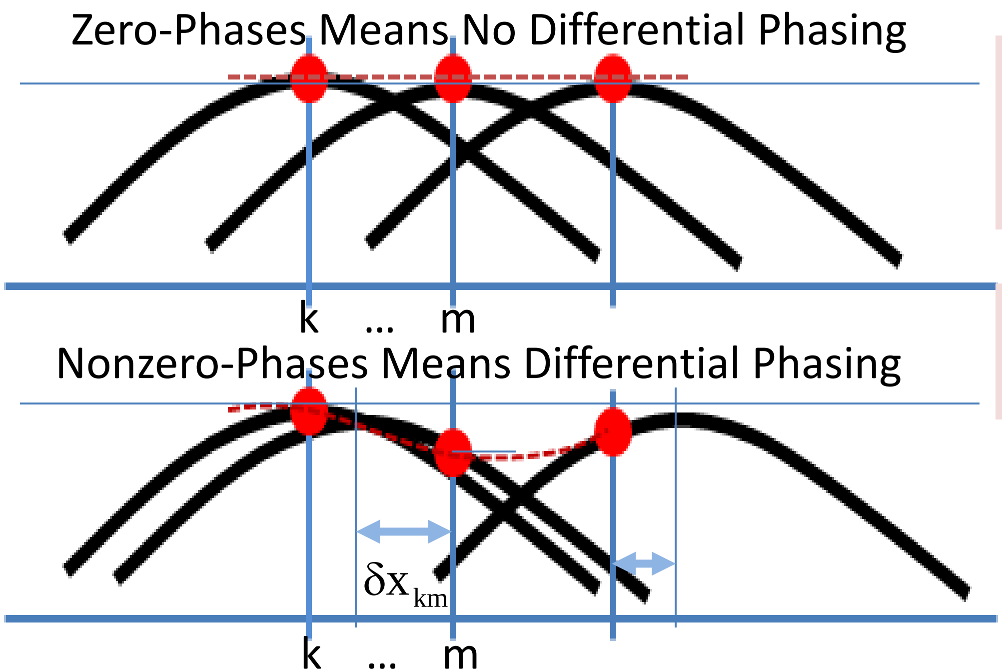

Single Mode “Zero-Phase” Motion produces a “deterministic” motion closer to coherent

Single Mode “Non-Zero-Phase” Motion produces a realistic “random field” motion

Differential Amplitude Variations due to Differential Random Phasing

Mode 1 Contribution

Freq	Part H	Part V
1 Hz	100%	98.2
8 Hz	84%	67%
25 Hz	7%	21%

At the lower frequencies, below 10 Hz, where a single mode (Mode 1) is governing, the zero-phase assumption practically neglects the differential phase variations between motion components due to incoherency.

Incoherency With Zero-Phasing (Loss of Physics)

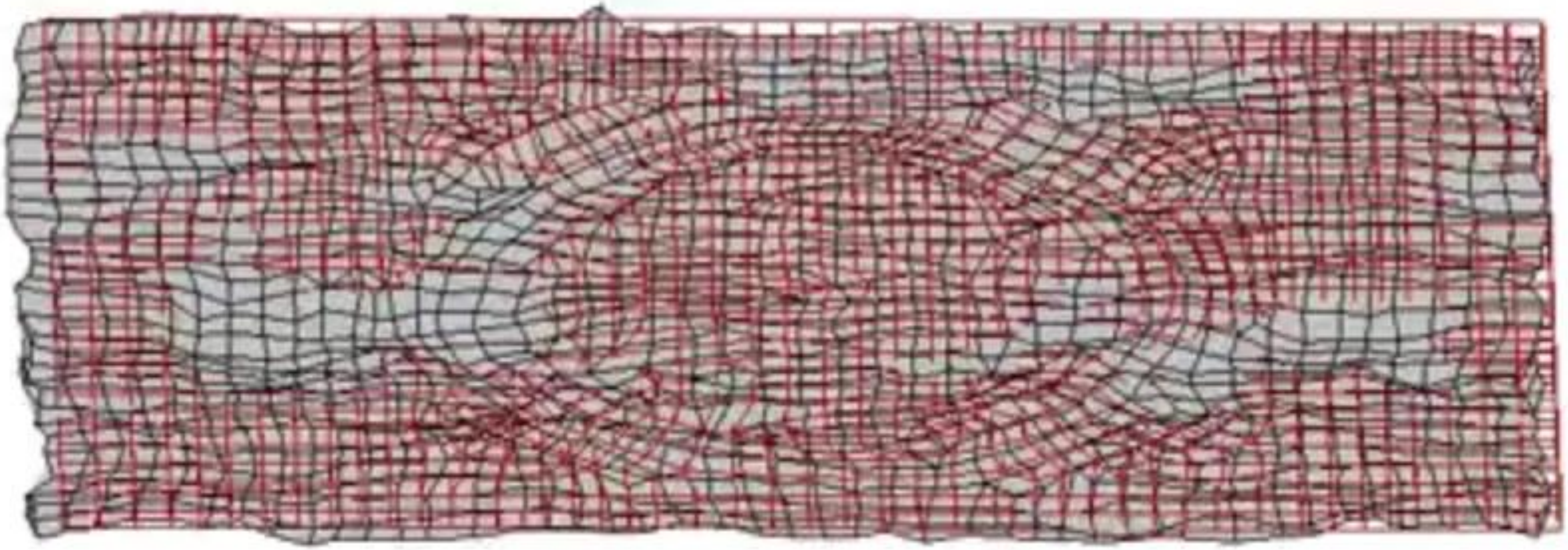

Incoherency With Random Phasing (No Loss of Physics)

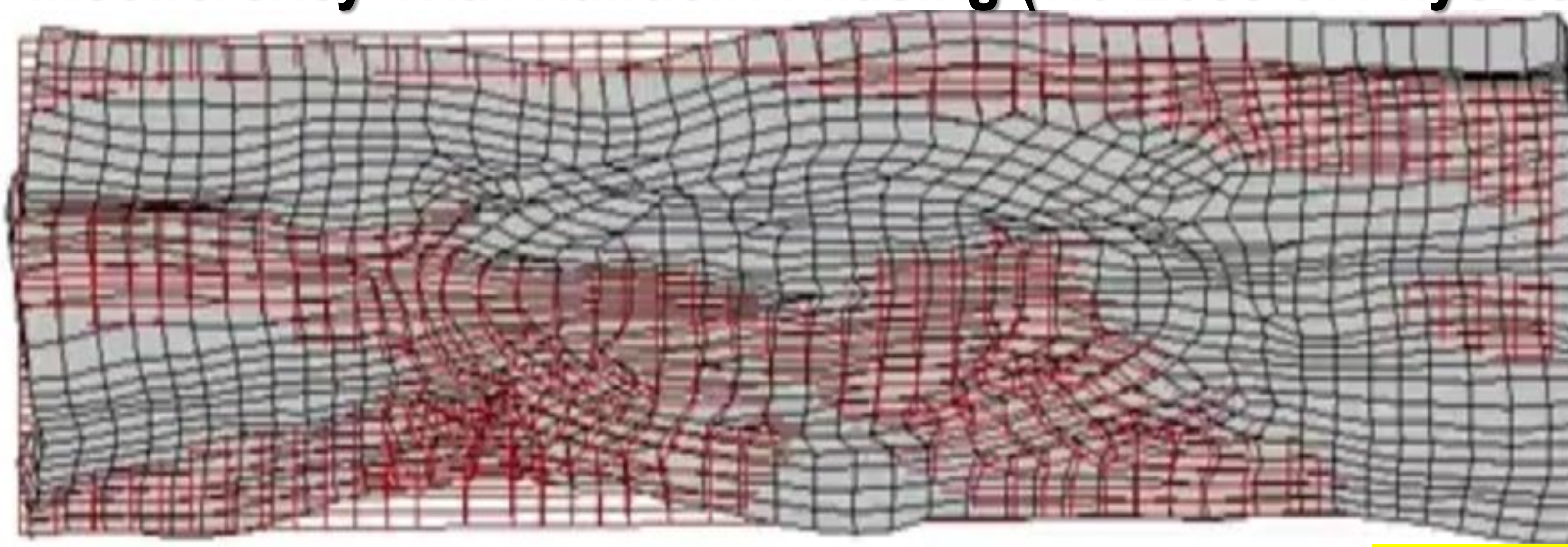

ANIMATIONS

2007 EPRI Validated Incoherent SSI Approaches Were Based on Industry Expert *Consensus*

The 2007 EPRI (TR 1015111) validated approaches are based on industry consensus. At that time the EPRI industry team (ARES, Bechtel,Bob Kennedy and Jim Johnson) uses the ClassiInco, ACS SASSI and SASSI Bechtel codes. The industry *consensus* was built around the SRSS approaches with 10 incoherent modes and assuming zero phasing for the SSI complex responses.

To match the team *"consensus" results* based on SRSS approaches, the Stochastic Simulation approach was used only with the "phase adjustment" option, that basically is zeroing the complex response phasing.

It should be understood that by neglecting the complex random phasing, the incoherent SSI responses are less incoherent, and by this creates a bias toward coherent responses. *This is usually conservative, but no always!*

Effect of Zeroing Phases for Low-Mid Frequencies Incoherent ISRS

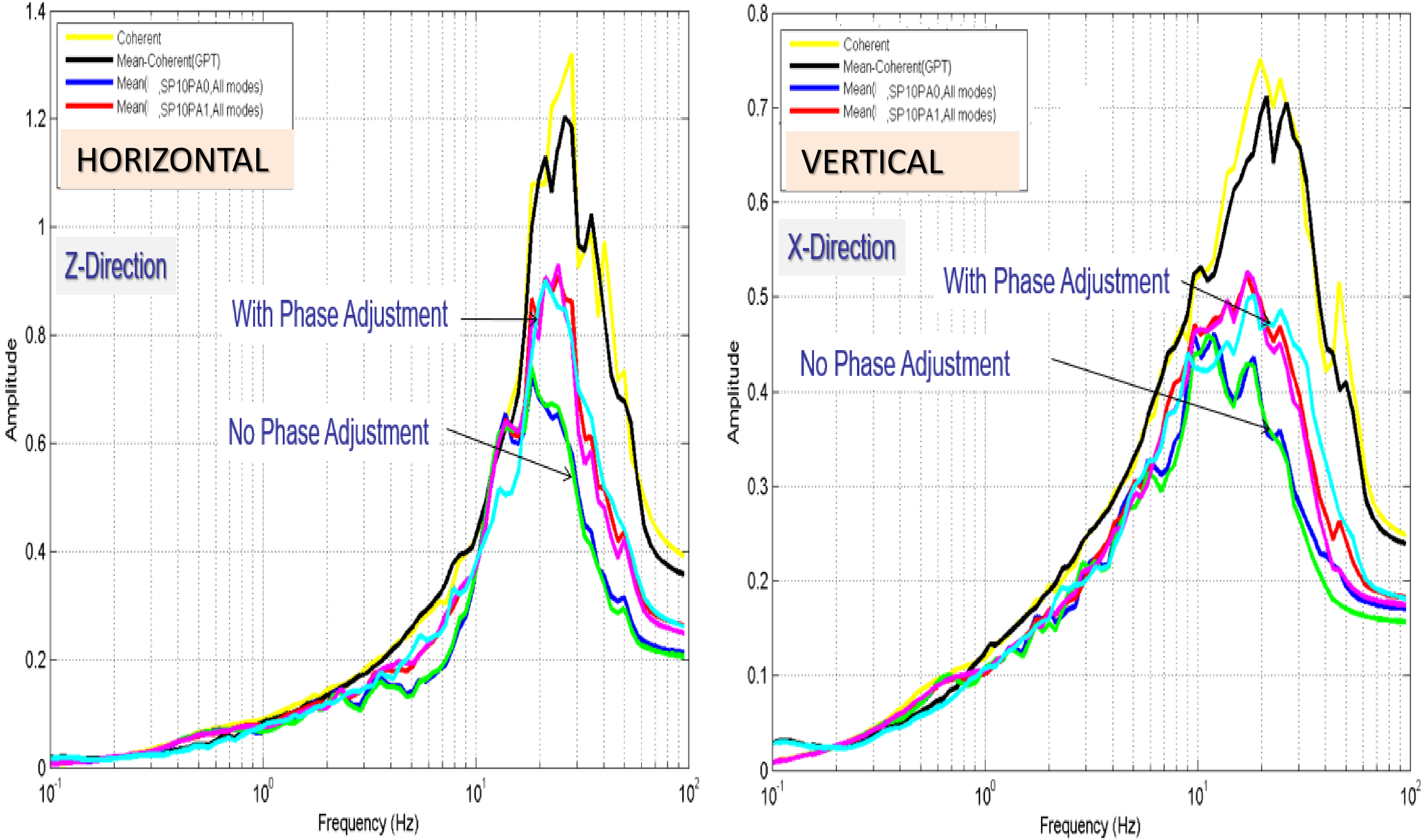

Flexible Foundations vs. Rigid Foundations

For *rigid foundations* the incoherency-induced stochasticity of the basemat motion is driven by the rigid body spatial variations (smooth, integral variations) of free-field motion. Kinematic SSI interaction is large, so that differential free-field motions are highly constrained by rigid basemat, i.e. shorter wavelength components are filtered out.

For *flexible foundations*, the incoherency-induced stochasticity of the basemat motion is driven by the local spatial variations (point variations) of free-field motion. Therefore, is much more complex and locally random, with an unsmoothed spatial variation pattern. Kinematic SSI is reduced, so that differential free-field motions are less constrained. Short wavelength are not filtered out.

To accurately capture the phasing of the local motion spatial variations that are directly transmitted to flexible basemat motions, the application of the Stochastic Simulation ("Simulation Mean" in EPRI studies) is recommended.

Mean RS for 5, 10, 15 and 20 Stochastic Samples For 3 Stick Model with Rigid Basemat (EPRI Studies, 2007)

Random FRS Samples

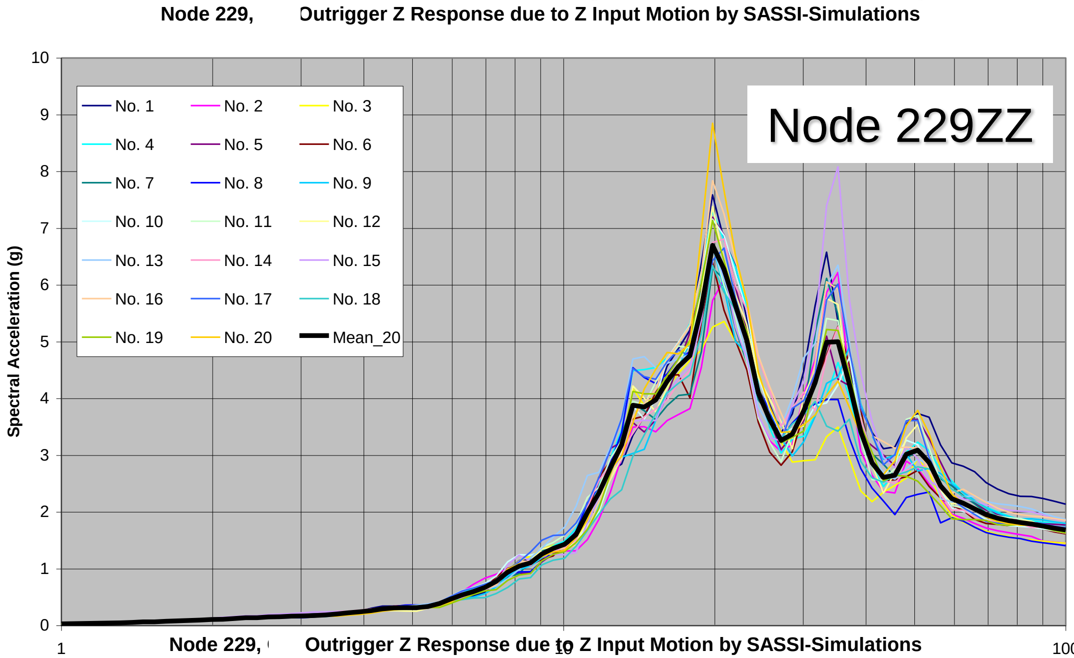

Mean FRS

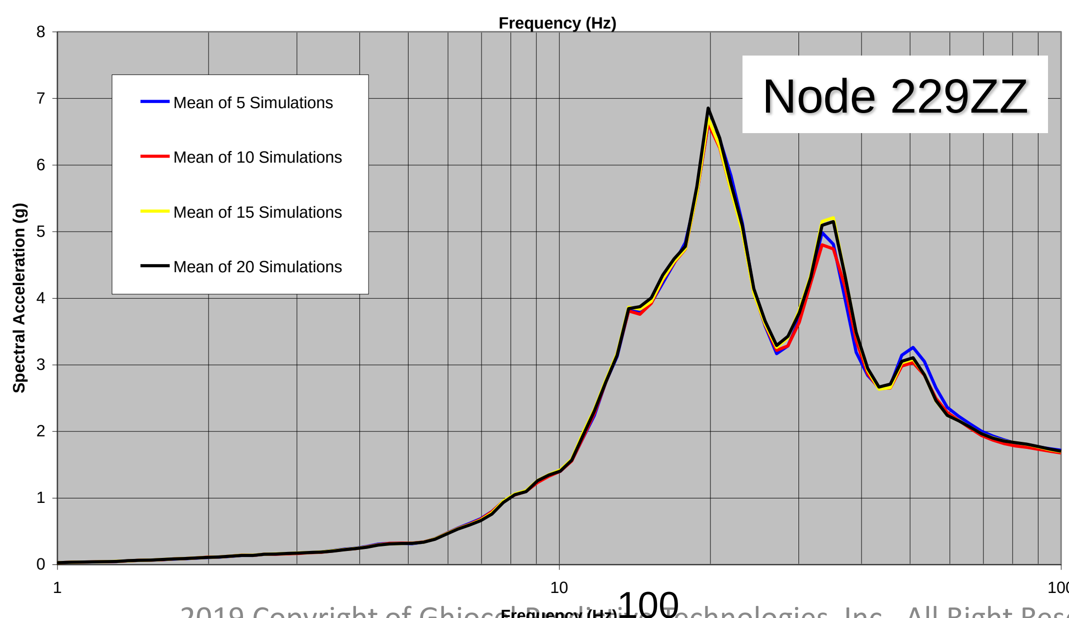

(included in EPRI Report, Figs. 4.1 and 4.2, page 4-5, by Short, Hardy, Merz and Johnson, Sept 2007)

We also compared with results from 50 random Samples – not shown.

ANIMATIONS

Stochastic Simulation Incoherent SSI Approach

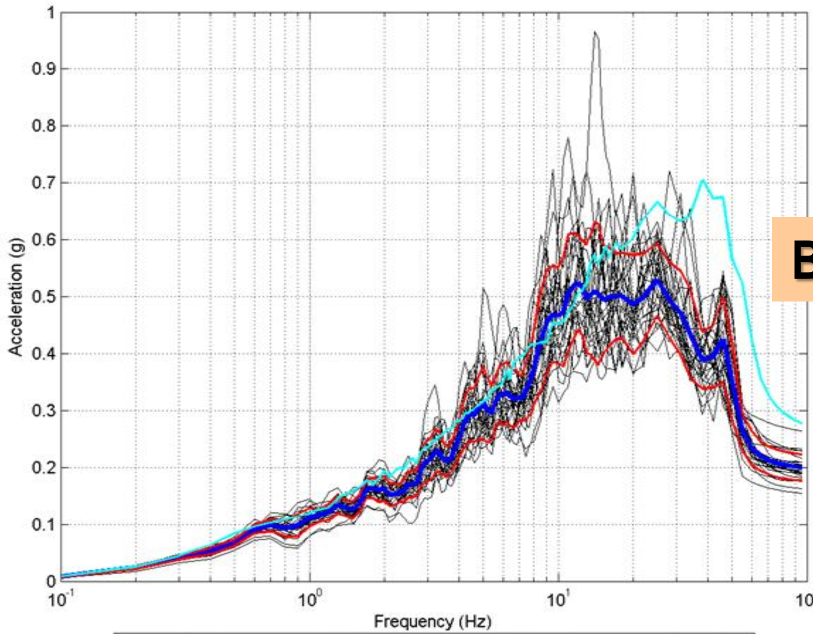

BASEMAT

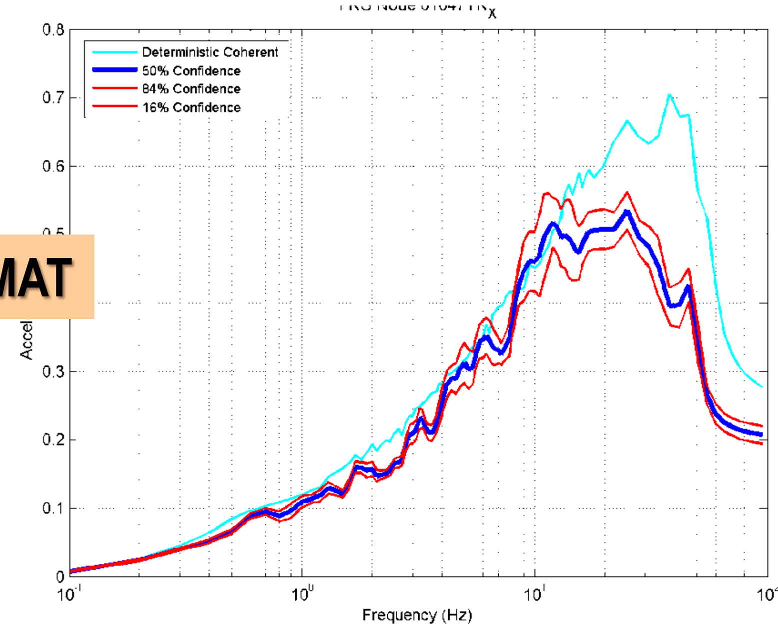

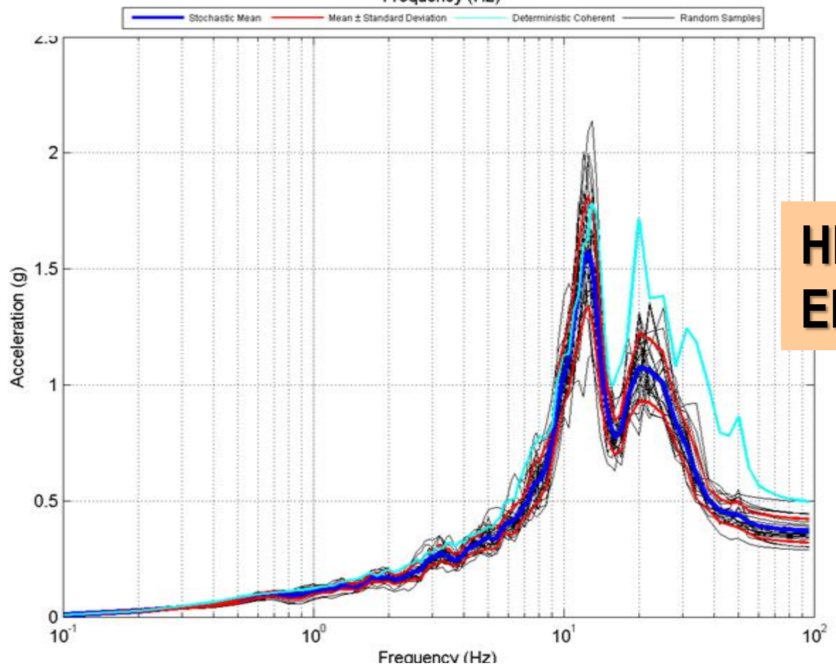

HIGHER ELEVATION

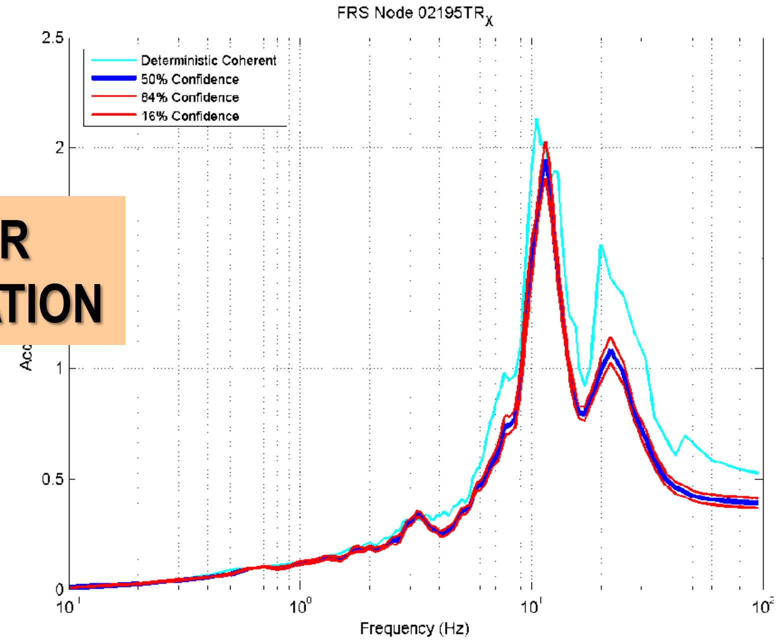

Deterministic Incoherent SSI Approaches (Simplistic Approaches)

ACS SASSI uses simplified superposition rules for combining incoherency modes or their random SSI modal effects:

i) Linear superposition of motion incoherency modes scaled with their standard deviation to simulate the free-field motion (AS in EPRI studies) – *single* SSI analysis

ii) Quadratic superposition of incoherency modal amplitude responses, applicable for the computed ATF or RS modal responses (SRSS in EPRI studies) – *multiple* SSI analysis

Five deterministic incoherent SSI approaches could be used:

1) Linear/algebraic summation (AS) w/ phase adjustment *(EPRI TR#1015111)*
2) Linear/algebraic summation (AS) w/o phase adjustment *
3) SRSS of ATF Amplitude w/ zero-phase *(EPRI TR#1015111)*
4) SRSS of ATF Amplitude w/ non-zero phase *
5) SRSS of RS (used in 1997 EPRI TR#102631, but not validated in 2007 EPRI TR#1015111) *

* Note: Not considered in the 2006-2007 EPRI studies (EPRI TR# 1015111)

Effects of Response Interpolation on Differential Phases

Records show Significant *Differential Phases (Incoherency)* for Close Frequencies

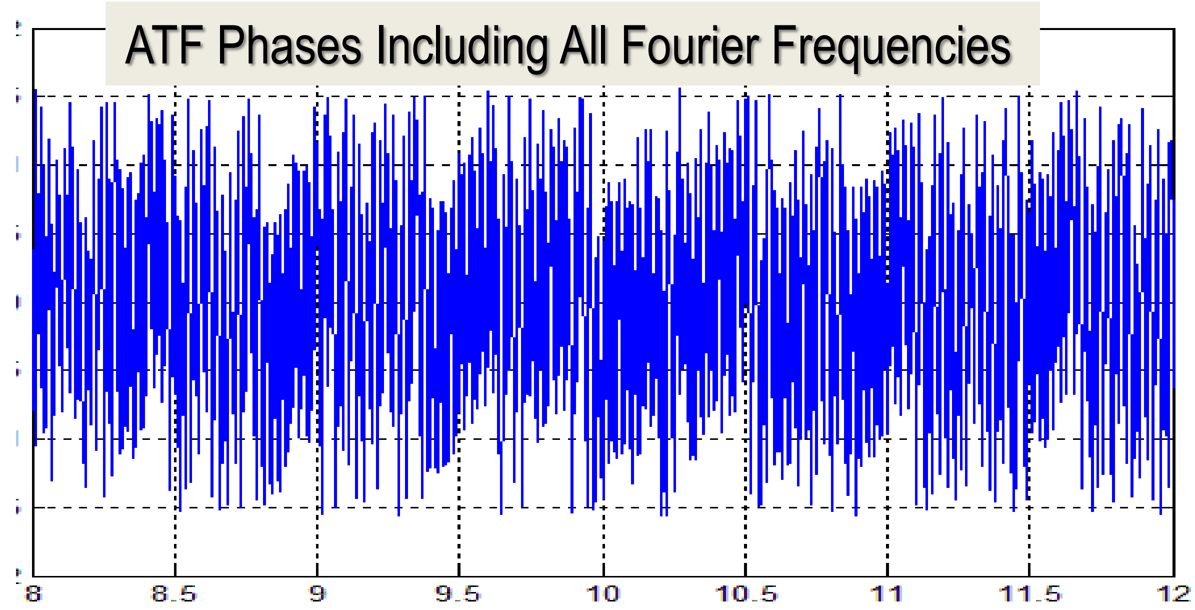

Interpolation smoothes, reduces *Differential Phases (Incoherency)* for Close Frequencies

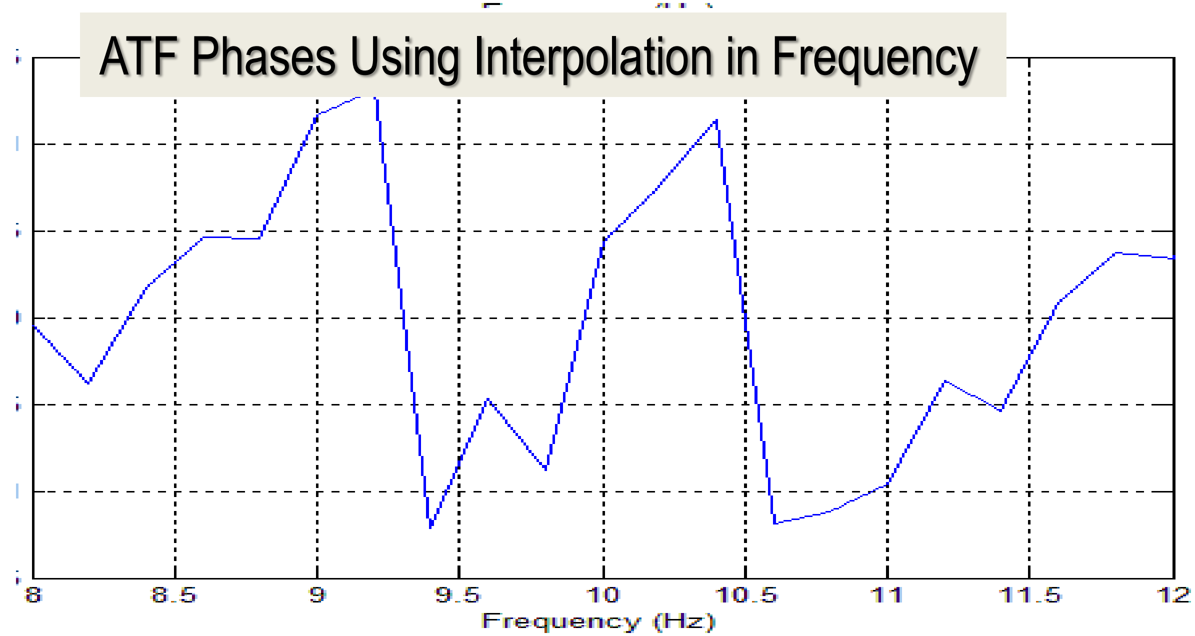

Incoherent SSI Solution Using MOTION & STRESS Spline Interpolation (Interpolation Option = 6)

ATF in Y-Direction

ATF in Z-Direction

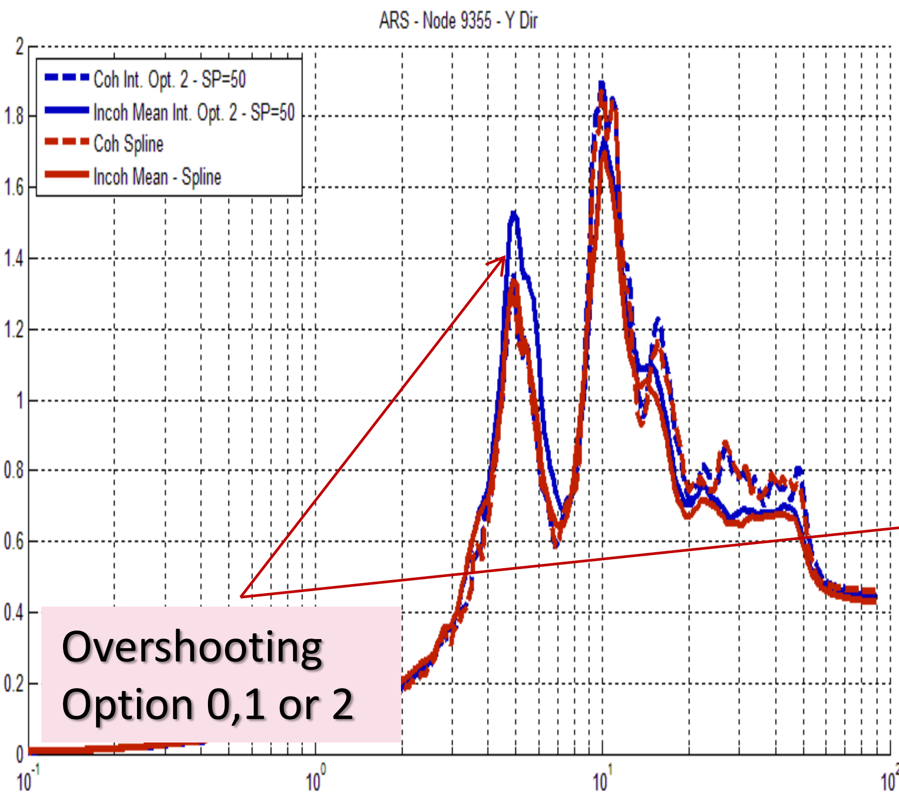

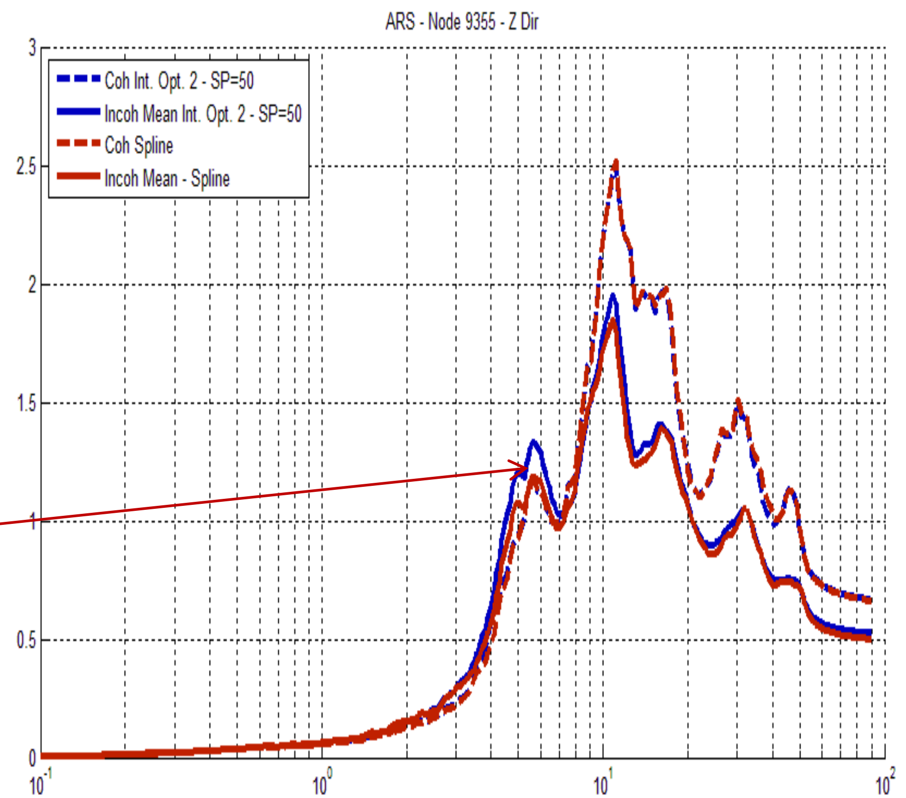

Embedded Models; Deterministic SSI May Fail

SAME node numbering order for all levels

DIFFERENT node numbering order for all levels

Mode 9 at 11.72 Hz

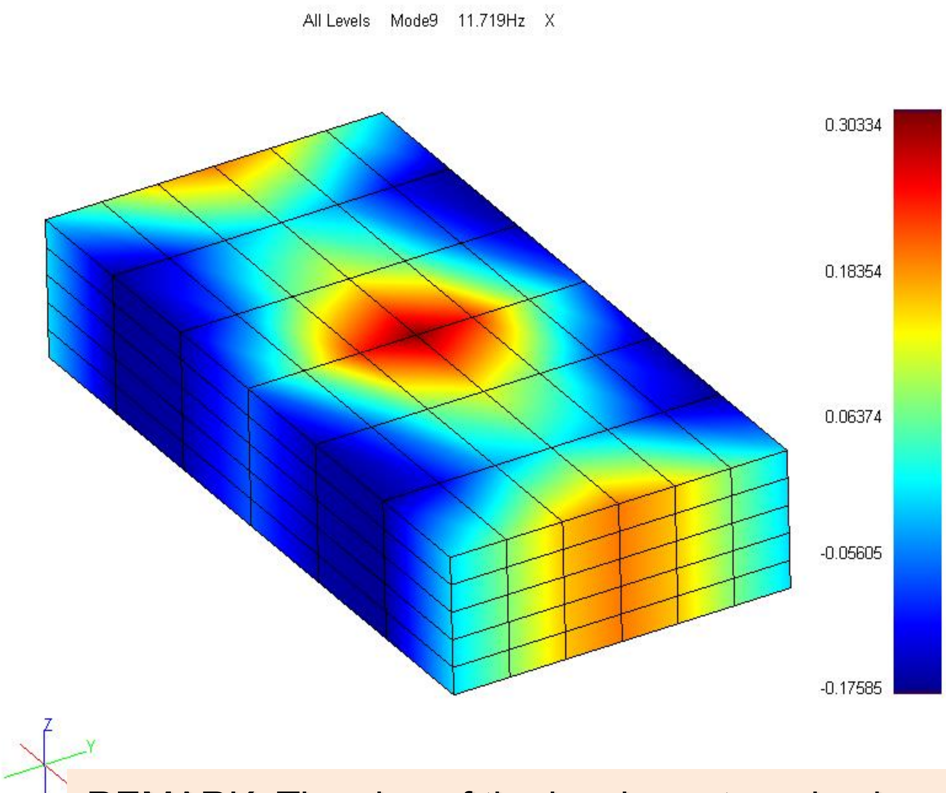

Mode 9 at 11.72 Hz

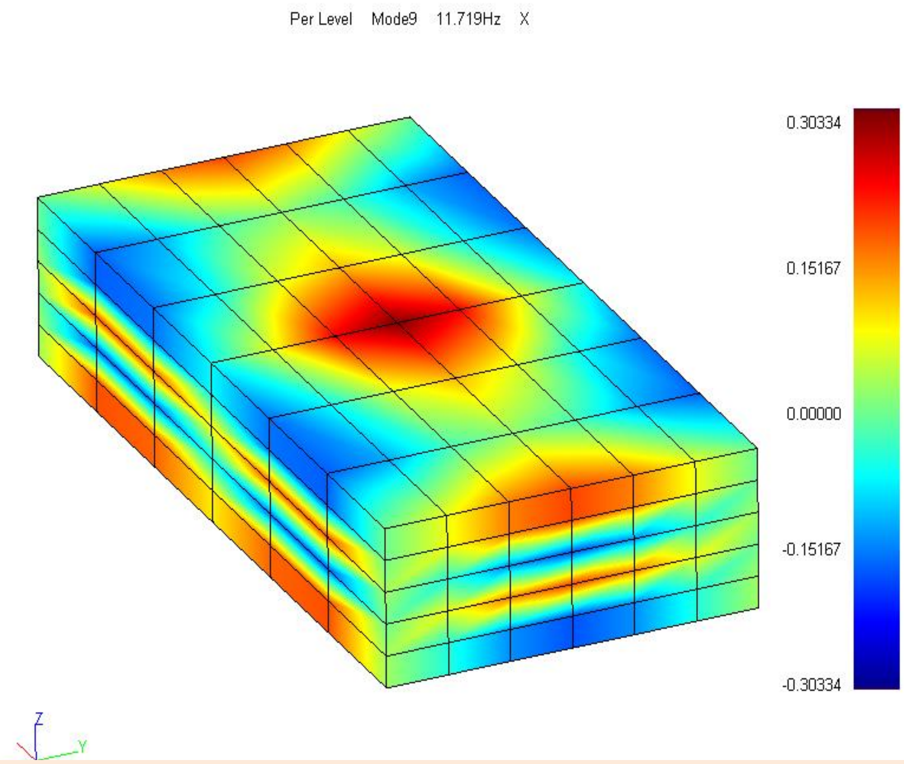

REMARK: The sign of the incoherent mode shapes is random, + or -, depending on node numbering. Deterministic SRSS approach uses an "arbitrary" criteria to maintain sign consistency between levels.

Mode 1 Sign Effect on Modal ATF & ISRS for X-Dir

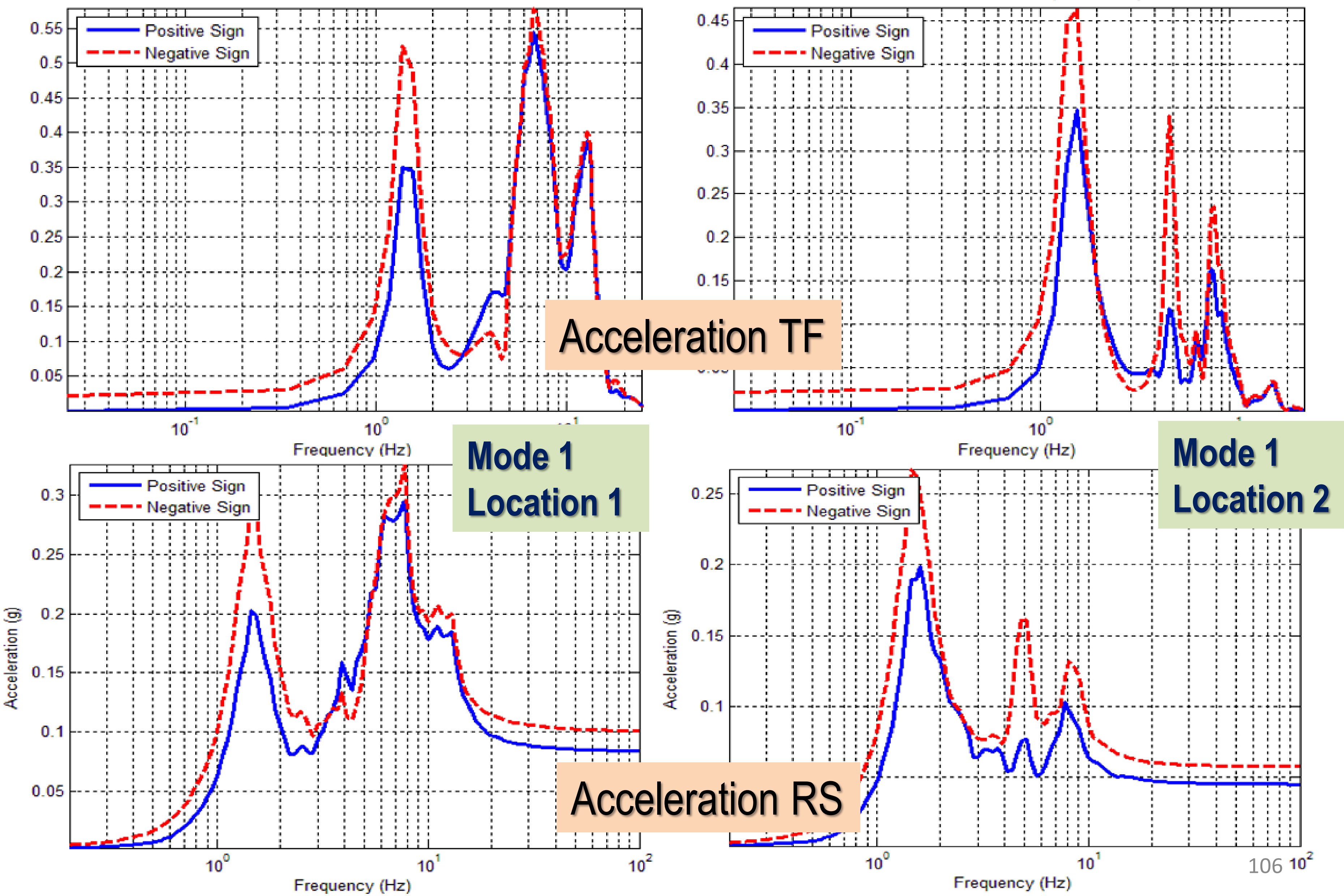

Incoherency Effects for Deeply Embedded Structures. 30 ft Embedded Concrete Pool Structure

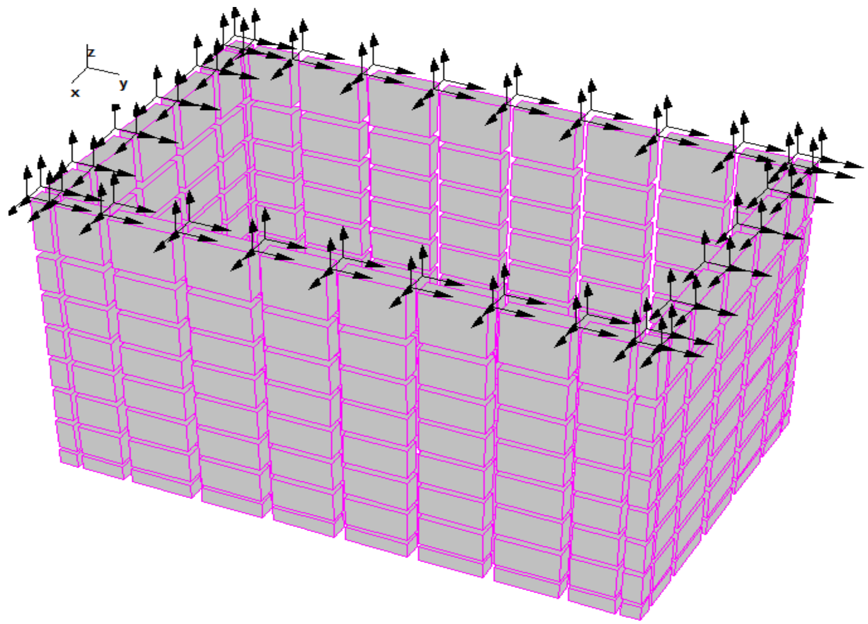

SSI Analysis Inputs:

- Structure: Embedded Concrete Pool Structure of 50ft x 80ft Size
- Soil Deposit: Soil layer with Vs=1,000fps above rock with Vs = 5500fps
- Control Motion: HF Seismic Input
- Incoherency: 2007 Abrahamson Coherence Function

Coherent and Incoherent SSI Motions and Stresses

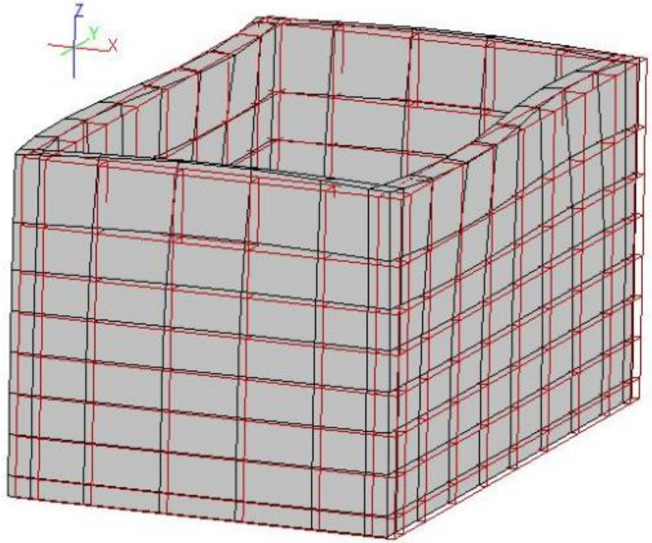

Accelerations

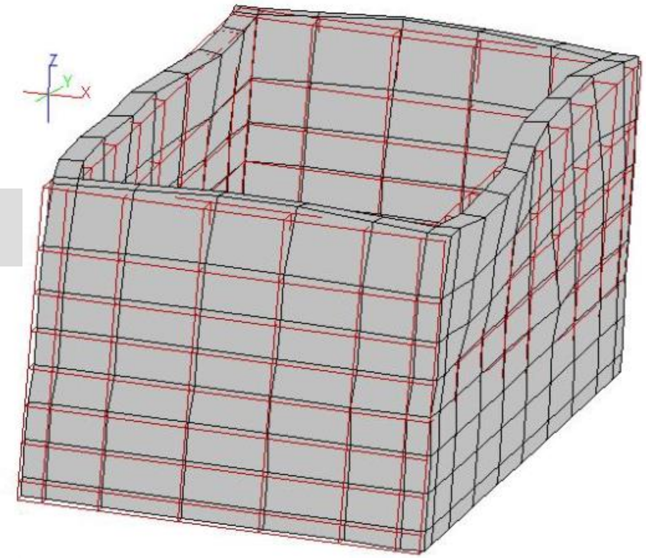

Coherent

Incoherent

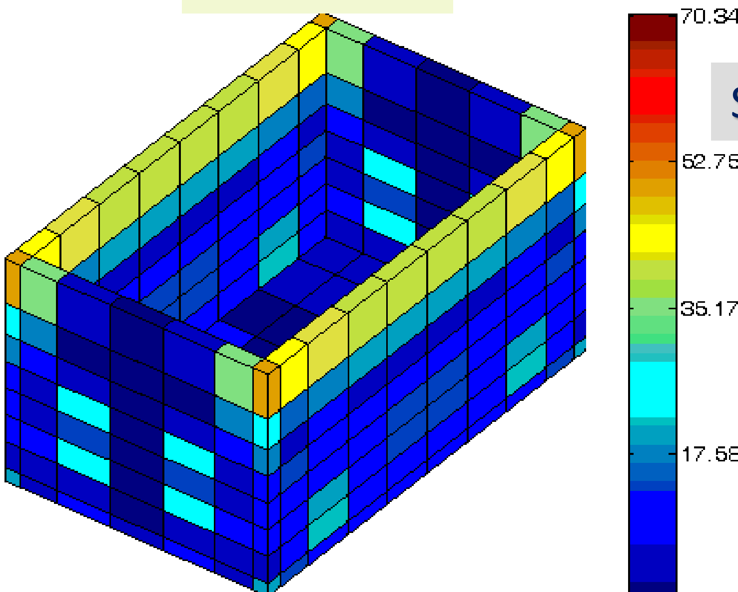

Stresses

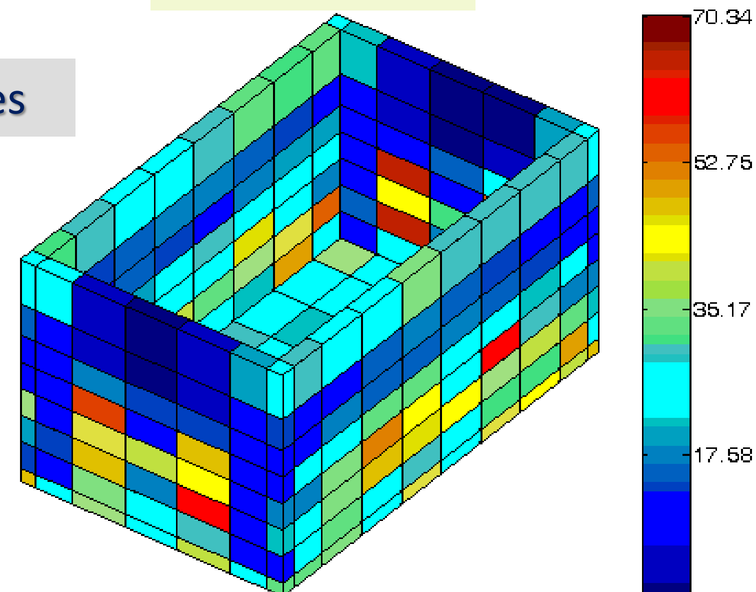

Coherent and Incoherent SYY Stresses in The Embedded Pool Walls

Coherent

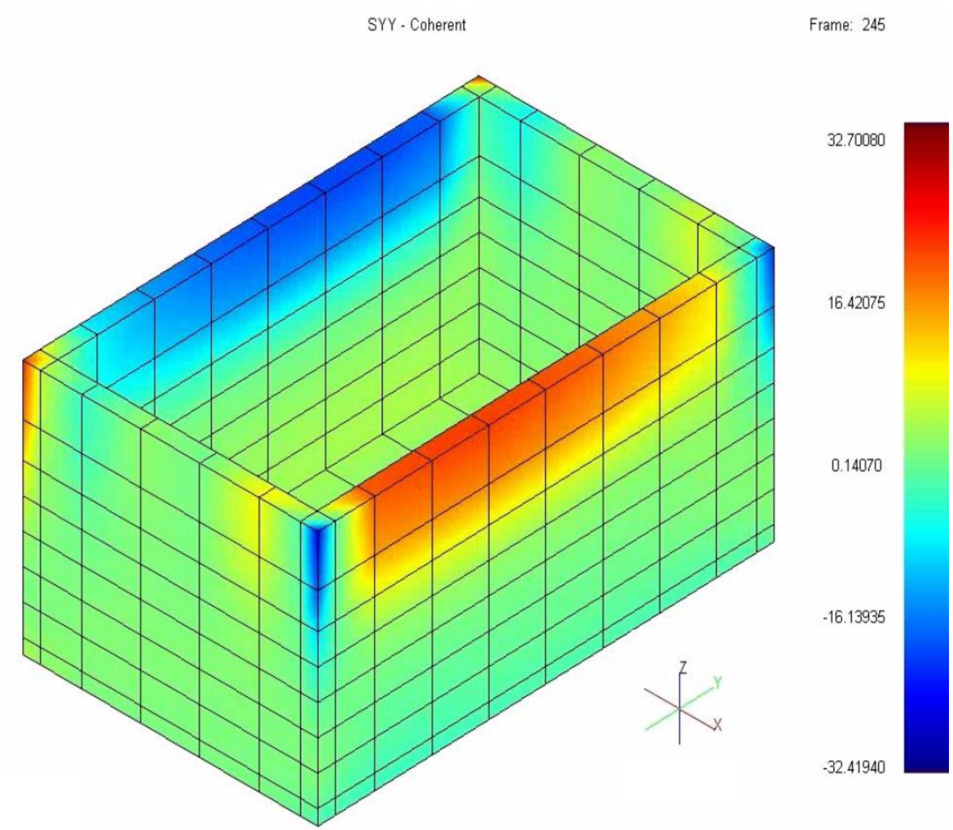

Incoherent

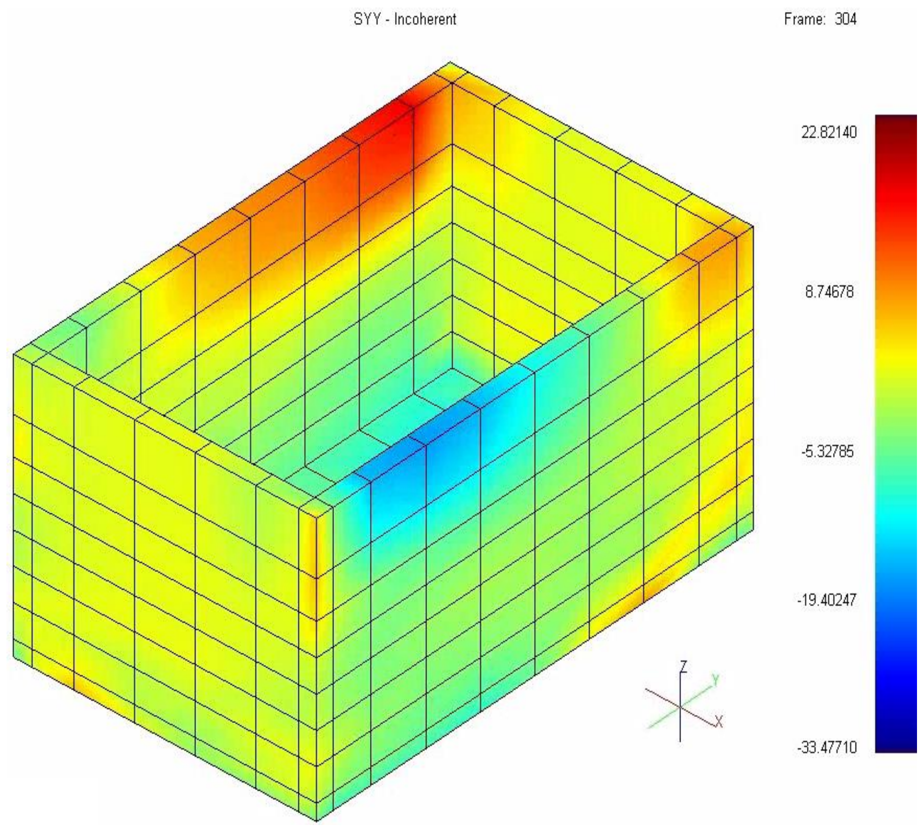

Remarks on Incoherency Effects on Soil Pressures for DES

For deeply embedded structures, the incoherency effects are to reduce the global resultant of the local soil pressures, but locally might produce “hot spot” pressures due to short wavelength soil motion components.

Wave scattering effects around deeply embedded structures are sensitive to motion incoherency.

3) Typical Application for Incoherent SSI Analysis

ACS SASSI Incoherent SSI Analysis Methodology

Incoherent Approach:

Stochastic Simulation with 20 Incoherent Samples with/without complex response phase adjustment

Coherence Function Model Options (TBD):

Generic Model: 2007 Abrahamson coherence function radial model (Model 5 for rock site, Model 6 for soil sites)

Site-Specific Model: Based on 2D probabilistic nonlinear site response analysis (using Option PRO to define this)

Wave Passage Effects (negligible for rock sites):

Rock Sites: Va = infinite (1.E+8)

Soil Site: Va = 2-4 Km/sec (produces more incoherency effects)

Typical R/B Complex Incoherent SSI Analysis (Key Reporting Aspects)

- Define Seismic Incoherent Input, Soil Layering & Embedded R/B SSI Model
- Define Incoherent SSI Methodology Based on SS
- Show Incoherent (Mean) vs. Coherent SSI Responses for:
  - ATF
  - ISRS
  - Maximum structural accelerations and displacements
  - Seismic soil pressures on foundation walls and basemat
  - Structural forces and moments, and out-of-plane bending moments in foundation walls and basemat
  - Vertical structural displacements at key equipment or primary cooling loop supports wrt to basemat center
- Conclusions

4. Limitations of the RVT SASSI Approach Implementation

Purpose:

The RVT SASSI approach as currently implemented is some SASSI versions (Deng and Ostadan, 2012) has the advantage that computes the seismic responses of the SSI system using directly the ground response spectra (GRS) input without the need of developing spectrum compatible input acceleration time histories.

The presentation discusses the theoretical basis of the RVT SASSI approach and explains why this approach can fail to provide reasonably accurate results for seismic SSI analyses.

Case studies include surface and embedded RB models, and deeply embedded SMR founded on rock and soil sites.

RVT SASSI Approach for Seismic SSI Analysis

The RVT based approach uses frequency domain convolution computations (no need to use time-histories) assuming a Gaussian seismic input

$S_X(\omega) = |H_{SSI}(\omega)|^2 |H_0(\omega)|^2 S_u(\omega)$ or $S_X(\omega) = |H_X(\omega)|^2 S_u(\omega)$

ISRS Responses:

XPSD = H2SSIX * H2SDOF * GPSD

Other SSI Responses:

XPSD = H2SSIX * GPSD

The RVT-based approaches include several options related to the *PSD-RS transformation*. These options are related to the stochastic approximation of the maximum SSI response over a time period T, i.e. during the earthquake intense motion time interval.

The maximum SSI response can be expressed using peak factors which are applied to the response motion standard deviation (RMS). These quantities depend on the duration T, the mean zero-crossing rate of the motion and probability level associated to maximum response (“first passage problem”).

RVT SASSI Approach for ISRS Responses

RVT Approach Flowchart:

Compute SSI Response TF ↓

Seismic GRS Input →(RS-PSD) Compute Seismic GPSD → Compute SSI Response PSD →(RS-PSD) Compute SSI Response ARS

SDOF Transfer Functions:

$$H_0(\omega) = \frac{\omega_0^2 + 2i\omega_0\xi_0\omega}{\left(\omega_0^2 - \omega^2\right) + 2i\omega_0\xi_0}$$

Absolute Accelerations (ARS-APSD)

$$H_0(\omega) = \frac{\omega}{\left(\omega_0^2 - \omega^2\right) + 2i\omega_0\xi_0}$$

Relative Velocities (VRS-VPSD)

$$H_0(\omega) = \frac{1}{\left(\omega_0^2 - \omega^2\right) + 2i\omega_0\xi_0}$$

Relative Displacements (DRS-RPSD)

Maximum SSI Response Based on RVT Solution

$$\bar{X}_{\max} = p\sigma_X$$
$$\sigma_{X_{\max}} = q\sigma_X$$

1) M Kaul-Unruh-Kana stochastic model (MK-UK) (1978, 1981) :

$$p = \left[-2\ln\left(-\left(\frac{\pi}{T}\right)\left(\frac{\sigma_X}{\sigma_{\dot{X}}}\right)\ln(P) \right) \right]^{1/2}$$

Please note that this *p* is not the mean peak factor, since it provides maximum peak factor for any given NEP P

2) A Davenport (AD) (1964) for p and Der Kiureghian (1980) for q

$$p = \sqrt{2\ln(\nu_0 T)} + \frac{0.5772}{\sqrt{2\ln(\nu_0 T)}} \qquad q = \frac{1.2}{\sqrt{2\ln(\nu_0 T)}} - \frac{5.4}{\left[13 + \left(2\ln(\nu_0 T)\right)^{3.2}\right]}$$

3) A Davenport Modified by Der Kiureghian (AD-DK) (1980,1981)

$$\nu_e T = \begin{cases} \max\left(2.1, 2\delta\nu_0 T\right) & ;0 < \delta \le 0.1 \\ \left(1.63\delta^{0.45} - 0.38\right)\nu_0 T & ;0.1 < \delta < 0.69 \\ \nu_0 T & ;0.69 \le \delta < 1 \end{cases} \qquad \delta = \sqrt{1 - \frac{\lambda_1^2}{\lambda_0 \lambda_2}}$$

Basic Assumptions for (Linear) RVT Solution

1) It is based on the assumption that the seismic ground motion is a Gaussian stationary stochastic process.

This assumption might not be true if highly non-Gaussian “seed” records are used to generate the design-basis input time histories. More generally, real earthquake motion are not Gaussian.

If the Gaussianity aspect is ignored, the RVT-based approach application becomes quite arbitrary, with results based on a case-by-case luck, and without a sound theoretical basis.

2) The ASCE 4-16 referenced RVT SASSI approach does not include the cross-correlations between the SSI response motions at different locations and between X, Y and Z components.

Inapplicable to multiple support time domain analysis of secondary systems.

2012 RVT Studies for SSI Stick Models

EPRI AP1000 NI Stick Model

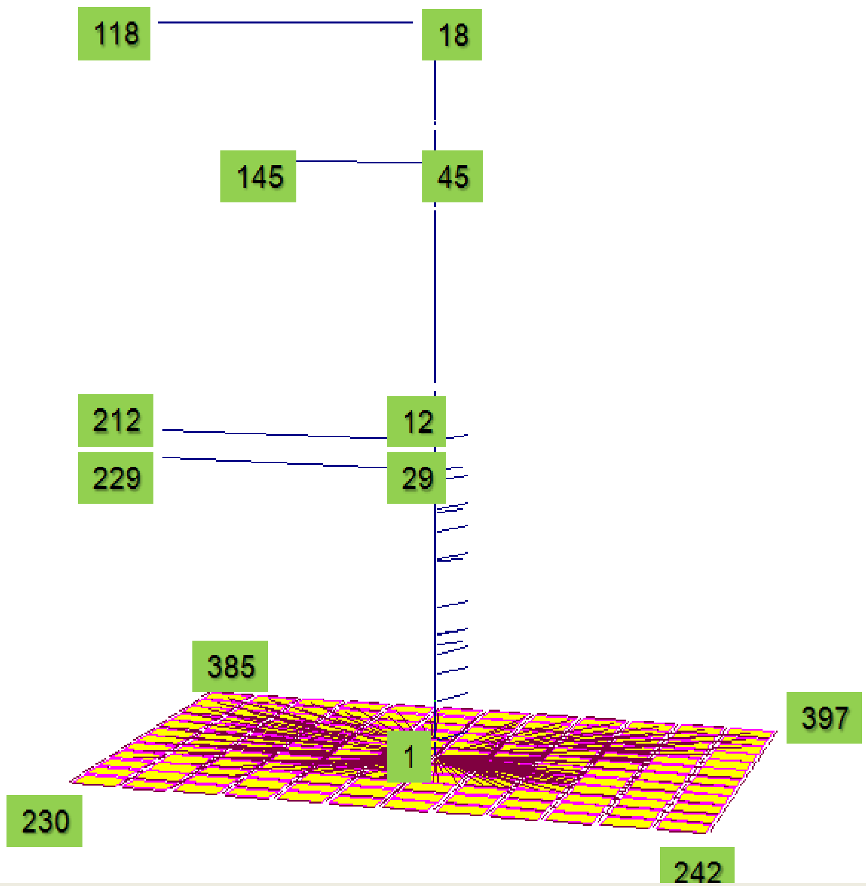

Case 1: Soil Site (BE Soil and Random Soil), Vs = 1,000 fps
Case 2: Rock Site (BE Soil and Random Soil), Vs = 6,000 fps

Ghiocel and Grigoriu, SMIRT22, 2013

RVT Approach vs. LHS (30) for Rock Site – Mean ISRS

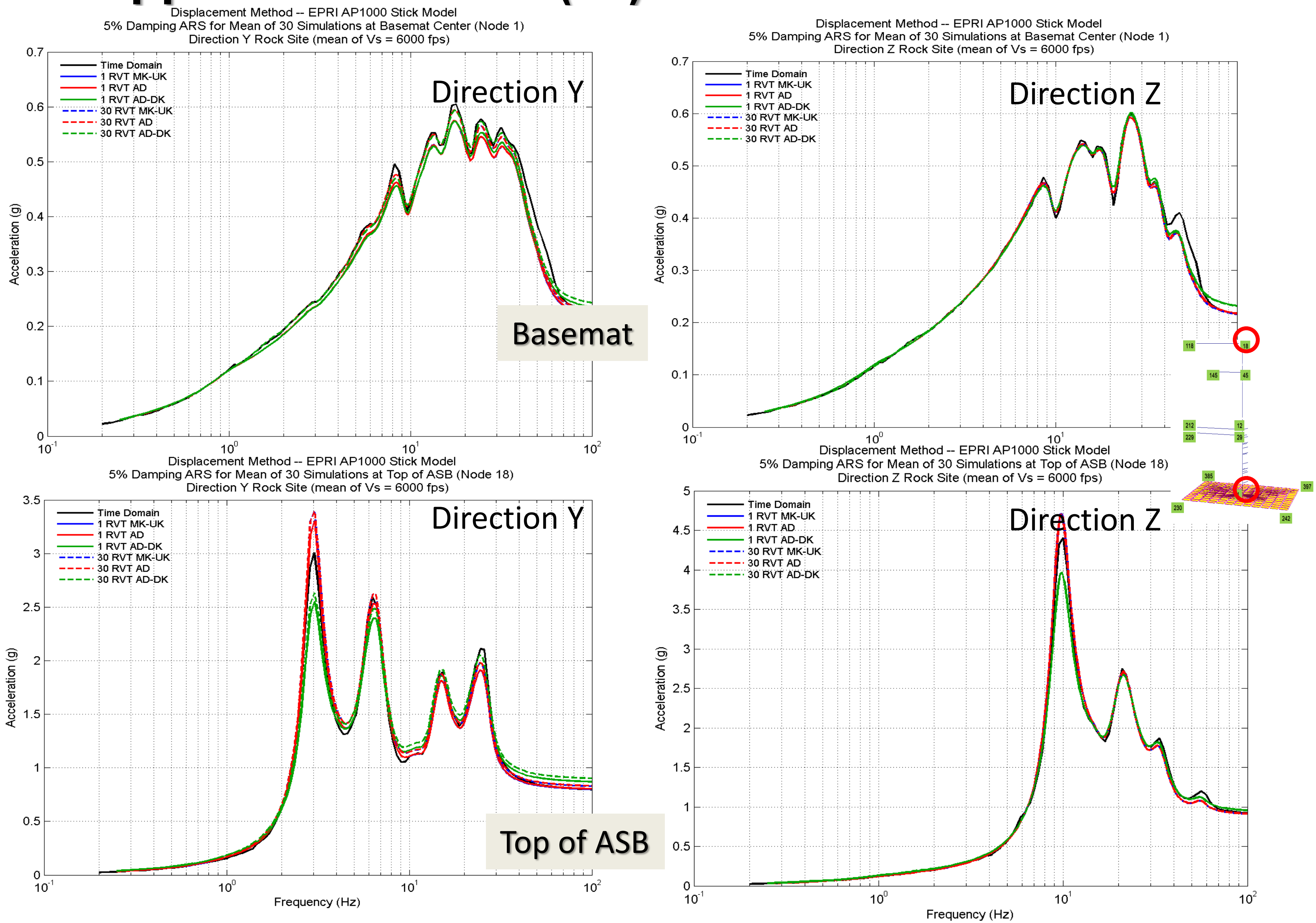

RVT Approach vs. LHS (30) for Soil Site – Mean ISRS

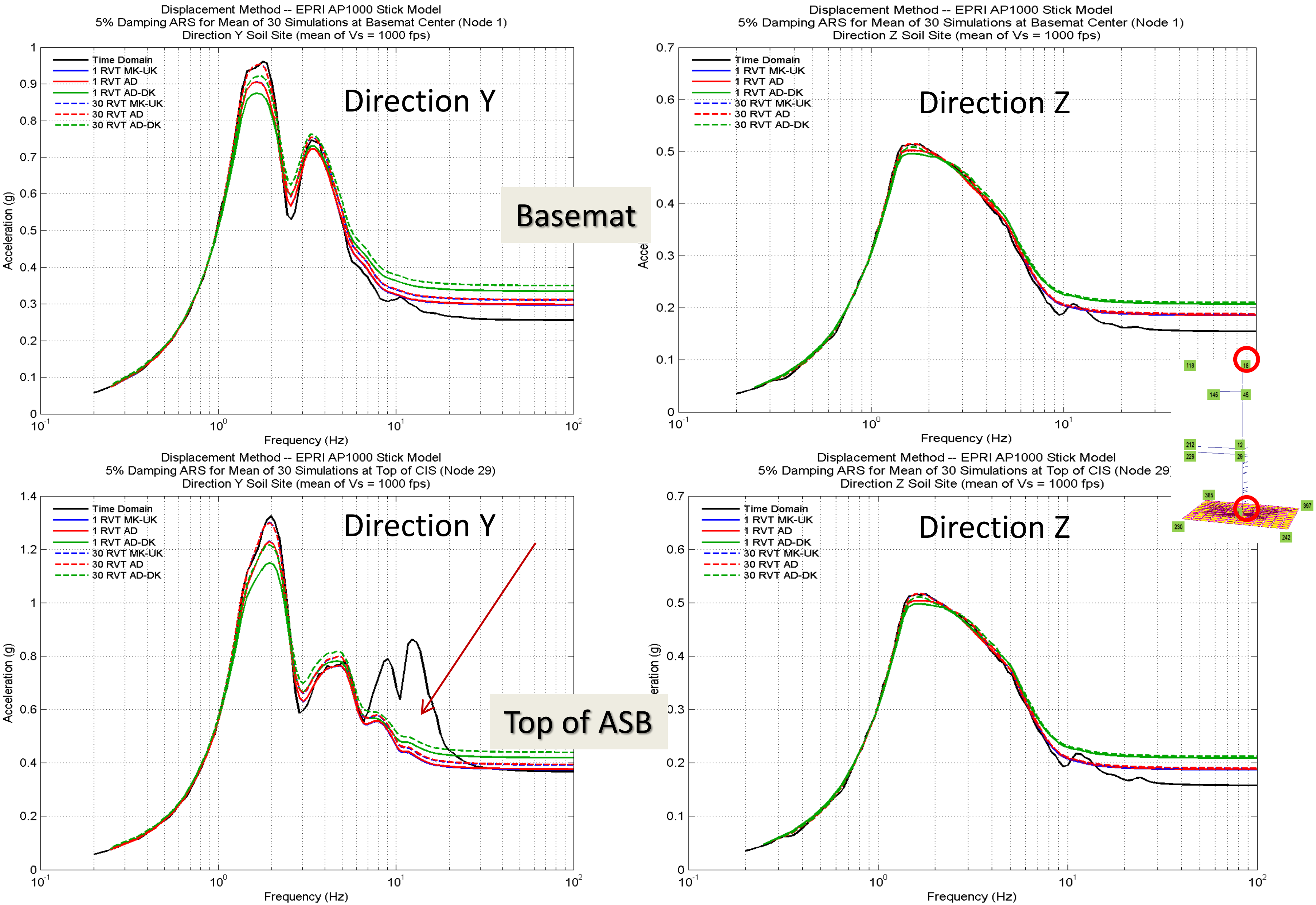

2014 Deeply Embedded SMR RVT SSI Analysis

Volume Size: 200 ft x 100 ft x 100 ft

140 ft Embedded SMR Model

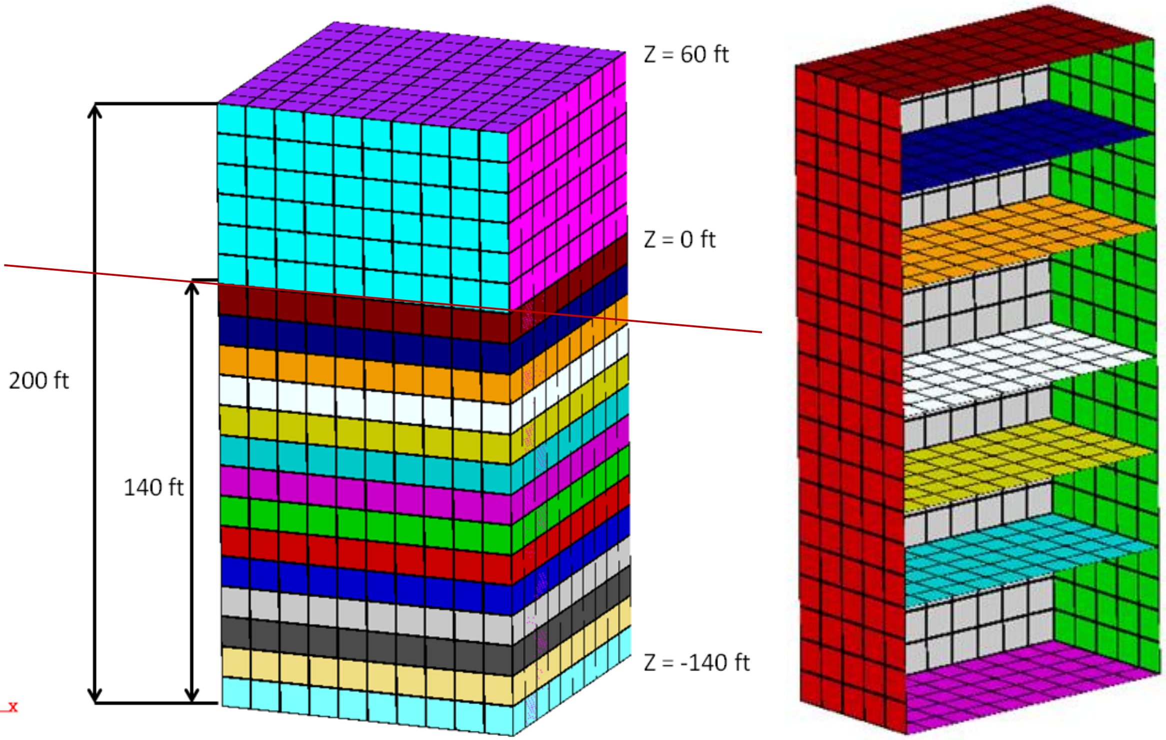

SMR size: 100 ft x 100 ft X 200 ft
Embedment: 140 ft
Mesh size: 10 ft X 10 ft X 10 ft
Number of Nodes: 2,580
Interaction Nodes: 1,815

Vs Soil Profile (fps)

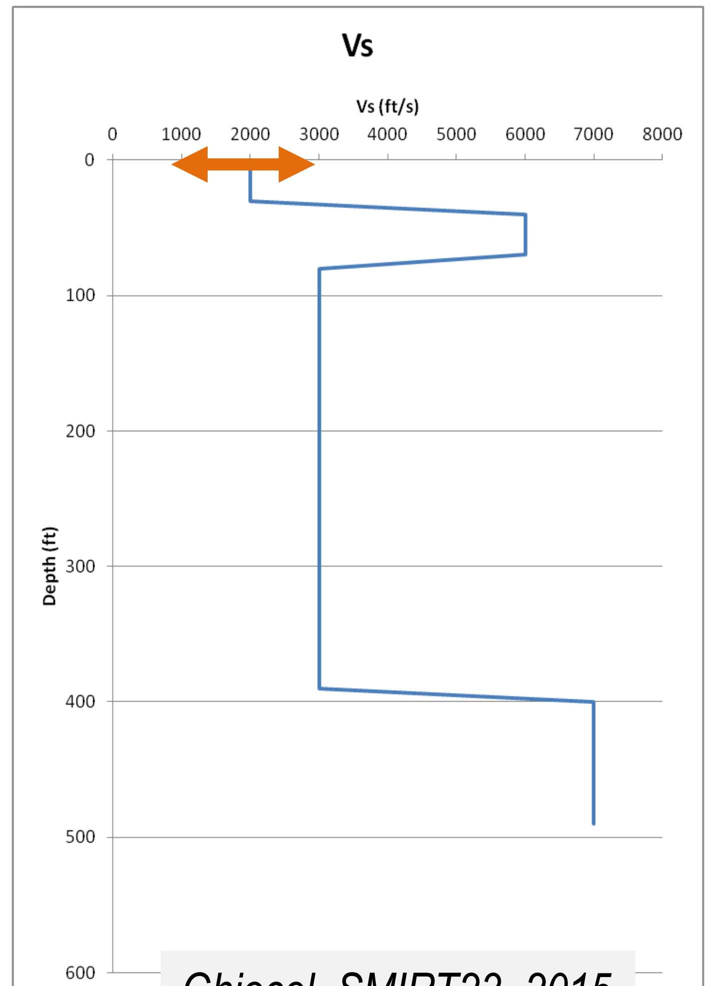

Ghiocel, SMIRT23, 2015

RVT vs. Deterministic SSI (5) for Nonuniform Soil ISRS at Basemat Level (Elevation 0ft)

Mean ISRS

Direction X

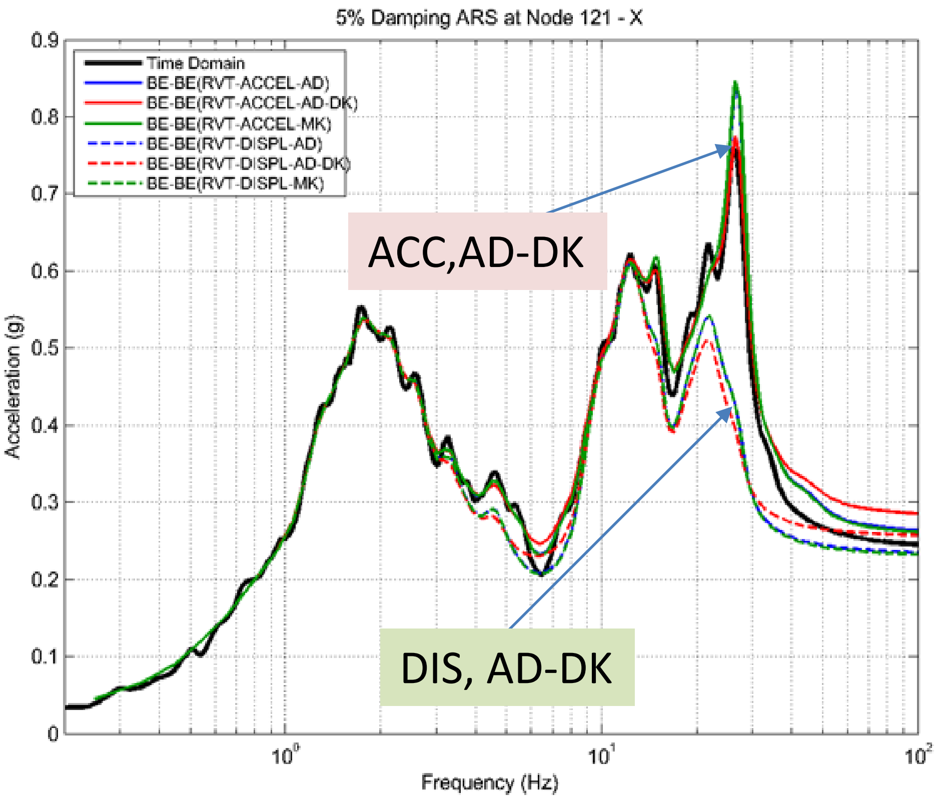

Direction Z

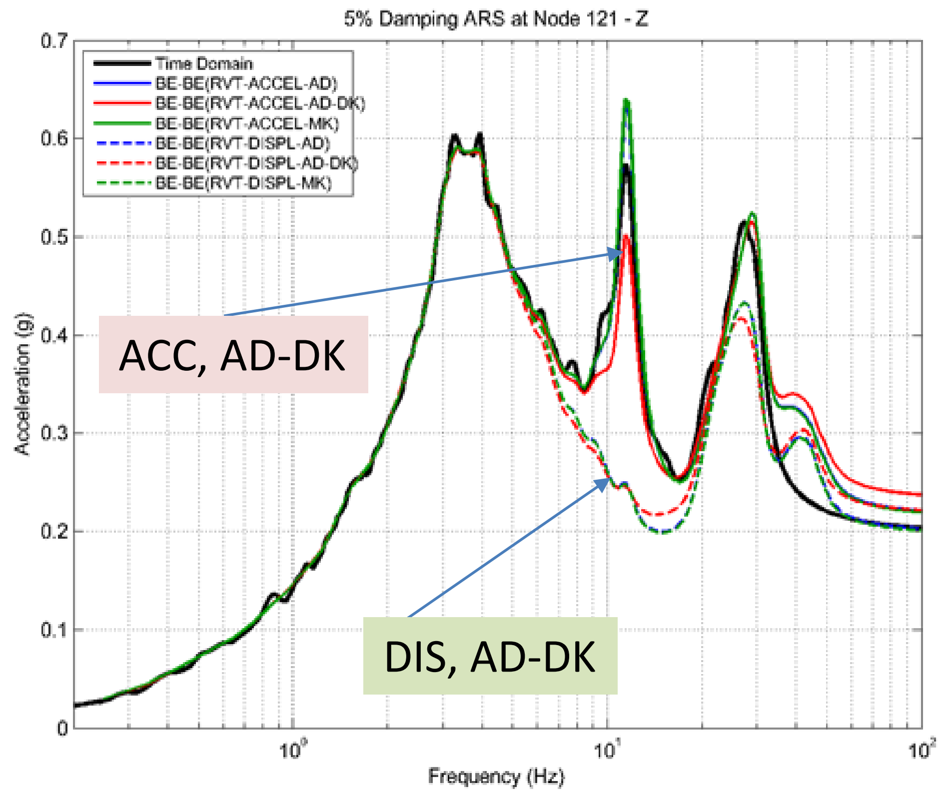

RVT vs. Deterministic SSI (5) for Nonuniform Soil at Roof Level (Elevation 200 ft)

Mean ISRS

Direction X

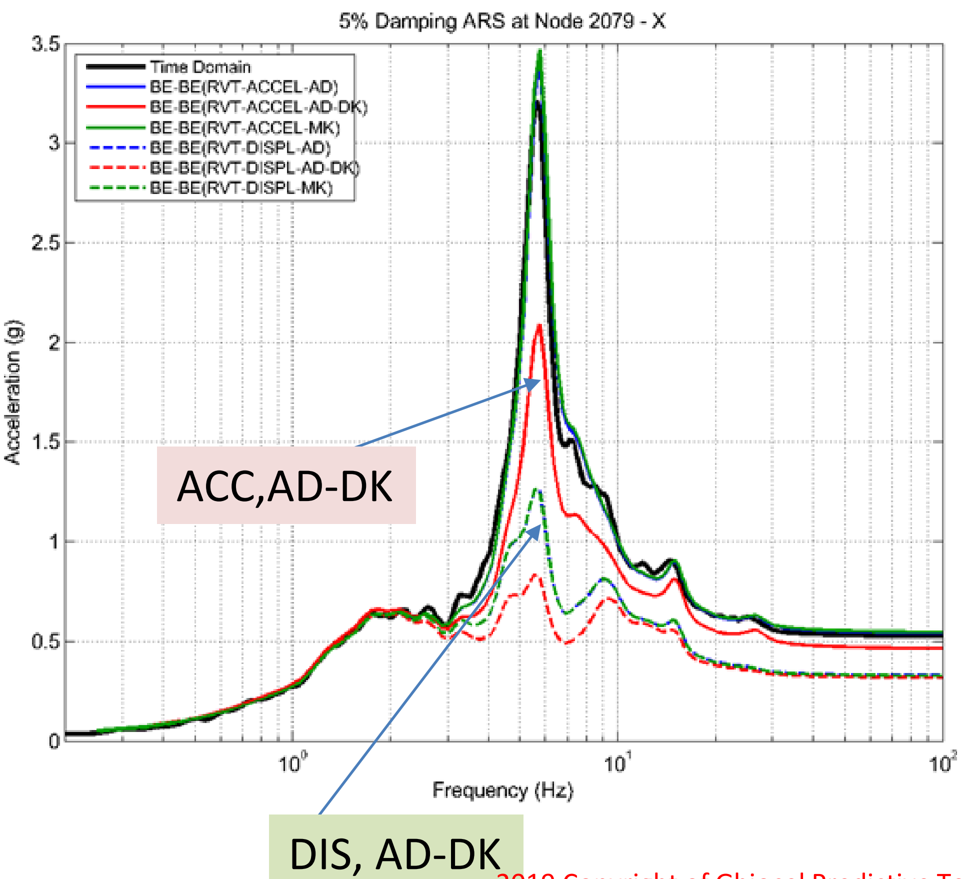

Direction Z

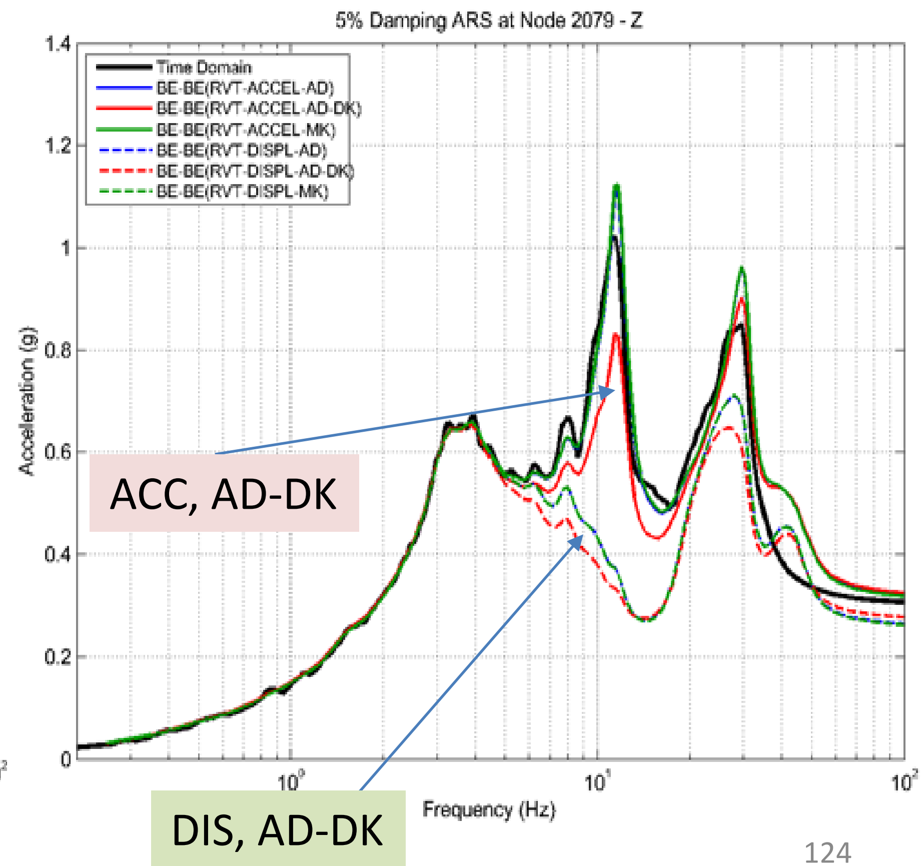

Concluding Remarks from Earlier Studies

The RVT SSI approach accuracy varies widely on a case-by-case basis.

- When the SSI responses are dominated by a single mode contribution, the RVT SASSI approach perform quite well.

- When multiple spectral peaks are present, then, there is a good chance of having missing ISRS peaks at higher frequencies (the 2^{nd} or 3^{rd} ISRS peak)

- The RVT SASSI approach is more accurate for the rock sites that have less SSI effects than for the soil sites that have larger SSI effects.

Earlier study results rised concerns on the RVT SASSI approach accuracy and its validation for SSI analysis. We decided not to include any RVT SSI analysis capability in our ACS SASSI software.

The Pitfall of RVT SASSI Approach: Single Peak Factor Used for MDOF SSI Systems

The RVT SASSI approach uses a single peak factor and single set of spectral moments based on AD-DK, which is applicable to *broad band spectra and SDOF responses to WN/FWN input motions* (Der Kiureghian's, 1980, 1981)

In the EERC 80-15 report, pages 8-9, the Der Kiureghian uses for MDOF systems separate peak factors for each system vibration mode. These modal *peak factors* (see eqs. 16-17) depend on the computed mean crossing rates that are *a function of the mode frequency and damping*. The SSI system modes, especially for soil sites, may have very different associated damping.

Each mode that produce a resonant spectral peak has its own peak factor.

Using a *single peak factor* is *accurate only for broad band ISRS that behave close to SDOF systems, not for MDOF SSI systems for which ISRS might have multiple peaks.*

Computation of SSI Response Peak Factors Using AD-DK SDOF System Solution Under WN/FWN Inputs

$$\overline{X}_{\max} = p\sigma_X$$
$$\sigma_{X_{\max}} = q\sigma_X$$

AD-DK Peak factors for mean (p) and std. dev. (q) of the maximum response, Xmax:

$$p = \sqrt{2\ln(\nu_0 T)} + \frac{0.5772}{\sqrt{2\ln(\nu_0 T)}} \qquad q = \frac{1.2}{\sqrt{2\ln(\nu_0 T)}} - \frac{5.4}{\left[13 + \left(2\ln(\nu_0 T)\right)^{3.2}\right]}$$

(after Der Kiureghian, 1980)

Mean-crossing rate for Gaussian process X

$$\nu_0 = \frac{1}{\pi}\frac{\sigma_{\dot{X}}}{\sigma_X} = \frac{1}{\pi}\sqrt{\frac{\lambda_2}{\lambda_0}}$$

Where spectral moments are defined by

$$\lambda_i = \int_0^\infty \omega^i S(\omega)\,d\omega$$

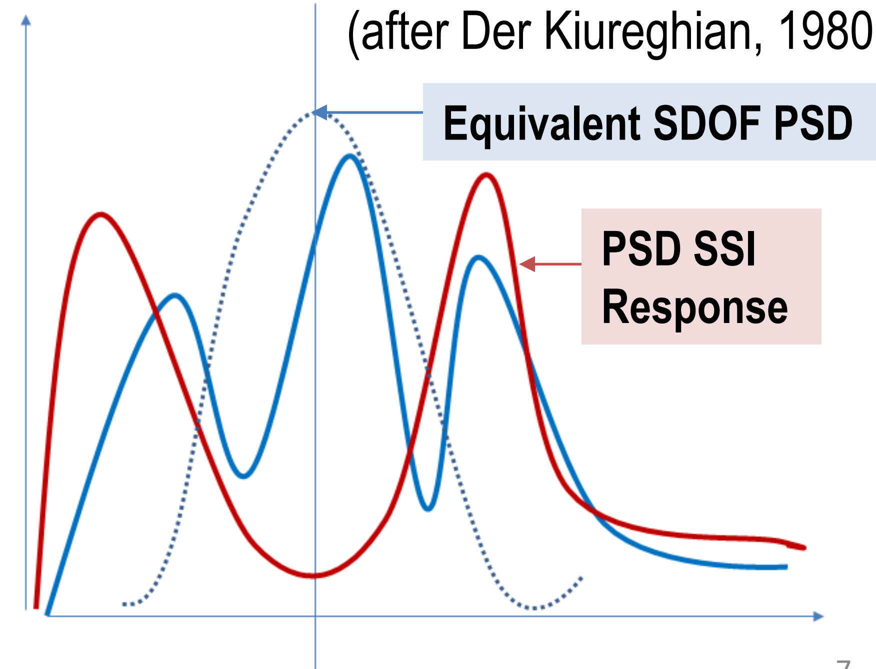

Only the 0 and 2nd order spectral moments are considered, so that PSD shape details are lost

10 slides skipped for public version

Embedded RB Complex on Rock and Soil Sites

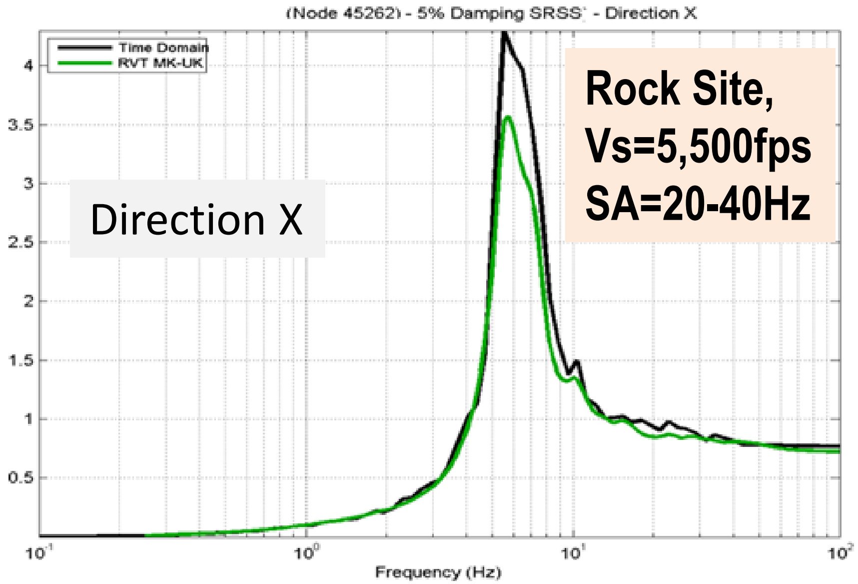

a) Horizontal RB ISRS at A Higher Elevation

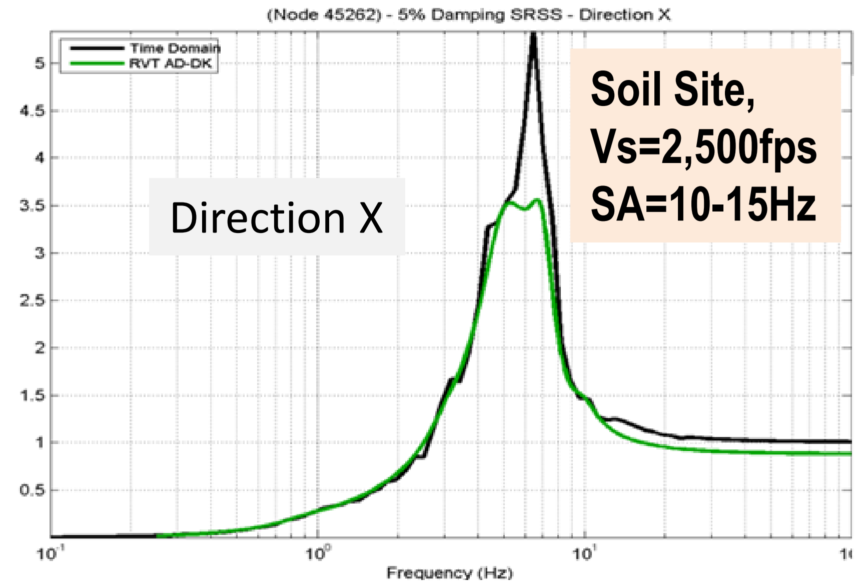

a) Horizontal RB ISRS at A Higher Elevation

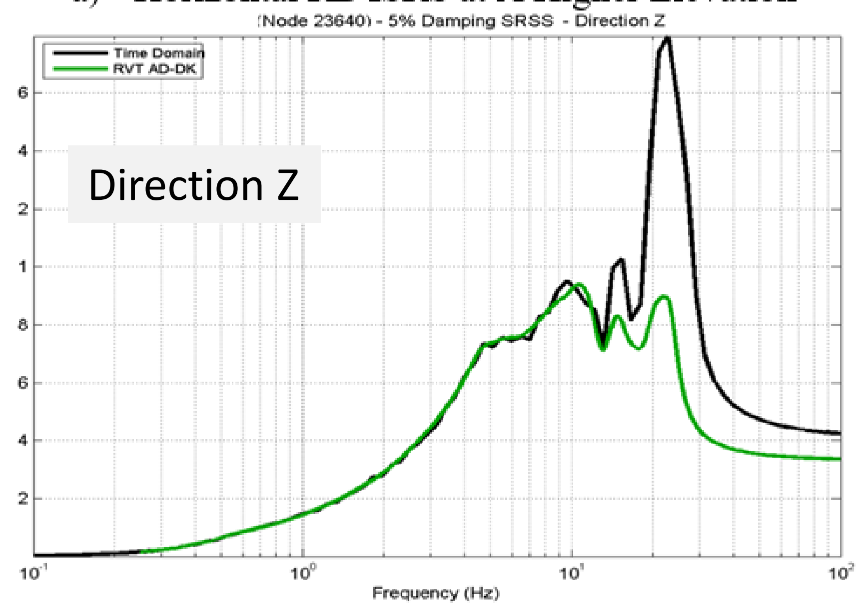

b) Vertical RB ISRS at A Higher Elevation

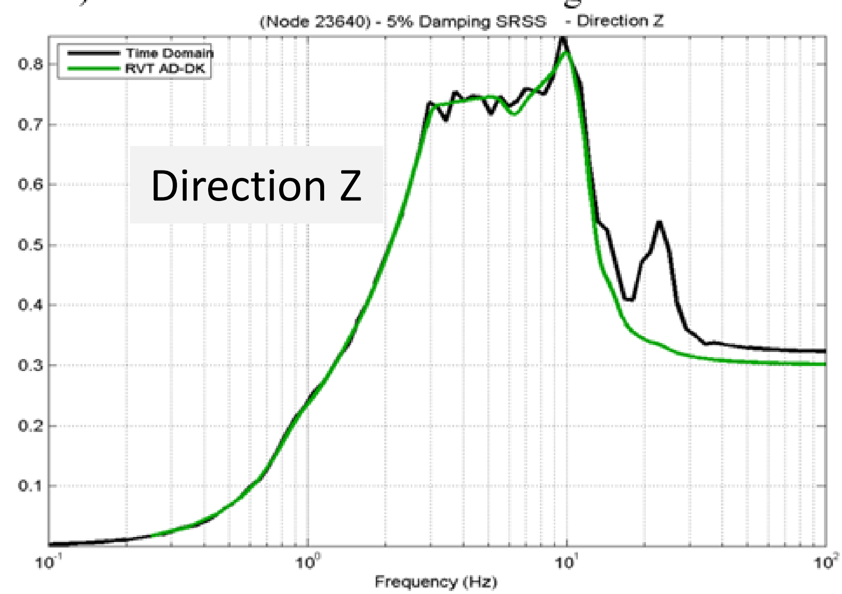

b) Vertical RB ISRS at A Higher Elevation

Deeply Embedded Building on Rock and Soil Sites

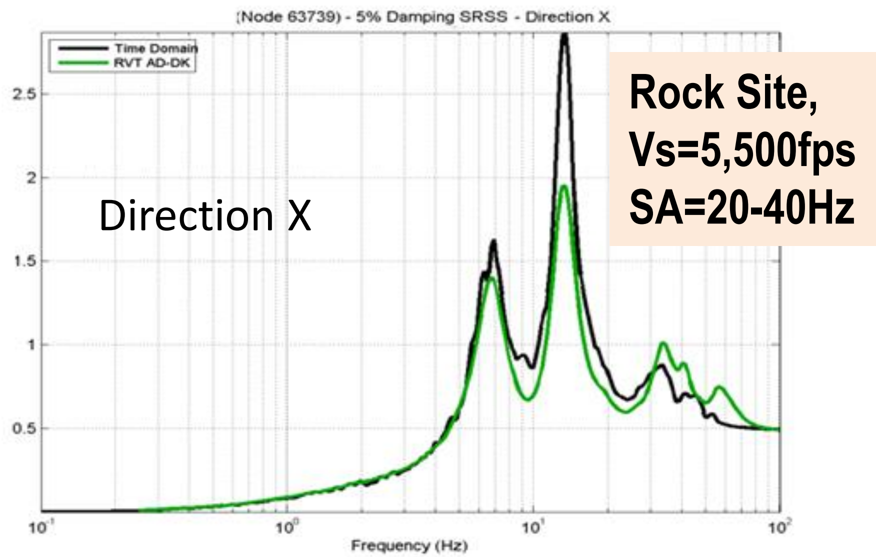

a) X Direction ISRS at A Higher Elevation

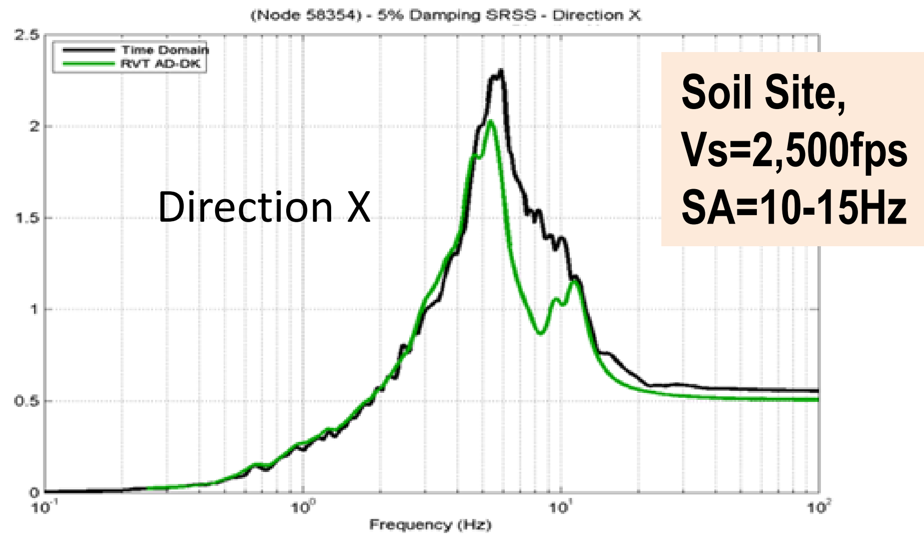

a) X Direction ISRS at A Higher Elevation

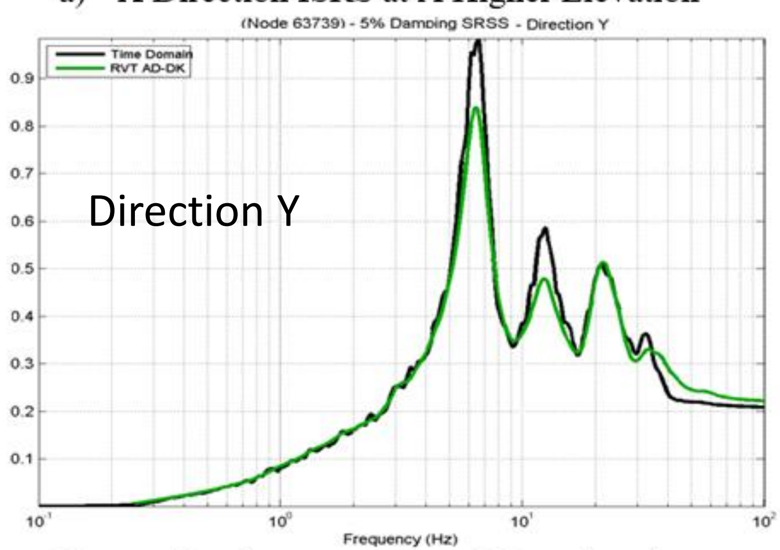

b) Y Direction ISRS at A Higher Elevation

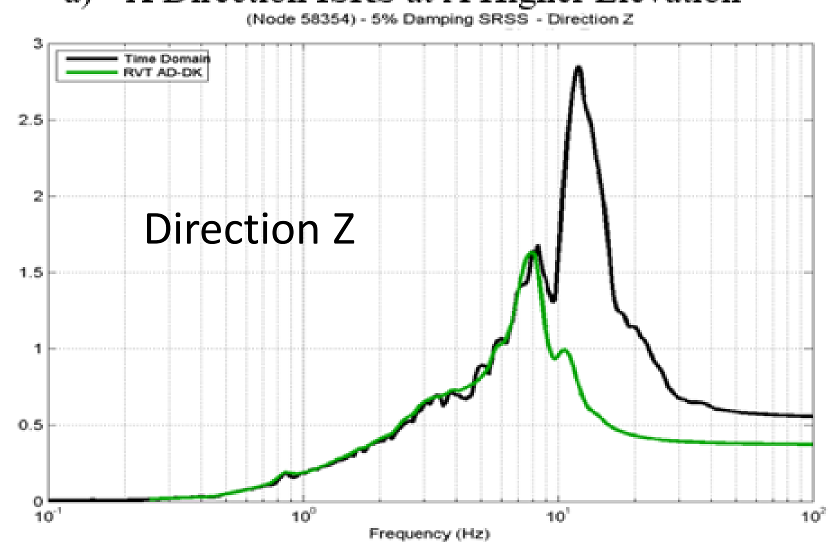

a) Z Direction ISRS at A Higher Elevation

Conclusions

The RVT SASSI approach accuracy varies widely on a case-by-case basis. *We selected on the worst case study examples*.

As explained herein, the theoretical basis of the RVT SASSI approach is on based on the RVT SDOF system solution.

This presentation should be considered as a warning for structural analysts, who are attracted for saving time by using the RVT SASSI approach to avoid having multiple input sets of acceleration time-histories.

The RVT SASSI approach, as currently implemented, and also recommended in ASCE 4-16, *should be used very cautiously* for performing seismic SSI analysis of the nuclear safety-related structures, and only after case-by-case detailed validations are performed for all three deterministic soil profiles, LB, BE and UB soils.

Key References

Davenport, A. (1964). “Note on the Distribution of the Largest Value of A Random Function with Application to Gust Loading*”, Proceedings. Institute of Civil Engineers, Vol. 28, 187-196*

Deng, N. and Ostadan, F. (2012) “Random Vibration Theory-Based Soil Structure Interaction Analysis”, *the 15th World Conference on Earth. Eng., Lisboa.*

Der Kiureghian, A. (1980). “Structural Response to Stationary Excitation”, *J of EMD, Vol. 106, EM6*

Der Kiureghian, A. (1981). “A Response Spectrum Method for Random Vibration Analysis of MDOF Systems*”, J of Earth. Eng. & Struct. Dyn., Vol. 9, 419-435*

Ghiocel, D.M. and Grigoriu, M.D. (2013). “Efficient Probabilistic Soil-Structure Interaction (SSI) Analysis for Nuclear Structures Using Reduced-Order Modelling in Probabilistic Space”, *SMiRT22 Conference, Division V, San Francisco, August 18-23*

Ghiocel, D.M. (2015). "Random Vibration Theory (RVT) Based SASSI Analysis for Nuclear Structures Founded on Soil and Rock Sites", *SMiRT23 Conference, Division V, August 14-19*

Igusa. T. and Der Kiureghian, A. (1983). “Dynamic Analysis of Multiple Tuned and Arbitrarily Supported Systems”, *University of California at Berkeley, EERC Report 83-07*

Unruh, J.F. and Kana, D.D.(1981).”An Iterative Procedure for Generation of Consistent Power Response Spectrum”, *Journal of Nuclear Engineering and Design, p. 427-435*